To the graduate council:

I am submitting herewith a thesis written by Richard Lee Graves entitled "Dynamic Stiffness and Damping of Single Piles in Loess." I have examined the final copy of this thesis for form and content and recommend that it be accepted in partial fulfillment of the requirements for the degree of Master of Science, with a major in Civil Engineering.

Edwin G. Burdette

Dr. Edwin G. Burdette, Major professor

We have read this thesis and
recommend its acceptance:

Accepted for the council:

Associate Vice Chancellor and
Dean of the Graduate School

DYNAMIC STIFFNESS AND DAMPING OF SINGLE PILES IN LOESS

A Thesis

Presented for the

Master of Science

Degree

The University of Tennessee, Knoxville

Richard Lee Graves

December, 1995

ACKNOWLEDGMENT

I would like to take this opportunity to express my gratitude to those who have helped me over the past several months. I would first like to thank my major professor, Dr. Edwin G. Burdette. Without his patience and guidance, this undertaking would not have been possible. I would also like to thank the rest of my committee members, Dr. David Goodpasture and Dr. James Harold Deatherage. They were both quick to offer their assistance when needed. Last, but not least, I want to thank Kevin Bowling for his many contributions.

ABSTRACT

Pluck tests were conducted to determine the lateral dynamic stiffness and damping of single piles embedded in loess. Two prestressed concrete, friction piles were tested just outside of Memphis, Tennessee. Each pluck test consisted of giving the pile head an initial deflection, then releasing it instantaneously. The dynamic stiffness and damping were determined from the free-vibration response of the pile. Each pile was tested at several initial deflections, which were progressively increased.

Dynamic stiffnesses ranged from 63 kips/inch at the smallest initial deflection to 13 kips/inch at the largest for one pile. For the other pile, the largest stiffness was 45 kips/inch and the smallest was 31 kips/inch. The smaller dynamic stiffness values determined for the first pile mentioned and the larger values determined for the second were believed to be artificially low due to saturated soil conditions. The damping ratios for the first pile ranged from 9% to 13% while those for the second pile ranged from 5% to 7%. Computer models of the test piles were developed to match the lateral stiffness determined from the tests. The models were then used to "transfer" the dynamic stiffness from the center of mass to the ground surface.

TABLE OF CONTENTS

LIST OF TABLES

LIST OF FIGURES

CHAPTER 1

INTRODUCTION

The Tennessee Department of Transportation (TNDOT) has recently become increasingly concerned about the manner in which it models bridges for seismic design. There are two main reasons for this concern. First, a significant amount of structural damage to bridges and other structures has resulted from earthquakes that have occured in the state of California in recent years. Second, portions of West Tennessee are subject to a significant risk of seismic activity according to AASHTO Specifications For Seismic Design of Highway Bridges (1).

TNDOT currently uses a computer software program called SEISAB, developed by Imbsen and Associates, to model its bridges for seismic analysis. The bridge being modeled is subjected to simulated seismic loadings, which impart shear, bending moments, and axial forces to each bent column and abutment. These forces are used in conjunction with forces caused by other loading conditions (i.e. dead, live, etc.) to design the bridge.

SEISAB allows the input of spring coefficients at the base of each bent column and at each abutment; these springs are meant to replace the stiffness of the soil that the bridge is founded on. Currently, TNDOT assumes the bent supports to be fixed against all translation and rotation while assigning spring coefficients to the abutments.

Two questions were raised: (1) does the assumption of fixed bent supports give reasonable results, and (2) if not, what would be appropriate values to use for spring coefficients? These questions prompted the initiation of the research project from which this thesis stems.

To answer the first question, a sensitivity study was conducted with SEISAB at the University of Tennessee (2,3). Spring coefficients were assigned to bridge bent column and abutment supports and varied to determine their relative contributions to column moments and axial forces. The results of the sensitivity study, some details of which are discussed in chapter two, indicate that the fixed support assumption can be unconservative.

In reference to the second question, a spring coefficient that one would use with SEISAB is the dynamic stiffness of the support corresponding to a particular degree-of-freedom. The first step in determining the dynamic stiffness of the support is to determine that of a single pile. The main focus of the second phase of the research project was to determine the lateral (horizontal) dynamic stiffness of a single pile, the reason for which is explained in chapter two.

The predominant type of soil in the western part of Tennessee is loess, which has some unique characteristics. "Loess" is a term used to describe a rather general soil category consisting of wind blown silts and clay. The engineering properties of loess can vary dramatically. Depending on the relative amounts of silt and clay, it may behave as either a cohesive soil or a cohesionless soil. Loess has another unusual characteristic in that it is considered to be a collapsible soil (4). At a relatively low water content, the compressive strength of loess can be very high. However, much of this strength is lost when the soil becomes saturated.

There has been a significant amount of research regarding the dynamic properties of sand and clay, but very little, if any, for that of loess. As a result, a series of full scale dynamic tests were conducted with two prestressed concrete friction piles located at a bridge construction site just outside of Memphis, Tennessee. The tests conducted during this investigation are referred to as "pluck" tests, whereby a pile was given an initial displacement and released instantaneously. The dynamic stiffness and damping of the soil-pile system were then obtained from the free vibration response of the pile.

The primary purpose of this thesis was to describe the results of the pluck tests performed to determine lateral stiffness. A description of the tests performed and a complete analysis of the data form the major portion of the work presented herein.

The final part of this investigation was to match the calculated stiffness of the test piles with a structural analysis program, using measured or estimated soil parameters, in order to predict the dynamic stiffness of other types of piles embedded in different types of loessial soils.

CHAPTER 2

REVIEW OF LITERATURE

The sensitivity study mentioned in chapter one was conducted using two actual bridges in West Tennessee. One is located in Madison County and the other in Haywood County. The Madison County bridge consists of two equal length spans (130'-6") with continuous, prestressed concrete I-beams. The bent columns are supported by prestressed concrete friction piles. The Haywood County bridge consists of three spans (31'-6", 31'-0", 31'-6") with continuous, prestressed concrete box girders. The superstructure is supported by free-standing friction piles. These bridges were selected for the study because they are typical of the types of bridges designed by TNDOT which are founded on loessial soil.

A total of six spring stiffness coefficients are available for use with SEISAB at the base of each pier and at each abutment to represent the foundation stiffness of the bridge being modeled. Three spring coefficients govern translation in the longitudinal, transverse, and vertical directions, with respect to the bridge centerline. In the remainder of this section, the longitudinal and transverse springs are referred to as horizontal springs. Of the remaining spring coefficients, two govern rotation in the longitudinal and transverse directions (rotational springs), and the third governs rotation about a vertical axis (torsional springs).

The spring coefficients were varied individually in order to determine the relative contribution of each to the overall structural response. Some analyses were with variations in bent support stiffness while fixing the abutment supports. Others were conducted with simultaneous variations in bent and abutment stiffnesses. The effects of skewness and a non-symmetrical structure were also considered in the study, although not simultaneously. The Madison county bridge was analyzed with various bent skew angles and with one span increased in length by twenty percent.

The general conclusions drawn from this study were as follows:

(1) Bent column forces were relatively insensitive to small variations in support stiffness.

(2) Variations in the vertical and torsional springs had very little effect on bent column forces while the effect of varying the rotational springs was somewhat larger.

(3) Variations in the horizontal springs had a significantly larger effect than variation in any of the other springs.

Researchers at the University of Michigan have conducted extensive full scale dynamic testing of single piles (5,6). The tests were conducted on eleven steel pipe piles located at three different sites in southeastern Michigan. The piles ranged in length from 50 feet to 160 feet and in diameter from 12.75 inches to 14 inches. Some piles were embedded in cohesive soils while others were embedded in cohesionless soils. Two types of tests were conducted on each pile: steady-state vibration tests and pluck tests.

The steady-state vibration tests consisted of forcing the pile to oscillate laterally in a harmonic fashion. This was accomplished with a vibratory oscillator that was attached to the top of the pile. The oscillator consisted of an eccentric rotating mass that produced an unbalanced force in the horizontal direction. A static weight (mass), consisting of steel plates bolted together, was added to the top of the pile in order to reduce the natural frequency of the soil-pile-mass system to the operating range of the oscillator. The oscillator was attached to the top of the pile mass. The mass was placed as close to the ground surface as possible to maximize the contribution of the soil to the response of the pile. The piles were driven at various force levels through a frequency range of 5 to 55 hertz. At each force level, the piles experienced the entire range of frequencies, stopping long enough at each frequency to reach a steady state. This procedure produced a response curve where the frequency occurring at the maximum displacement amplitude was the resonance frequency. The maximum amplitude and resonant frequency were used to calculate the natural frequency and damping of the system, assuming a single-degree-of-freedom system with viscous damping. These values were then used to determine the dynamic lateral stiffness.

The pluck test consisted of striking the pile, as close to the center of gravity of the attached mass as possible, with a wooden plank. The system damping and natural frequency were determined from the free vibration response of the pile. The dynamic stiffness of the soil-pile-mass system was not determined from the pluck test. A single-degree-of-freedom system was also assumed for calculations involving the pluck test.

Maximum displacement amplitudes 0.0005 inches to 0.025 inches were recorded during the steady-state vibration tests. Damping ratios ranging from 2.8 to 22.7 percent and dynamic stiffnesses ranging from 32.4 to 157 kips per inch were reported.

It would be more accurate to consider the soil-pile-mass system described here as a two-degree-of-freedom system (coupled translational and rocking modes). However, Gle and Woods were able to make the single-degree-of-freedom assumption based on the degree of separation between the translational and rocking resonant frequencies. That is, the rocking resonance frequency was believed to be large enough relative to the translational resonance frequency that it would not interfere with the translational response of the system. The test results confirmed this belief as a well defined rocking resonance was never obtained.

Gle and Woods reported that, in general, the resonance frequencies were lower for the pluck tests compared with the steady-state vibration tests. However, there was good agreement between the resonance frequencies from the two procedures for the higher amplitude tests. The damping ratios obtained from the pluck tests were reported to be generally higher, almost twice as high for the higher amplitude tests, than those obtained from the steady-state vibration tests. This phenomenon was attributed to the difference in the two test procedures. During a steady-state vibration test, the soil is subjected to a large number of cyclic deformations of approximately equal magnitude, which is not characteristic of a pluck test. These repetitive deformations result in a permanent deformation of the soil, which causes the pile to lose contact with the soil during a portion of each cycle. The reason for the decrease in damping in this situation is that the soil contributes much more to the overall damping of the system than the pile.

Full scale dynamic tests were also conducted at the University of Houston pile test facility by researchers from the University of Texas at San Antonio and the University of Houston (7). Both a single pile and a nine-pile group were tested as part of this research. Because the investigation reported herein concerns only single piles, the tests involving pile groups are not discussed.

The tests were conducted on a steel, 10.75 inch diameter, pipe pile embedded 43 feet in stiff, overconsolidated clay. A massive concrete cap was attached to the pile head. The testing program began with a series of steady-state vibration tests. Approximately one year after the conclusion of this phase, pluck tests and slow cyclic loading tests were conducted on the pile. The pluck tests were performed at increasing levels of horizontal static load. The slow cyclic loading tests consisted of horizontal loads as well as rotational (moment inducing) loads, applied vertically upward to a bottom corner of the pile mass.

Natural frequencies and damping values for the translational (horizontal) mode were determined at each load level for the soil-pile-mass system from the response curves generated by the pluck tests and steady-state vibration tests. The dynamic stiffnesses were then calculated with these values. Once the field test results were obtained, single-degree-of-freedom analyses and two-degree-of-freedom (coupled translational and rocking modes) modal analyses were used to determine the natural frequencies of the system analytically. The slopes of the slow cyclic loading tests ("static" stiffnesses) were converted to pseudo-dynamic stiffnesses by increasing them to account for soil creep effects and rate of loading (strain rate). In addition, steady-state response curves were synthesized with theoretical equations, using the translational pseudo-dynamic stiffnesses, as just described, and damping values obtained from the pluck tests.

Blaney and O'Neill reported that the horizontal natural frequencies of the soil-pile-mass system calculated by the analytical methods compared well with those obtained from the pluck tests. In addition, the natural frequencies for the rocking mode determined from the two-degree-of-freedom modal analyses were well separated from those for the translational mode, which is consistent with the observation made by Gle and Woods. Horizontal natural frequencies and dynamic stiffnesses obtained from the synthesized response curves also compared well with those obtained from the steady-state vibration tests.

CHAPTER 3

FIELD TEST PROCEDURE AND SITE INFORMATION

3.1 INTRODUCTION

The pluck tests conducted as part of this research project consisted of four main components. These components include the piles, pile mass, load and release mechanisms, and instrumentation used to monitor and record the free-vibration response of the pile as well as the lateral force to which the piles were subjected. Discussions of each of these components, the determination of site soil properties, and experimental procedure are presented in the following sections.

3.2 SUBSURFACE INVESTIGATION

A geotechnical investigation was conducted at the field test site by Hall, Blake, and Associates, Inc. on January 12, 1995. Four bore holes, each thirty feet deep, were drilled as part of this investigation, two holes in the vicinity of each pile. The distance between the piles was approximately seventy-nine feet. Figure 1 [1] shows the location of the bore holes relative to the piles. At each pile, a split-spoon sampler was used in one bore hole to

---

[1] All Figures and Tables may be found in the Appendix

conduct standard penetration tests (SPT) while a Shelby tube sampler was used in the other hole to obtain undisturbed soil samples for laboratory testing.

Descriptions of the soil in the vicinity of each pile are presented as Tables 1 and 2. Loess was encountered from the ground surface to a depth of approximately 8.5 feet in the vicinity of both piles. All soil classifications were made according to the Unified Soil Classification System.

Tables 3 and 4 provide a summary of the soil properties determined from the borings. Both the field blow counts, which were determined directly from the standard penetration tests, and the corrected blow counts are presented in the tables. Details of the method by which the corrected blow counts were obtained were not included in the soils report submitted to the research team. In general, however, field blow counts are corrected as follows (8):

$$N_{corr.} = C_N \times N \times \eta_1 \times \eta_2 \times \eta_3 \times \eta_4 \qquad (EQ.\ 3.1)$$

in which,

C_N = Adjustment for overburden pressure.

η_1-η_4 = Correction factors which accout for deviations from standard testing procedure and equipment.

The adjustment for overburden pressure is determined from the following relationship:

$$C_N = \left(\frac{P_0^{\prime\prime}}{P_0^{\prime}} \right)^{1/2} \qquad (EQ.\ 3.2)$$

in which,

P_0'' = Reference overburden pressure (taken as 2.0 ksf).

P_0' = overburden pressure at test depth.

The soil densities, damping ratios, shear moduli, and shear wave velocities were estimated with empirical equations that are based on past dynamic tests conducted on soils of the northern Mississippi embayment region. The unconfined compressive strengths were estimated from the results of hand penetrometer tests.

3.3 TEST PILES

The pluck tests described herein were conducted on two fourteen inch square, prestressed concrete piles. Both piles were originally to be driven a minimum of thirty to thirty five feet into the ground in order to prevent the pile tips from translating during the course of the pluck tests. Due to the stiffness of the soil at the test site, however, piles one and two were driven only to depths of fifteen and seventeen feet, respectively. Both piles were driven on July 27, 1994. Once driven, each pile was cut off at approximately three feet from the ground surface to accommodate the steel mass that was attached to the top of the pile.

3.4 PILE MASS

In order to reduce the free-vibration response of each pile to that of a single-degree-of-freedom system, a sizeable static weight (mass) was attached to the pile head. The mass consisted of a holder and fifty-four steel plates, two of which were used to transfer the lateral load to the piles. These two plates are referred to as pull plates, for obvious reasons, and the others are referred to as standard plates. The pile mass was located as close to the ground as possible in order to maximize the contribution of the soil to the free-vibration response of the pile. When the mass is located farther from the ground surface, the response of the pile more closely resembles that of a cantilever.

Section and top views of the mass holder are shown in Figures 2 and 3, respectively. A thirty inch section of 16" x 16" x 1/2" structural steel tube was enclosed at one end by a 15 1/2" x 15 1/2" x 1" plate, which formed the top of the holder. Four, one inch diameter holes were drilled in the top plate to accommodate anchor bolts protruding from the top of each pile, the purpose of which was to provide a secure bond between the pile and mass holder. Seven inches from the other end of the tube, 11" x 1 1/4" plates were cut and attached as shown to form the platform on which the mass plates rested. Two small 1/2" thick plates were attached below these plates to provide an additional point of load application. Once the mass was placed on the pile, set screws were threaded through four holes, one on each side of the tube, and tightened against the pile. Steel shim plates were placed between the set screws and the pile to prevent them from digging into the concrete. The total weight of the holder was 754 pounds.

The mass plates, each 1/2" thick, were rectangular in shape with sides measuring thirty-eight and thirty-nine inches. The sides were of different lengths to aid in the placement of the plates. During placement, the plates were staggered so that no two consecutive plates had the same length sides facing a particular direction, thus providing a finger-hold for those responsible for the placement process. A 16 1/2" x 16 1/2" hole was cut in the center of each plate, which provided space between the plate and the outside of the tube. Four 1 1/2" diameter holes located at the corners of each plate were aligned with similar holes in the mass holder. Threaded rods were then placed through these holes to tie the mass plates and holder together.

The standard plates and pull plates were identical with the exception of an additional smaller plate, used to transfer the lateral load to the pile mass, that was attached to each pull plate (Figure 4). The pull plates were located such that the lateral load would be applied at the center of mass. Each mass plate weighed 171.5 pounds, which, when added to the weight of the holder, resulted in a total mass weight of 10,018 pounds.

3.5 LOAD AND RELEASE MECHANISMS

The horizontal force that provided the initial deflections of the pile head during the pluck tests was supplied by a hydraulic, center-hole jack. Profile and plan views of the test setup are shown in Figures 5 and 6, respectively. The force was delivered to the pile by jacking against a steel frame, which was comprised of a structural steel tube and wide flange sections configured as shown. High strength threaded bars, coupled together, were used to transfer the load from the reaction frame to the pile head. These bars, commonly called Dywidag bars because of the manufacturer (Dywidag Systems International), are typically used for post-tensioning concrete. In order to prevent excessive rebound movement of the Dywidag bar and its contents after the load was released, a plate was located on the inside of the tube, bolted to the back of the reaction frame. The load reaction frame was mounted to an unreinforced concrete pad, both of which were designed by

Kevin Bowling, a graduate student at the University of Tennessee, and David McAlister, a former graduate student at the University of Tennessee. For additional information concerning the design of the reaction frame, concrete slab, and associated equipment, the reader is referred to an M.S. thesis by David McAlister (9).

Of particular concern during the pluck tests was the speed with which the load was released. In order to obtain a meaningful free-vibration response from a soil-pile system, the load must be released instantaneously. This instantaneous release was accomplished with a special quick-release mechanism, manufactured by Peck and Hale in West Sayville, New York, located as indicated in Figure 5. The load was released by pulling a rope attached to the quick-release mechanism in a direction essentially perpendicular to the applied load. At relatively low loads, the quick release mechanism was disengaged relatively easily without mechanical intervention. However, the aid of a power winch was necessary at higher loads.

3.6 INSTRUMENTATION

Although pile head displacement is of primary importance when determining the dynamic properties of a soil-pile-mass system, acceleration and velocity can be used as independent means of displacement verification.

Displacement is obtained either by integrating velocity once or acceleration twice.

The lateral displacement of the pile head during free-vibration was monitored by linear variable displacement transducers (LVDT). The LVDT's were manufactured by Solartron Metrology and had an operating range of $\pm$ one inch. Ultra low frequency seismic accelerometers, manufactured by Wilcox Research Inc., were used to monitor the acceleration of the pile head. The operating range and sensitivity of the accelerometers were $\pm$ 1g (units of gravity) and 5 volts/g, respectively. The pile head velocity was measured with a linear velocity transducer (LVT), which had a linear operating range of two inches (note units of length - not velocity). The LVT was manufactured by Lucas Schaevitz. A twenty-five kip doughnut type load cell, manufactured by Interface, was used to monitor the lateral load applied to the pile head. During the pluck tests, information from the motion and load sensing devices was processed and recorded by a data acquisition system, DTVEE, installed on a personal computer. The main component of this system was a model DT2836 data acquisition board.

Figure 7 shows the location of the motion sensors on the pile mass during the first series of tests. Two LVDT's, one LVT, and four accelerometers were used during the first series of pluck tests. One accelerometer was placed on top of the mass and oriented so that only vertical accelerations were measured. Another accelerometer was placed on the tube below the mass and oriented so that it sensed only out-of-plane, with respect to the plane of loading, accelerations of the pile mass. The remaining devices were oriented to sense motion in the plane of loading.

3.7 TEST PROCEDURE AND SITE LAYOUT

The full-scale testing began with pile number one on December 16, 1994. The layout of the test site is shown in Figure 8. The x and y-axes in the figure are used later in this section as a reference when indicating the directions of the horizontal loads applied to the test piles. The pile head was given initial deflections, measured at the bottom of the mass, ranging from 0.042" to 0.25" in ascending order. Several tests were conducted at each initial deflection in order to provide a sufficient amount of data. During a typical test, the deflection at the bottom of the mass was monitored by the person operating the loading jack with a voltmeter. The applied load was also being monitored with a digital strain indicator (Vishay). Once the desired deflection was reached, the order was given to release the load. At the same time, the load was recorded on paper.

The point of load application was alternated between the center of gravity and bottom of the mass at each initial deflection. In order to compare the static and dynamic stiffnesses of the soil-pile-mass system, the load had to be applied at the center of mass. At the same time, the dynamic stiffness obtained from the free-vibration response of the system was the stiffness at the center of mass, which was located approximately twenty-seven inches from the ground surface. The original purpose for applying the load at the bottom of the mass was to provide a relationship between the stiffness at the center of mass and at a location closer to the ground surface, which would aid in determining the "true" dynamic stiffness of the system at the ground surface. However, the computer models of the test piles were used for this purpose.

Pile number two was tested the following day. For this series of tests, the velocity transducer and the accelerometer measuring pile head accelerations in the vertical direction were replaced by two LVDT's, one at the center of gravity and the other at the bottom of the mass. Due to problems encountered with the computer at some point during the series of tests, the remaining accelerometers were removed from the pile mass.

The pluck tests on pile number two were conducted in a manner similar to those conducted on pile number one with initial deflections ranging from 0.038" to 0.11". Several tests were conducted at an initial deflection of approximately 0.1" to assess the repeatability of results.

On March 20, 1995, the research team returned to the site to conduct two additional series of tests on pile number two. The first series of tests was conducted with the load applied in the same direction as the original series (y-direction), with initial pile head deflections ranging from 0.048" to 0.097". For the second series of tests, the load was applied perpendicular to the original direction (x-direction). A portion of these tests was conducted with initial deflections ranging from 0.02" to 0.096" in ascending order. Once the maximum deflection was reached, additional tests were conducted with initial deflections descending to 0.019" to observe the rebound characteristics of the soil. Two accelerometers and two LVDT's were used during the tests conducted on this day. One of each was placed at the center of gravity and at the bottom of the mass. The lateral load was applied at the center of mass for all tests.

CHAPTER 4

EVALUATION OF TEST DATA

4.1 INTRODUCTION

The lateral dynamic stiffness was determined for each test pile at each initial deflection. The static stiffness was also determined and compared with the dynamic stiffness to assess the effect of dynamic loading on the soil-pile system. The procedure used to determine the static and dynamic stiffness values is explained in the following sections.

4.2 DYNAMIC STIFFNESS

In general, the amount of computational effort required to perform the dynamic analysis of a structure decreases with the number of degrees-of-freedom necessary to adequately describe the response of the structure. Obviously, a single-degree-of-freedom structure would require the least amount of computational effort to analyze. The steel mass was attached to the top of each test pile to reduce the free-vibration response of the soil-pile-mass system as closely as possible to that of a single-degree-of-freedom system, consisting of lateral translation only. The effect of a rocking mode, caused by rotation of the mass, on the lateral response of the system was assumed to be insignificant. This assumption was based on the results of tests conducted by Gle and Woods and Blaney and O'Neill (discussed in chapter 2), which indicated no significant interference from a rocking mode. No irregularities in pile response, which could be attributed to rocking of the pile mass, were observed during the tests conducted as part of this investigation, thus justifying the aforementioned assumption. This statement is valid only for the motion detected at the center of gravity of the mass. A small amount of mass rotation was detected by sensing devices located at other points on the mass; however, this had little, if any, effect on the results of the pile tests.

A mathematical relationship exists between the dynamic stiffness, mass, and natural frequency of a single-degree-of-freedom system, which can be expressed as follows (10):

$$k=m\omega_n^2 \qquad (EQ.\ 4.1)$$

in which:

k = dynamic stiffness of the system.

m = system mass.

ω_n = undamped natural circular frequency of the system.

The first step in determining the dynamic stiffness of the system is to obtain the period of oscillation, which is the damped natural period, T_D, of the system, directly from the free-vibration response curve (Figure 9). For the remainder of this section, any mention of a frequency, whether damped,undamped, cyclic or circular, should be interpreted by the reader as the natural frequency of the system. The damped cyclic frequency, f_D, measured in units of cycles per second or hertz, is, simply, the inverse of the damped natural period. The damped circular frequency can then be determined from the following expression:

$$\omega_D = 2\pi f_D \qquad (EQ.\ 4.2)$$

Before the undamped circular frequency can be determined, the system damping must first be evaluated. Although structural damping is often found to be amplitude dependent, viscous (velocity related) damping is typically assumed, as it is here, in order to simplify the dynamic analysis of a structure. Contributions to the overall system damping of an embedded pile are made by the pile and the soil, which are referred to as geometric and radiation damping, respectively. The soil contributes much more to the overall damping of the system than the pile alone. The natural logarithm of the ratio of any two consecutive peaks from the free-vibration response curve is referred to as the logarithmic decrement, δ, which can be expressed as follows:

$$\delta = \ln\left(\frac{v_n}{v_{n+1}}\right) \qquad (EQ.\ 4.3)$$

in which v_n is the amplitude of a displacement peak and v_{n+1} is the amplitude of the following peak. The ratio of peaks j cycles apart is, simply, j times the logarithmic decrement. Therefore, the system damping ratio, ξ, expressed as a percent of critical damping, can be evaluated using any pair of peaks (both must be of the same sign) with the following expression:

$$\xi = \sqrt{\frac{\left(\ln\frac{v_n}{v_{n+j}}\right)^2}{(2\pi j)^2+\left(\ln\frac{v_n}{v_{n+j}}\right)^2}} \qquad (EQ.\ 4.4)$$

Once the damping ratio has been determined, the undamped circular frequency can be calculated as:

$$\omega_n = \frac{\omega_D}{\sqrt{1-\xi^2}} \qquad (EQ.\ 4.5)$$

Having evaluated the undamped circular frequency, one can use equation 4.1 to calculate the dynamic stiffness of the system.

4.3 STATIC STIFFNESS

The maximum pile head deflection, occurring just before release, at the point of load application was used to determine the static stiffness of the system. The applied load, pile head deflection, and static stiffness are related by the following expression:

$$k_{st} = \frac{P}{\Delta} \qquad \text{(EQ. 4.6)}$$

in which P is the applied load and Δ is the pile head deflection. The deflection used to calculate the static stiffness was determined by subtracting the resting position of the pile mass at the end of the previous test from the maximum measured deflection.

CHAPTER 5

COMPUTER MODELS OF TEST PILES

5.1 INTRODUCTION

In order to minimize the need for full-scale pile testing, the expense of which can become significant, the ability to predict the dynamic lateral stiffness of a pile embedded in loess without the benefit of a full-scale test was desired. The method chosen to accomplish this goal consisted of matching the lateral stiffness, as determined from the pluck test, of each pile tested with a computer model of the corresponding soil-pile system.

Computer models of both test piles were generated with the structural analysis program GTSTRUDL. Before the models could be used as intended, the stiffness of the soil surrounding the test piles had to be represented in some fashion. After considering various methods for this purpose, the method discussed in section 5.2 was chosen. This particular method was chosen primarily because it is relatively straightforward and easy to follow. In addition, it relies on commonly used static soil strength parameters, which are generally more familiar and better understood than the corresponding dynamic strength parameters. The results of the pluck tests showed that the static stiffnesses were, in general, very close to the dynamic stiffnesses; therefore, either could be used. The soil stiffness profiles resulting from this "matching" process could, theoretically, be used to predict the lateral stiffness of other types and sizes of piles embedded in loessial soils with a variety of stiffness characteristics.

In addition to matching the lateral stiffness of the test piles, the models were also used to transfer the dynamic stiffness from the center of mass to the ground surface. Details of this procedure are discussed in the following chapter. Descriptions of the models, including the method used to represent the soil stiffness, are presented in the following sections.

5.2 BASIS FOR APPROACH TO REPRESENTING SOIL STIFFNESS

The method used to represent the soil stiffness in the computer models of piles one and two was based on a method proposed by Gary Norris and Robert Sack (11). Pluck tests were conducted to evaluate the lateral dynamic stiffness of two bridges located in the state of Nevada. The bent piers and abutments of both bridges were supported by pile groups. From the results of the pluck tests, the lateral stiffness of each pile group was back-calculated. Norris and Sack then wanted to solve for the pile group stiffnesses analytically. They first solved for the lateral stiffness of a single isolated pile, then of the pile group, by accounting for the contribution from the pile cap and the so-called group effect which is based on the pile spacing and arrangement. Only that portion of the solution pertaining to the determination of the soil stiffness is considered here.

The approach used by Norris and Sack relies on classical beam-on-elastic foundation formulations whereby the stiffness of the soil surrounding the pile is represented by a continuous bed of springs. These springs were defined using a subgrade modulus profile approach, which can be described by the following relationship:

$$E_s = fx \qquad (EQ.\ 5.1)$$

in which,

f = Coefficient of variation of lateral subgrade reaction with depth.

x = Depth below ground surface.

E_s = Modulus of subgrade reaction at depth x.

The relationships between the coefficient of variation of lateral subgrade reaction and the unconfined compressive strength, Q_u, of fine grained soils and relative density, D_r, of coarse grained soils are shown in Figure 10. Notice that f is in units of tons/ft^3, which, when multiplied by x, in feet, results in units of tons/ft^2 for E_s. The curve for coarse grained soils and the curve consisting of alternating long and short dashes, which is for normally consolidated cohesive soils, are based directly on recommendations by Terzaghi (12) and Davisson (13). For overconsolidated cohesive soils, Terzaghi suggested that E_s be taken as $33.5Q_u$ (E_s constant with depth and f=0). However, Norris and Sack believed that a linear variation of E_s would be more appropriate. Accordingly, they developed a linear relationship for overconsolidated cohesive soils that produced the same pile response as the constant subgrade modulus profile.

The relationships depicted in Figure 10 reflect not only the stiffness of the soil, but the stiffness of the pile as well. In other words, they represent the stiffness of the soil relative to that of the pile. The curves were formulated with respect to "average pile conditions", which were not defined in the literature, and they correspond to particular levels of soil strain. Because of their association with these strain levels, although numerical values were not given, the relationships were referred to as design-level subgrade modulus gradients. Norris and Sack conducted an analysis relative to their particular situation (pile tops embedded five to ten feet below the ground surface), which is typical in highway bridge applications, and found that these soil strain levels corresponded to an average pile top deflection of one tenth of an inch.

According to Norris and Sack, this magnitude of pile top deflection exceeds the maximum deflection that a pile would experience, at this depth, as the result of an earthquake. Based on this belief and the reasoning that the soil stiffness increases as the strain level, and hence the pile top deflection, decreases, they developed a set of curves (Figure 11) to adjust the design-level modulus gradients (coefficients of lateral subgrade reaction) accordingly. In addition to the increase in soil stiffness with decreasing strain levels, the curves reflect the fact that the subgrade modulus increases in proportion to the pile width B. As noted earlier, the pile stiffness and the soil stiffness are reflected in the subgrade modulus.

The soil properties, Q_u and D_r, used herein to determine the soil stiffness, were based on blow counts from the standard penetration tests conducted at the bridge sites. Cyclic effects due to repeated loading were assumed to be small relative to other pile head stiffness modifications, which were necessary to account for the contribution from the pile cap and the pile group effects, and were, therefore, neglected. It should be emphasized that the aforementioned procedure was used in the work reported herein only to provide initial estimates of the soil stiffness for use with the computer models of piles one and two.

5.3 COMPUTER MODELS OF TEST PILES

Both test piles were modeled with the structural analysis program GTSTRUDL. The models are graphically represented in Figure 12, and sample GTSTRUDL input files are provided as Appendix C. As mentioned previously, piles one and two were driven to depths of seventeen and fifteen feet, respectively. Each pile was divided into several members with nodes, or joints, which are represented by the darkened circles at the ends of each member. The two nodes on each pile above the ground surface represent the points of load application. The top node (node one) was located at the center of gravity of the steel mass. The reader will notice that the distances from the ground surface to the top two nodes on pile two are exactly four inches greater than the distances to the same nodes on pile one. The reason for this difference is not that pile two was cut off four inches farther from the ground surface, but to account for soil missing from the perimeter of the pile.

The location of the nodes at and below the ground surface was based on the soil profile data provided in Tables 1 and 2. The soil surrounding each pile was divided into several individual layers with the upper and lower boundaries defined by the midpoints between soil samples. For example, the lower boundary for the top soil layer, which was also the upper boundary for the next layer, was located (2.5+3.0)/2 = 2.8 feet (Table 1), rounded to the nearest tenth of a foot, below the ground surface. The upper boundary for the top layer and the lower boundary for the bottom layer were, of course, defined by the ground surface and the bottom of the pile, respectively. Nodes were placed at the boundaries of each soil layer. In order to avoid large differences in node spacings, additional nodes were placed within the boundaries of some of the soil layers.

The pile properties that were important in the computer modeling consisted of the modulus of elasticity and weight density of the concrete and the area moment of inertia. The modulus of elasticity was estimated from the following relationship:

$$E = 57\sqrt{f'_c} \qquad (EQ.\ 5.1)$$

in which f'_c is the compressive strength of the concrete. The units of E and f'_c are ksi and psi, respectively. The concrete compressive strength was taken as 5,000 psi, which resulted in an elastic modulus of E = 4,030 ksi. The area moment of inertia was calculated as:

$$I = \frac{bh^3}{12} \qquad (EQ.\ 5.2)$$

in which b and h are the cross-sectional dimensions of the pile, both of which were 14". The resulting moment of inertia was I = 3,201 inches^4. In addition to modeling the static response of the test piles, GTSTRUDL was also used to determine the fundamental (lowest) natural frequencies, which were then compared with the measured frequencies. This task required the input of the concrete density (weight density). By specifying the pile material as concrete, GTSTRUDL uses the default value of 8.68 x 10^{-5} kips/inch^3. This value is based on a unit weight of 150 pounds/foot^3. The pile mass was assumed to be "lumped" at the top node in the computer models.

5.4 EVALUATION OF SOIL STIFFNESS

Determination of the soil stiffness was based on the unconfined compressive strength, Q_u, and relative density, D_r, for the fine grained and coarse grained soils, respectively. The relative densities were estimated from correlations (reference 8, which was cited in chapter 3) with the standard penetration test blow counts, soil densities, and soil descriptions (i.e. dense or loose for cohesionless soils), which are presented in Tables 1 through

4. The unconfined compressive strengths were taken directly from Tables 3 and 4. Each soil layer was assigned a value of Q_u or D_r, depending on the soil type, as indicated in Figure 12. The value corresponding to a particular soil layer was assumed to be constant within that layer.

The design level subgrade modulus gradients for piles one and two, which are presented in Table 5, were determined from Figure 10. These gradients were then amplified in accordance with Figure 13, which was based on the relationships in Figure 11 (Norris and Sack provided a means of developing a design-level modulus amplification curve corresponding to any pile width).

The method presented in section 5.2 was not based on pile tops located at the ground surface, much less above the ground surface. Rather, it was assumed that the pile tops were located at a depth of approximately five to ten feet. The best approximation to this assumption was to use the pile deflections at the ground surface in conjunction with Figure 13. Since these deflections were not measured during the pile tests, they were estimated through a trial-and-error process with GTSTRUDL.

For example, the design-level modulus gradient was amplified according to an assumed ground surface deflection. The computer program was then executed and the resulting ground surface deflection determined. If this deflection did not match the assumed deflection, the process was repeated with a new assumed ground surface deflection.

The soil stiffness was represented in the computer models by spring constants; one constant was placed at each pile node. Various stages of the procedure by which these spring constants were determined are illustrated in Figures 14 and 15. Pile one was the subject of this example. Figure 14 shows a subgrade modulus profile, which was determined with the use of equation 5.1. This profile resulted from increasing the design-level modulus gradients with an amplification factor of, in this case, 2.2. The modulus gradient within the soil layer located between nodes 7 (5.5 ft.) and 9 (7.8 ft.) in Table 5 is identical to those within the bottom two layers by coincidence only.

Values of the spring constants were calculated based on tributary length of pile. The subgrade modulus was evaluated at points midway between each node, and the soil stiffness within the zones created by this process was assumed to be concentrated at the corresponding nodes. For example, the stiffness assigned to node 10 (Figure 14) was determined as follows:

$$E_{s(10)} = \frac{(697\ kcf + 855\ kcf)}{2} \times (10.8\ ft - 8.8\ ft) \qquad (EQ.\ 5.2)$$

$$E_{s(10)} = 1{,}552\ ksf$$

The value of the spring constant was then calculated with the following relationship:

$$K_{10} = 1,552\ ksf \times \frac{14}{12}\ ft \times \frac{1}{12}\ \frac{feet}{inch} = 151\ kips/inch \quad (EQ.\ 5.3)$$

in which 14/12 is the pile width in feet. All of the spring constants for this example are displayed in Figure 15.

Once the spring constants were input, the computer program was executed with the simulated horizontal load applied at the proper location. If the resulting pile deflection did not match the measured deflection, the subgrade modulus gradients were changed, and the procedure was repeated. The deflections at the bottom of the mass were used because of inaccuracies in the measurement of deflections at the center of gravity of the mass. This subject is discussed in the following chapter.

CHAPTER 6

PRESENTATION AND DISCUSSION OF RESULTS

6.1 INTRODUCTION

The static stiffness, damping, and dynamic stiffness were determined for piles one and two from the response data recorded during each test. Representative field data plots and the results of the data evaluation are presented in the following sections. The results of the work done with the computer models of piles one and two are presented as well.

In general, field operations seldom proceed exactly as expected. The full-scale pile testing conducted as part of this investigation was not an exception as problems were encountered. These problems and their effects on the results of the pile tests are also discussed.

6.2 PREPARATORY INFORMATION

Each pile test in a particular series of tests was assigned a letter of the alphabet and referred to thereafter by this designation. Test A in each series was conducted only to provide "zero" (base) readings for all of the instrumentation; therefore, Test B was the first actual test.

As explained in chapter 3, the point of application of the horizontal load was alternated between the center of gravity and bottom of the mass for the tests conducted on December 16 and 17, 1994. Table 6 indicates the location of the applied load for each of these tests. The load was applied at the center of the mass for all tests conducted on March 20, 1995.

In general, only the first four or five cycles from the free-vibration response curve were considered when calculating the damping and dynamic stiffness values for each test. After this point, the quality of the curves degraded and the displacement amplitudes became very small. Therefore, the use of cycles in this region would have increased the probability of inaccurate results. All static stiffness, dynamic stiffness, and damping values were determined according to the procedure outlined in chapter 4. When calculating the damping ratios, several pairs of displacement peaks were considered (not just consecutive peaks), both positive and negative. The average damping ratios are reported herein. All pertinent data used in calculating the damping and dynamic stiffness values are presented in appendix D.

6.3 REPRESENTATIVE FIELD DATA PLOTS

Representative data plots from a few of the pile tests are displayed in Figures 16 through 21. Figures 16 and 17 show the displacement of the pile at the center of gravity and bottom of the mass, respectively, during the test. The lead wires for the LVDT's were connected differently, which created the appearance that the center and bottom of the mass were moving in opposite directions. The large and sudden increase in displacement just after the start of the test, which was a typical occurrence, was caused by a buildup and sudden release of fluid pressure in the hydraulic jack. In general, the data plots of the pile head displacement at the bottom of the mass were not as clear as the plots of displacement at the center.

Figure 18 shows a plot of the load cell data from the same test. It is apparent in the figure that the output signal was anything but clean. The maximum applied load for this particular test was 5.36 kips, which is approximately equal to the width of the band of noise in the plot. This problem was characteristic of all tests conducted on December 16 and 17. Luckily, the maximum load for each test was recorded on paper; otherwise, no reliable load data would have been obtained.

In an attempt to correct this problem for the tests conducted on March 20, a 10 kΩ resistor and a 1,000 μF capacitor were installed in the circuit on the output side of the load cell. This addition to the circuitry did succeed in reducing the noise level; however, it also created an undesired time dependency in the output signal.

Figure 19, which is typical of the load cell data from all tests conducted on March 20, provides a good illustration of this new problem. The data plot should show a sudden increase in load corresponding to the increase in pile head displacement that occurred near the beginning of this and every other test. The plot should also show an instantaneous return of the load to zero upon release. In effect, the resistor-capacitor combination functioned as a voltage buffer in that it allowed no abrupt changes in the measurement of the load. The sensitivity of the load cell for these tests was 3.0 kips/volt.

Figures 20 and 21 show the out-of-plane accelerations at the bottom of the mass and the vertical accelerations at the top of the mass, respectively. As a reminder, the vertical accelerations were measured to provide a rough estimate of the amount of rocking (rotation) experienced by the pile mass during free-vibration. As apparent in the figures, these accelerations consisted only of a few "spikes" just after the load was released. Accordingly, they were believed not to have significantly affected the results of the pile tests.

The accelerometers measuring accelerations in the direction of the applied load did not yield usable results. After the pile testing was completed, it was determined that the magnitude of lateral accelerations experienced by the pile mass exceeded the working range of the accelerometers. The velocity transducers used during the pile tests conducted on December 16 also failed to function as expected.

6.4 ADDITIONAL PROBLEMS ENCOUNTERED

Another problem encountered during the pile tests consisted of relative movement (slipping) between the pile mass plates. At some point during the first few tests conducted on December 17, it was noticed that the pull plates were not aligned with the surrounding plates as they had been before. The nuts on the threaded rods holding the mass plates together were immediately tightened to prevent further slipping. Although the problem with the plates was presumably solved, relative movement between the mass holder and the pile itself remained a possibility.

Evidence of what appeared to be the result of a loose mass was noticed in the free-vibration response of pile two during tests B and C, which were conducted during this same time period. The time-displacement data recorded during test B is presented in Figure 22. When compared with a typical free-vibration response curve (i.e. Figure 16 b), it is apparent that the transition from one displacement peak to the next in Figure 22 is not as smooth as it should be.

The displacements of the second and third positive or negative peaks are approximately the same; likewise with the fourth and fifth peaks.

A combination of the weather and the manner in which the LVDT at the center of the mass was supported is believed to have presented a problem for the tests conducted on December 16. The weather conditions on this particular day were anything but favorable for field testing as it rained, heavily at times, throughout much of the day.

The LVDT at the center of the mass was clamped to a section of a structural steel tube several feet in length. The tube was, in turn, clamped to tripod stands at each end, which were allowed to rest essentially on the ground surface. On the other hand, the LVDT at the bottom of the mass was supported by steel angles driven firmly into the ground. Thus, there was certainly some potential for a problem to occur with the measurement of displacements at the center of mass.

The aforementioned problem was noticed as an irregularity in the displacements of the pile mass at the end of some of the tests. Figures 23 through 30 show the final displacement of the pile mass (mass resting position) for all tests. Some general information regarding these figures is provided prior to a detailed discussion of the problem.

The final displacements illustrated in the figures are displacements relative to the base displacement, which was determined from test A. The series of tests represented in Figures 29 and 30 is an exception as the final displacement for test B was used as the base displacement. This displacement was used because both LVDT's were reset prior to the start of test B. The final displacements for test C are not presented because the data recorded during this test were inadequate.

As indicated in Figures 23 through 30, the pile mass did not return to its original position at the end of each test. However, this pattern is not particularly evident in Figures 27 and 28. The cause of these "permanent" displacements appeared to be two-fold. First, the soil on the back side of the pile expanded during the loading process; and second, there was not sufficient time between tests for the soil to rebound completely.

One general trend apparent in the figures, setting the obvious exceptions aside for now, is the progressively increasing final displacements in the direction of the applied load (positive y-direction). This trend coincided with a similar trend in the magnitude of the maximum static loads and deflections. As the maximum load was increased, generally with each test, the time required to reach this load also increased. As a result, the soil was allowed more time to expand.

Most important is the difference between the trends in final displacements at the center and bottom of the mass. For example, if the final displacement at the bottom of the mass increased from one test to the next, the displacement at the center should also have increased. However, this was not the case for, primarily, the last several tests conducted on December 16 (Figures 23 and 24) beginning with test O. It appears as though the center and bottom of the mass were moving in opposite directions, which is, of course, impossible. This illusion was most likely created by progressive movement of the center LVDT toward the mass, with the exception of test R. The loose surface soil conditions combined with the lack of a firm anchorage for the LVDT support apparently allowed the entire support to slide under its own weight.

6.5 PILE 1 TEST RESULTS

The results from this series of tests are summarized in Tables 7 and 8. The static stiffness values are presented in Table 7 while the dynamic stiffness values and damping ratios (expressed as a percent of critical) are presented in Table 8. No results were obtained for test B as the recorded data were inadequate. Results were, likewise, not obtained for tests C and I because the quick-release mechanism failed to release. Static stiffness values for tests J and K are not presented in Table 7 because the maximum loads were not obtained. During each of these tests, the rebound plate (Figure 6) was located too close to the structural tube, thus transferring much of the applied load directly to the reaction frame instead of the pile. Static stiffness values ranged from 125 kips/inch to 83.8 kips/inch for the tests in which the horizontal load was applied at the bottom of the mass. For the tests in which the load was applied at the center of the mass, the static stiffness values ranged from 55.6 kips/inch to 24.1 kips/inch. It should be noted that the maximum pile head deflections corresponding to the location of the applied load were used to calculate the static stiffness values.

The largest dynamic stiffness encountered was 62.8 kips/inch, which occurred at the smallest pile head deflection. The smallest dynamic stiffness, which occurred at the largest deflection, was 12.8 kips/inch.

Figure 31 shows a plot of the static and dynamic stiffness vs. initial (maximum) deflection for this series of tests. Since the dynamic stiffness is, inherently, the stiffness at the center of the mass, only those values from the tests in which the load was applied at this location are plotted.

Most apparent in the figure is the abrupt and continued separation between the static and dynamic stiffness, which begins at an initial deflection of approximately 0.22 inches (test O). This separation is somewhat exaggerated due to movement of the LVDT toward the mass, as explained in section 6.4. This movement caused an underestimation of the static deflection, which led to the calculation of inflated static stiffness values.

After accounting for these inflated values, a separation still exists between the static and dynamic stiffness. One factor that can result in a lower dynamic stiffness is the degradation of the soil stiffness due to repeated cycles of approximately equal displacement amplitudes. However, the displacement amplitudes of the pile during free-vibration progressively decreased.

One explanation for these artificially low dynamic stiffness values involves the adverse weather conditions and previous disturbance of the soil due to the pile driving process. As a reminder, both test piles were driven on July 7, 1994, less than five months prior to commencement of the testing program. It is certainly possible that this relatively short amount of time was not sufficient for the soil to regain all of its original strength. Each time the pile was displaced, rain water seeped between the pile and soil. This continued water seepage served to further weaken the already disturbed soil. The fact that the dynamic stiffness and not the static stiffness was affected by this phenomenon can also be explained. The magnitude of the initial deflection (Table 7) was generally much larger than the displacement amplitudes during free-vibration (Appendix D). The pile most likely passed through the weak zone of soil and into less affected (stronger) soil during the loading process.

Figure 32 shows a plot of the damping ratios (expressed as a percent of critical) vs. initial deflections at the bottom of the mass. In the case of an embedded pile, the soil generally accounts for the majority of the system damping. One explanation for the increase in damping with initial deflection is that the soil was involved in the system response to a greater extent at the larger deflections.

6.6 PILE 2 TEST RESULTS; 12-17-94 PILE TESTS

The results of these tests are summarized in Tables 9 and 10. The dynamic stiffness for test C was not determined due to inadequate data. Equipment problems precluded the determination of any results for test L. The static stiffness values ranged from 39.9 kips/inch to 32.9 kips/inch for the tests in which the load was applied at the center of the mass. For the tests with the load applied at the bottom, the static stiffness values were between 72.8

kips/inch and 49.7 kips/inch. Dynamic stiffness values ranging from 39.1 kips/inch to 30.6 kips/inch were obtained. The damping ratios varied only slightly as the highest was 7.2% and the lowest 5.3%.

It is apparent from the plot in Figure 33 that very little difference existed between the static and dynamic stiffness values determined from these tests. Figure 34 shows how the damping ratios varied with the initial deflections at the bottom of the mass. Again, a slight increase in damping with initial deflection is evident with the exception of the second data point, which represents the damping for test D. The cause of the abnormally high damping ratio for this test is not clear.

6.7 PILE 2 TEST RESULTS; 3-20-95 PILE TESTS

Two series of tests were conducted on this day. The first series was conducted with the horizontal load applied in the y-direction, which was the same direction as the original tests in December. At the conclusion of these tests, another series of tests was conducted with the load applied in a perpendicular direction (x-direction). The load was applied at the center of the mass for all tests conducted on this day. The results of both series of tests are presented in Tables 11 through 14. Results were not obtained for tests C and U as the length of the tests exceeded the time allotted to record the data.

The static and dynamic stiffnesses for the tests in which the load was applied in the y-direction are plotted against the initial deflection at the center of the mass in Figure 35. The dynamic stiffness values are only slightly higher for the first few tests. In Figure 36, the damping ratios are seen to remain almost perfectly constant throughout the range of initial deflections.

The results of the second series of tests are illustrated a little differently. As a reminder, the first several tests were conducted with progressively increasing initial deflections. Then, additional tests were conducted while decreasing the initial deflections in a similar manner. To avoid confusion, the static stiffness values and dynamic stiffness values are plotted separately with all tests represented. The lower set of values in Figures 37 and 38 are data from the additional tests. In a separate plot, the static and dynamic stiffness values are plotted together; however, only the first group of tests is represented.

Both the static stiffness and dynamic stiffness values did rebound to a large extent, although not completely, once the initial deflections (Figures 37 and 38) were decreased. The static and dynamic stiffness values are plotted together in Figure 39. It is clear that the dynamic stiffness is significantly lower than the static stiffness for the first group of tests, all of which were conducted at relatively small initial deflections. As with pile one, the "weak zone" theory can be used to explain this behavior. The displacement amplitudes as well as the initial deflections for all of the other tests were considerably larger than those for the tests in this group. As a result, the pile most likely passed through the weak zone and into a stiffer soil.

The damping ratios for all of the tests conducted with the load applied in the x-direction are plotted in Figure 40. The familiar trend is, once again, evident. In addition, it does not seem to matter whether the initial deflections are increasing or decreasing, as the damping ratios follow essentially the same path regardless.

The dynamic stiffness values from all three series of tests conducted on pile two are compared in Figure 41. Although the dynamic stiffnesses were very close together, the stiffness values for the tests conducted on March 20 with the load applied in the y-direction were generally higher than the others. This difference was probably the result of the soil having regained some of its strength during the time between the December and March pile tests.

6.8 RESULTS OF STIFFNESS MATCHING PROCEDURE WITH COMPUTER MODELS

Following the December 1994 field tests, piles one and two were modeled with the structural analysis program GTSTRUDL. The computer models, including the initial soil stiffness profiles, were developed according to the procedure outlined in chapter 5. Tests S through V conducted on December 16 are not represented herein because the deflections at the bottom of the mass were not sufficiently accurate. After the testing was completed, it was determined that these deflections had exceeded the working range of the LVDT.

The subgrade modulus amplification factors for each pile, as determined from Figure 13, are presented in Table 15. Once the design-level modulus gradients were amplified accordingly, the computer program was executed. The resulting deflection at the bottom of the mass was then compared with the corresponding measured deflection. This portion of the procedure is summarized in Tables 16 and 17 for piles one and two, respectively. As evident in the tables, the deflections were overpredicted to a large extent in all cases; however, those of pile two were predicted somewhat better. The fact that this procedure was used only to provide initial estimates of the soil stiffness should be emphasized.

The subgrade modulus gradients were then increased until the deflection from the computer model matched the measured deflection. The required increase in the modulus gradients over the initial estimates (stiffness correction factors), and the total increase over the design-level gradients for each test are presented in Tables 18 and 19. The total increase required was equal to the modulus amplification factor multiplied by the stiffness correction factor.

The initial deflections for pile two were divided into two categories, approximately 0.05" and 0.1". As apparent in Table 19, the values in column 4 are relatively consistent for each category with the exception of tests D and G. The value for test D is high because the bottom LVDT, in some way, moved toward the pile mass between tests C and D (Figure 25), which resulted in a measured deflection that was too low. This error, in turn, led to an overcorrection of the soil stiffness in the computer model. Movement of the LVDT does not seem to have been the reason for the low total correction value for test G. However, an error in the measurement or recording of the applied load would produce a similar result. Discarding these two values resulted in average total increase factors of 3.79 for a 0.05" deflection and 2.57 for a 0.1" deflection. With these values, one can construct average soil stiffness profiles for each of the corresponding initial deflection categories. The total stiffness increase values for pile one (Table 18) were considerably more scattered than those for pile two. As a result, the same procedure was not attempted.

The measured pile frequencies and those obtained from the computer models with the final soil stiffness profiles are compared in Tables 20 and 21. These frequencies for pile one did not compare well as the difference between them grew progressively larger with each test. This trend reflects the difference between the static and dynamic stiffnesses obtained from the field tests. The frequencies for pile two, on the other hand, compared very well in all cases.

6.9 TRANSFERRING OF DYNAMIC STIFFNESS TO GROUND SURFACE

The dynamic stiffnesses from all tests conducted on piles one and two were transferred to the ground surface using correction factors determined with the computer models. However, only those models corresponding to the tests in which the load was applied at the bottom of the mass were used for this purpose. The soil stiffness profiles, as determined with the computer models, corresponding to these tests were believed to be more representative of the true soil stiffness than those corresponding to the tests in which the load was applied at the center of mass. The load for each of the other tests was applied directly to the outside of the pull plates, which was essentially a single point. Due to the manner in which the mass was attached, however, the load was transferred to the pile at more than one point. The location of the point at which the load resultant acted on the pile, although close, most likely did not coincide with the location of the applied load. As a result of this uncertainty, the accuracy of the soil stiffness profiles determined from these tests was in question. In hindsight, this concern was probably unwarranted as small errors in the development of the stiffness profiles would have made little difference. This fact is clearly evident in Tables 16 through 19. In each case, the increase in the initial stiffness profile required to match the measured deflection (stiffness correction factor) was much greater than the difference between the measured and predicted deflections. For example, the difference between the measured and predicted deflections from test B (Table 17) was 31%; however, the increase in the initial stiffness profile required to match the measured deflection was 73% (Table 19). As a reminder, the predicted deflections were determined with the initial stiffness profiles.

In each model, the mass was transferred to the ground surface. The dynamic stiffness was then determined from equation 4.1 with the resulting lateral frequency. Correction factors for all tests considered, which are presented in Tables 22 and 23, were calculated as the ratio of the dynamic stiffness of the model to that of the actual soil-pile-mass system.

In the case of pile two, the correction factors were all very close (Table 23); therefore, the average value of 2.23 was used. The dynamic stiffness obtained at the center of mass from each test was multiplied by this value to obtain the stiffness at the ground surface. This correction factor was also used for the tests conducted in March since the same pile and essentially the same soil were involved.

A different approach was used with pile one because the correction factors were considerably more scattered (Table 22). Figuratively speaking, Table 22 was divided into three sections. Tests D and E were in one section, tests L, M, and N in another, and test R was in the remaining section. The average correction factors from these three sections were 2.55, 4.33, and 5.38, respectively. The average value from the first section was used to transfer the dynamic stiffness from tests D through H. Likewise, the average values from the second and third sections were used to transfer the stiffness from tests J through P, and Q through V, respectively. The corrected dynamic stiffness values for all of the tests are presented in Table 24.

CHAPTER 7

SUMMARY AND CONCLUSIONS

The Tennessee Department of Transportation (TNDOT) currently uses the computer program SEISAB to model bridges for seismic design. SEISAB determines the shears, moments, and axial forces in the bent columns and abutments due to simulated seismic loadings. After performing an analysis of a particular bridge, TNDOT considers the maximum of these resulting forces in the design of the individual components. When modeling a bridge with SEISAB, the user has the option to input spring coefficients, six at each bent column and abutment, which represent the foundation soil stiffness. Three springs govern translation in the longitudinal, transverse, and vertical directions, with respect to the bridge centerline. The longitudinal and transverse springs are referred to herein as lateral springs. Two additional springs govern rotation about longitudinal and transverse axes and are referred to as rotational springs. The remaining spring, referred to as a torsional spring, governs rotation about a vertical axis. If no spring coefficients are input, the bents and abutments are taken by SEISAB to be fixed against all translation and rotation. Under current modeling practices, TNDOT assumes the bent columns to be fixed while placing springs at the abutments.

As a result of the substantial amount of structural damage caused by the occurrence of recent earthquakes, particularly in the state of California, the importance of foundation soil stiffness, in general, has never been more evident. According to AASHTO, portions of West Tennessee are at a significant risk for future seismic activity. This fact, combined with the heightened sense of awareness concerning foundation soil stiffness, led TNDOT to question the appropriateness of its fixed bent support assumption when modeling bridges.

To investigate this matter further, TNDOT contracted with The University of Tennessee to carry out a research project. First, a sensitivity study was conducted with SEISAB to assess the effects of variations in foundation stiffness. Two bridges located in West Tennessee were the subjects of this study. These particular bridges were selected because of their simplistic design and the fact that they are founded on loess, which is prevalent in this part of the state. Both bridges were analyzed with fixed supports and with springs at each support, the magnitudes of which were varied in several combinations. The results of the study showed that, at least for the bridges considered, the dynamic response was sensitive to variations (albeit relatively large variations) in the lateral and, to a lesser extent, the rotational spring stiffnesses.

Having concluded that the fixed bent support assumption may be inadequate, the researchers addressed the next issue, which concerned the appropriate spring coefficients to use with SEISAB. A thorough review of the available literature failed to provide this information. As a result, a full-scale testing program was initiated to assess the dynamic stiffness of single piles embedded in loess. Based on the results of the sensitivity study, it was decided that the lateral stiffness would be the initial focus.

Two prestressed concrete piles were tested at a bridge construction site just outside of Memphis, Tennessee. Piles one and two, so designated, were driven to a depths of seventeen and fifteen feet, respectively. Both piles were fourteen inches square.

The chosen method of testing was the pluck test whereby the pile head was given an initial displacement(deflection), then released. The system damping and dynamic stiffness were determined from the free-vibration response of the pile. In order to reduce the response of the pile to that of a single-degree-of-freedom system, a large steel mass was attached to the pile head. The static stiffness, equal to the horizontal load just before release divided by the corresponding pile head deflection (initial deflection), was also determined and compared with the dynamic stiffness.

Piles one and two were tested on December 16 and 17, 1994, respectively. Each pile was subjected to several pluck tests with progressively increasing initial deflections. Pile two was subjected to two additional series of tests on March, 20, 1995. The first series of tests was conducted with the horizontal load applied in the same direction as the original tests. For the second series, however, the load was applied perpendicular to the original direction. During this series of tests, the initial deflections were progressively decreased once the maximum initial deflection was reached. These tests were conducted to assess the rebound characteristics of the soil.

The dynamic stiffness of pile one ranged from 63 kips/inch at the lowest initial deflection to 13 kips/inch at the highest. From the tests conducted on December 17, the dynamic stiffness of pile two ranged from 39 kips/inch to 31 kips/inch. Part of the reason that the stiffness of pile one decreased more than the stiffness of pile two was that higher initial deflections were experienced by pile one. However, the weather was also believed to have been a factor as it rained throughout much of the day on the 16th. The soil surrounding the pile continued to weaken as it became more saturated. The dynamic stiffness of pile two from the first series of tests conducted on March 20 was, in general, slightly higher than the stiffness from the original tests. This difference was attributed to the time that elapsed between the two series of tests. The soil was still wet during the December 17 tests from the rain experienced the previous day, but was allowed to dry and regain some of its strength afterward. The dynamic stiffnesses determined from the second series of tests on pile two were consistent with those determined from the two previous series. However, lower initial deflections were induced during the first few tests in this series, and the stiffnesses were higher at these initial deflections.

In general, the static stiffnesses compared well with the dynamic stiffnesses, which was expected. Exceptions were the last several tests conducted on December 16 and the first group of tests from the second series conducted on March 20. In those cases, the static stiffness was higher. Weakened soil due to excess moisture is believed to have been a contributing factor in this difference for all of the tests. Movement of the deflection measuring device also played a role in the difference in stiffnesses from the December 17 tests. This movement resulted in the calculation of artificially high static stiffnesses.

The damping ratios for pile one ranged from approximately 9% to 13% while those for pile two ranged from 5% to 7%. Very little change in damping ratio throughout the testing was observed for either pile. During the tests that were conducted to assess the rebound characteristics of the soil, the dynamic stiffness did increase considerably, although not to the original values. This behavior indicates a certain amount of permanent deformation in the soil. Several tests were also conducted at the same initial deflection to assess the repeatability of results. No change in stiffness was observed throughout the course of these tests.

A subsurface investigation of the test site was conducted between December 1994 and March 1995. Standard penetration tests were performed and soil samples obtained as part of this investigation. Loess was observed to a depth of approximately 8.5 feet in the vicinity of each test pile. Beneath the loess were layers of sand and clay. The unconfined compressive strengths, q_u, of the loess were estimated from hand penetrometer tests conducted with the soil samples. The results of these tests indicated that the soil surrounding pile one was stiffer than the soil surrounding pile two. The fact that the dynamic stiffness of pile one was greater than the dynamic stiffness of pile two, at least in the beginning, is consistent with this finding.

Computer models of each test pile were developed so that the lateral stiffness of other embedded piles could be predicted. The stiffness of the surrounding soil was represented by springs along the length of the pile. The stiffness of these springs was varied until the pile head deflection in the model matched the measured deflection. The models could have been used to match the pile frequencies, and thus the dynamic stiffnesses, instead of the static deflections just as effectively. The models were also used to "transfer" the dynamic stiffness of the test piles from the center of the mass to the ground surface.

LIST OF REFERENCES

LIST OF REFERENCES

1 Guide Specifications for Seismic Design of Highway Bridges. 1994. American Association of State Highway and Transportation Officials.

2 Cook, Tommy Lynn. 1994. "Modeling of Soil-Pile Interaction for Bridge Foundations Under Seismic Loading," Thesis Submitted in partial Fulfillment of the Requirements for the Degree of Master of Science. University of Tennessee, Knoxville, Tennessee.

3 Cook, Tommy L., Burdette, Edwin G., Graves, Richard L., Goodpasture, David W., and Deatherage, J. Harold. 1995. "Effect of Varying Foundation Stiffness on Seismically Induced Loads in Bridge Bents: a Sensitivity Study," Transportation Research Board, Paper No. 950919.

4 Reznik, Yakov M. 1993. "Plate Load Tests of Collapsible Soils," Journal of Geotechnical Engineering. ASCE, Vol 119. No. 3, pp 608-615.

5 Gle, Dennis Ray. 1981. "The Dynamic Lateral Response of Deep Foundations," Dissertation Submitted in Partial Fulfillment of the Requirements for the Degree of Doctor of Philosophy. University of Michigan, Ann Arbor, Michigan.

6 Gle, Dennis Ray, and Woods, Richard D. 1984. "Suggested Procedure for Conducting Dynamic Lateral Load Tests on Piles," Laterally Loaded Deep Foundations: Analysis and Performance. ASTM Special Technical Paper No. 835, pp 157-171.

7 Blaney, Geoffrey W., and O'Neill, Michael W. 1991. "Procedures for Prediction of Dynamic Lateral Pile Group Response in Clay from Single Pile Tests," Geotechnical Testing Journal. ASTM, Vol 14, March, pp 3-12.

8 Bowles, Joseph, E. 1988. Foundation Analysis and Design. McGraw-Hill.

9 McAlister, David H., 1994. "Development of Dynamic Test for Analyzing Free-Vibrations of Bridge Piers," Thesis Submitted in Partial Fulfillment of the Requirements for the Degree of Master of Science. University of Tennessee, Knoxville, Tennessee.

10 Penzien, Joseph, and Clough, Ray W. !975. Dynamics of Structures. McGraw-Hill.

11 Norris, G. M., and Sack, Robert L. 1986. "Evaluation of Lateral Stiffness of Pile Groups for Seismic Analysis of Highway Bridges," Proceedings of the 22nd Symposium on Engineering Geology and Soils Engineering. February 24-26, 1986, Boise, Idaho.

12 Terzaghi, K. 1955. "Evaluation of Coefficients of Subgrade Reaction," Geotechnique. Vol. 5, No. 4, pp 297-326.

13 Davisson, M. T. 1970. "Lateral Load Capacity of Piles," Highway Research Record. No. 333, pp 104-112.

APPENDIXES

APPENDIX A

TABLES

Table 1 Soil profile data for pile 1.

SAMPLE DEPTH (FT)	COLOR & DESCRIPTION	CONSISTENCY (CLAY)	DENSITY (SAND)	UNIFIED CLASS.
1.0-2.5	brown mottled clayey silt	stiff	-----	ML
3.0-5.0	same	stiff	-----	ML
6.0-7.0	same	moderate	-----	ML
8.5-10.0	brown mottled clayey sand	-----	medium dense to loose	SC
13.5-15.0	gray clayey silt with sand	-----	medium dense to loose	SM-u
18.5-20.0	reddish brown clayey sand and gravel	-----	dense to medium dense	SP
23.5-25.0	brown - orange sand	-----	very dense	SP
28.5-30.0	brown sand	-----	very dense	SP

Table 2 Soil profile data for pile 2.

SAMPLE DEPTH (FT)	COLOR & DESCRIPTION	CONSISTENCY (CLAY)	DENSITY (SAND)	UNIFIED CLASS.
1.0-2.5	brown clayey silt	stiff	-----	ML
3.0-5.0	same	stiff	-----	ML
6.0-7.0	light gray clayey silt	moderate	-----	ML
8.5-10.0	light gray mottled clay	soft	-----	CL
13.5-15.0	brown sand	-----	medium dense	SP
18.5-20.0	coarse sand and gravel	-----	dense	GP
23.5-25.0	brown sand	-----	very dense	SP
28.5-30.0	mottled sand	-----	very dense	SP

Table 3 Soil properties near pile 1.

DEPTH (FEET)	FIELD BLOW COUNT	CORRECTED BLOW COUNT	COMPRESSIVE STRENGTH (KSF)	SOIL DENSITY (PCF)	DAMPING RATIO (%)	SHEAR MODULUS (PSI)	SHEAR WAVE VELOCITY (FT/SEC)
1.3	11	30	7.0	118	4.37	6284	496
3.8	14	29	5.5	118	4.11	8815	588
6.0	8	14	3.0	115	3.87	8670	592
8.5	10	16	-----	113	4.47	9877	635
12.5	10	13	-----	112	3.90	11902	700
17.5	24	27	-----	118	5.59	14609	756
22.5	55	55	-----	119	3.18	16253	797
27.5	61	55	-----	119	2.81	17832	835

Table 4 Soil properties near pile 2.

DEPTH (FEET)	FIELD BLOW COUNT	CORRECTED BLOW COUNT	COMPRESSIVE STRENGTH (KSF)	SOIL DENSITY (PCF)	DAMPING RATIO (%)	SHEAR MODULUS (PSI)	SHEAR WAVE VELOCITY (FT/SEC)
1.3	18	50	5.50	118	4.37	6284	496
3.8	10	21	5.26	116	4.09	8049	566
6.0	7	13	2.20	114	3.86	8240	579
8.5	3	5	1.18	102	6.21	4204	436
12.5	20	27	-----	116	4.01	12281	700
17.5	35	40	-----	121	5.84	15503	771
22.5	59	59	-----	119	3.19	16228	796
27.5	54	49	-----	119	2.81	17810	834

Table 5 Design-level subgrade modulus gradients for piles one and two.

DEPTH (FEET)	DESIGN-LEVEL MODULUS GRADIENT (KCF/FT)	
	PILE 1	PILE 2
0 TO 2.8	85.0	65.0
2.8 TO 5.5	65.0	64.0
5.5 TO 7.8	36.0	27.5
7.8 TO 11.8	36.0	16.0
11.8 TO 17	36.0	72.5

Table 6 Point of load application for December, 1994 pile tests.

TEST	PILE 1	PILE 2
A	----------	----------
B	----------	CENTER OF MASS
C	----------	CENTER OF MASS
D	BOTTOM OF MASS	BOTTOM OF MASS
E	BOTTOM OF MASS	BOTTOM OF MASS
F	CENTER OF MASS	BOTTOM OF MASS
G	CENTER OF MASS	CENTER OF MASS
H	CENTER OF MASS	CENTER OF MASS
I	----------	CENTER OF MASS
J	BOTTOM OF MASS	CENTER OF MASS
K	BOTTOM OF MASS	CENTER OF MASS
L	BOTTOM OF MASS	----------
M	BOTTOM OF MASS	BOTTOM OF MASS
N	BOTTOM OF MASS	BOTTOM OF MASS
O	CENTER OF MASS	BOTTOM OF MASS
P	CENTER OF MASS	BOTTOM OF MASS
Q	CENTER OF MASS	BOTTOM OF MASS
R	BOTTOM OF MASS	BOTTOM OF MASS
S	CENTER OF MASS	BOTTOM OF MASS
T	CENTER OF MASS	BOTTOM OF MASS
U	CENTER OF MASS	BOTTOM OF MASS
V	CENTER OF MASS	BOTTOM OF MASS

Table 7 Static stiffness of pile 1.

TEST	LOAD (KIPS)	PILE HEAD DEFLECTION (INCHES)		STATIC STIFFNESS (KIPS/INCH)
		C.G.M.	BOTTOM	
A	-----	-----	-----	-----
B	-----	-----	-----	-----
C	-----	-----	-----	-----
D	4.49	0.0528	0.0419	107.0
E	5.41	0.0547	0.0432	125.0
F	3.91	0.0702	0.0421	55.6
G	7.78	0.2081	0.0961	37.5
H	9.08	0.2213	0.1134	41.1
I	-----	-----	-----	-----
J	-----	0.1459	0.1167	-----
K	-----	0.1259	0.1010	-----
L	10.2	0.1274	0.1039	98.2
M	13.2	0.1670	0.1348	97.9
N	12.7	0.1618	0.1342	94.6
O	10.8	0.2206	0.1373	49.0
P	9.66	0.2870	0.1326	33.5
Q	14.9	0.4064	0.2138	36.9
R	17.2	0.2576	0.2053	83.8
S	19.5	0.6092	0.2860	32.0
T	21.7	0.8076	0.2470	26.9
U	19.8	0.7885	0.2487	25.1
V	20.6	0.8533	0.1882	24.1

NOTE:

Static stiffness corresponds to pile head deflection @ location of applied load.

Table 8 Damping and dynamic stiffness of pile 1.

TEST	DAMPED FREQUENCY (CYC./SEC.)	DAMPING RATIO (%)	UNDAMPED FREQUENCY (CYC./SEC.)	UNDAMPED FREQUENCY (RAD./SEC.)	DYNAMIC STIFFNESS (KIPS/INCH)
A	---------	---------	---------	---------	---------
B	---------	---------	---------	---------	---------
C	---------	---------	---------	---------	---------
D	7.80	9.30	7.83	49.20	62.8
E	7.40	8.66	7.44	46.72	56.6
F	7.13	9.35	7.16	45.00	52.5
G	6.50	11.99	6.55	41.16	43.9
H	6.13	11.73	6.17	38.79	39.0
I	---------	---------	---------	---------	---------
J	5.66	12.90	5.71	35.89	33.4
K	5.71	13.10	5.76	36.16	33.9
L	5.60	11.74	5.64	35.44	32.6
M	5.17	13.48	5.22	32.77	27.8
N	4.92	12.35	4.96	31.15	25.2
O	4.94	12.50	4.98	31.27	25.4
P	4.92	12.10	4.95	31.12	25.1
Q	4.31	13.30	4.35	27.32	19.4
R	4.32	13.46	4.36	27.39	19.5
S	3.98	13.60	4.02	25.24	16.5
T	3.72	12.87	3.75	23.55	14.4
U	3.90	12.32	3.82	24.03	15.0
V	3.51	11.46	3.53	22.17	12.8

Table 9 Static stiffness of pile 2 for tests conducted on December 17, 1994.

TEST	LOAD (KIPS)	PILE HEAD DEFLECTION (INCHES)		STATIC STIFFNESS (KIPS/INCH)
		C.G.M.	BOTTOM	
A	--------	--------	--------	--------
B	2.17	0.0553	0.0434	39.2
C	2.56	0.0647	0.0518	39.6
D	2.75	0.0485	0.0378	72.8
E	3.33	0.0606	0.0523	63.7
F	3.67	0.0684	0.0562	65.3
G	2.66	0.0761	0.0581	35.0
H	2.90	0.0789	0.0580	36.8
I	2.61	0.0683	0.0535	38.1
J	4.39	0.1306	0.1009	33.7
K	4.49	0.1369	0.1058	32.9
L	--------	--------	--------	--------
M	5.60	0.1281	0.1058	52.8
N	5.31	0.1259	0.1046	50.6
O	5.07	0.1219	0.1017	49.7
P	4.93	0.1141	0.0956	51.6
Q	5.36	0.1263	0.1050	51.0
R	5.36	0.1255	0.1052	51.0

<u>NOTE:</u>

Static stiffness corresponds to pile head @ location of applied load deflection.

Table 10 Damping and dynamic stiffness of pile 2 for tests conducted on December 17, 1994.

TEST	DAMPED FREQUENCY (CYC./SEC.)	DAMPING RATIO (%)	UNDAMPED FREQUENCY		DYNAMIC STIFFNESS (KIPS/INCH)
			(CYC./SEC.)	(RAD./SEC.)	
A	--------	--------	--------	--------	--------
B	6.17	5.07	6.18	38.84	39.1
C	--------	--------	--------	--------	--------
D	6.08	7.24	6.10	38.29	38.0
E	6.15	5.29	6.16	38.72	38.9
F	6.26	5.67	6.17	38.75	38.9
G	6.08	5.77	6.09	38.24	37.9
H	6.08	5.71	6.09	38.28	38.0
I	6.06	5.74	6.07	38.14	37.7
J	5.85	6.25	5.87	36.86	35.2
K	5.71	6.95	5.72	35.95	33.5
L	--------	--------	--------	--------	--------
M	5.70	6.63	5.71	35.90	33.4
N	5.61	6.94	5.62	35.33	32.4
O	5.61	6.81	5.62	35.34	32.4
P	5.55	6.44	5.56	34.94	31.7
Q	5.49	6.76	5.51	34.60	31.0
R	5.46	6.66	5.47	34.36	30.6

Table 11 Static stiffness of pile 2 for tests conducted on March 20, 1995 with the load applied in the y-direction.

TEST	LOAD (KIPS)	PILE HEAD DEFLECTION (INCHES)		STATIC STIFFNESS (KIPS/INCH)
		C.G.M.	BOTTOM	
A	--------	--------	--------	--------
B	2.29	0.0626	0.0479	36.6
C	2.46	0.0608	0.0460	40.5
D	2.36	0.0609	0.0473	38.8
E	4.56	0.1231	0.0969	37.0
F	4.48	0.1231	0.0965	36.4
G	4.41	0.1214	0.0962	36.3

NOTE:

(1) Load applied at center of mass for all tests.

(2) Pile head deflection @ center of mass was used to calculate static stiffness.

Table 12 Damping and dynamic stiffness of pile 2 for tests conducted on March 20, 1995 with the load applied in the y-direction.

TEST	DAMPED FREQUENCY (CYC./SEC.)	DAMPING RATIO (%)	UNDAMPED FREQUENCY		DYNAMIC STIFFNESS (KIPS/INCH)
			(CYC./SEC.)	(RAD./SEC.)	
A	--------	--------	--------	--------	--------
B	6.36	6.53	6.37	40.04	41.6
C	6.35	6.97	6.36	39.98	44.1
D	6.30	6.99	6.31	39.66	40.8
E	6.00	6.94	6.01	37.77	37.0
F	5.88	7.02	5.90	37.05	35.6
G	5.83	6.89	5.85	36.75	35.0

Table 13 Static stiffness of pile 2 for tests conducted on March 20, 1995 with the load applied in the x-direction.

TEST	LOAD (KIPS)	PILE HEAD DEFLECTION (INCHES)		STATIC STIFFNESS (KIPS/INCH)
		C.G.M.	BOTTOM	
A	--------	--------	--------	--------
B	1.95	0.0346	0.0248	56.4
C	--------	--------	--------	--------
D	1.73	0.0348	0.0245	49.8
E	1.57	0.0332	0.0234	47.3
F	1.69	0.0328	0.0234	51.5
G	2.46	0.0676	0.0485	36.4
H	2.27	0.0649	0.0470	35.0
I	2.47	0.0688	0.0497	35.9
J	3.38	0.0985	0.0714	34.3
K	3.29	0.0974	0.0711	33.8
L	3.24	0.0971	0.0713	33.4
M	3.23	0.0964	0.0704	33.5
N	4.43	0.1307	0.0962	33.9
P	4.31	0.1287	0.0945	33.5
Q	4.18	0.1269	0.0936	32.9
R	2.96	0.0924	0.0684	32.0
S	1.96	0.0591	0.0436	33.2
T	1.15	0.0262	0.0190	43.9
U	--------	--------	--------	--------
V	4.22	0.1270	0.0935	33.2

NOTE:

(1) Load applied at center of mass for all tests.

(2) Pile head deflection @ center of mass was used to calculate static stiffness.

Table 14 Damping and dynamic stiffness of pile 2 for tests conducted on March 20, 1995 with the load applied in the x-direction.

TEST	DAMPED FREQUENCY (CYC./SEC.)	DAMPING RATIO (%)	UNDAMPED FREQUENCY (CYC./SEC.)	UNDAMPED FREQUENCY (RAD./SEC.)	DYNAMIC STIFFNESS (KIPS/INCH)
A	--------	--------	--------	--------	--------
B	6.60	5.36	6.61	41.53	44.7
C	--------	--------	--------	--------	--------
D	6.52	6.38	6.53	41.02	43.6
E	6.42	6.02	6.43	40.42	42.4
F	6.46	5.93	6.47	40.67	42.9
G	6.23	6.57	6.24	39.21	39.9
H	6.17	6.41	6.18	38.82	39.1
I	6.11	6.45	6.13	38.49	38.4
J	5.97	6.85	5.98	37.58	36.6
K	5.94	6.75	5.95	37.40	36.3
L	5.89	7.16	5.90	37.10	35.7
M	5.86	6.87	5.88	36.92	35.3
N	5.78	7.49	5.80	36.42	34.4
P	5.75	7.26	5.77	36.25	34.1
Q	5.71	7.22	5.72	35.96	33.5
R	5.77	7.22	5.78	36.33	34.2
S	5.84	6.49	5.86	36.80	35.1
T	6.07	6.16	6.08	38.21	37.9
U	--------	--------	--------	--------	--------
V	5.74	7.21	5.76	36.16	33.9

Table 15 Subgrade modulus amplification factors for models of test piles.

TEST	SUBGRADE MODULUS AMPLIFICATION FACTOR	
	PILE 1	PILE 2
A	-------	-------
B	-------	2.20
C	-------	-------
D	2.20	2.30
E	2.20	1.90
F	2.20	1.80
G	1.40	1.85
H	1.20	1.80
I	-------	1.90
J	-------	1.30
K	-------	1.30
L	1.30	-------
M	1.00	1.20
N	1.00	1.20
O	1.00	1.25
P	1.00	1.30
Q	1.00	1.20
R	1.00	1.20
S	-------	-------
T	-------	-------
U	-------	-------
V	-------	-------

Table 16 Comparison of measured deflections at bottom of pile mass and deflections predicted by computer model - pile 1.

TEST	DEFLECTION (INCHES)		DIFFERENCE (%)
	MEASURED	PREDICTED	
D	0.0419	0.0759	81
E	0.0432	0.0914	112
F	0.0421	0.0834	98
G	0.0961	0.2123	121
H	0.1134	0.2702	138
L	0.1039	0.2348	126
M	0.1348	0.3566	165
N	0.1342	0.3431	156
O	0.1373	0.3564	160
P	0.1326	0.3188	140
Q	0.2138	0.4917	130
R	0.2053	0.4647	126

Table 17 Comparison of measured deflections at bottom of pile mass and deflections predicted by computer model - pile 2.

TEST	DEFLECTION (INCHES)		DIFFERENCE (%)
	MEASURED	PREDICTED	
B	0.0434	0.0567	31
D	0.0378	0.0562	49
E	0.0523	0.0756	45
F	0.0562	0.0858	53
G	0.0581	0.0760	31
H	0.0580	0.0840	45
I	0.0535	0.0735	37
J	0.1009	0.1512	50
K	0.1058	0.1546	46
M	0.1058	0.1655	56
N	0.1046	0.1569	50
O	0.1017	0.1462	44
P	0.0956	0.1390	45
Q	0.1050	0.1584	51
R	0.1052	0.1584	51

Table 18 Stiffness correction factors and total increase in subgrade modulus gradient over design-level gradient - pile 1.

TEST	INITIAL DEFL. @ BOTTOM OF MASS (INCHES)	STIFFNESS CORRECTION FACTOR	TOTAL INCREASE IN MODULUS GRADIENT
D	0.0419	2.83	6.23
E	0.0432	3.73	8.21
F	0.0421	3.70	8.14
G	0.0961	4.45	6.23
H	0.1134	5.10	6.12
L	0.1039	4.10	5.33
M	0.1348	5.30	5.30
N	0.1342	5.00	5.00
O	0.1373	5.88	5.88
P	0.1326	5.05	5.05
Q	0.2138	4.65	4.65
R	0.2053	4.05	4.05

Table 19 Stiffness correction factors and total increase in subgrade modulus gradient over design-level gradient - pile 2.

TEST	INITIAL DEFL. @ BOTTOM OF MASS (INCHES)	STIFFNESS CORRECTION FACTOR	TOTAL INCREASE IN MODULUS GRADIENT
B	0.0434	1.73	3.81
D	0.0378	2.12	4.88
E	0.0523	1.99	3.78
F	0.0562	2.20	3.96
G	0.0581	1.71	3.16
H	0.0580	2.11	3.80
I	0.0535	1.90	3.61
J	0.1009	2.20	2.86
K	0.1058	2.10	2.73
M	0.1058	2.20	2.64
N	0.1046	2.05	2.46
O	0.1017	1.90	2.38
P	0.0956	1.95	2.54
Q	0.1050	2.06	2.47
R	0.1052	2.06	2.47

Table 20 Comparison of measured pile frequencies and frequencies from computer model - pile 1.

TEST	FREQUENCY (HERTZ)		DIFFERENCE (%)
	MEASURED	GTSTRUDL	
D	7.83	7.43	5.11
E	7.44	7.91	6.32
F	7.16	7.90	10.3
G	6.55	7.43	13.4
H	6.17	7.40	19.9
L	5.64	7.17	27.1
M	5.22	7.16	37.2
N	4.96	7.06	42.3
O	4.98	7.33	47.2
P	4.95	7.08	43.0
Q	4.35	6.94	59.5
R	4.36	6.72	54.1

Table 21 Comparison of measured pile frequencies and frequencies from computer model - pile 2.

TEST	FREQUENCY (HERTZ)		DIFFERENCE (%)
	MEASURED	GTSTRUDL	
B	6.18	5.95	3.72
D	6.10	6.28	2.95
E	6.16	5.95	3.4
F	6.17	6.01	2.6
G	6.09	5.72	6.1
H	6.09	5.95	2.3
I	6.07	5.89	3.0
J	5.87	5.59	4.8
K	5.72	5.53	3.3
M	5.71	5.49	3.9
N	5.62	5.40	3.9
O	5.62	5.36	4.6
P	5.56	5.44	2.2
Q	5.51	5.41	1.8
R	5.47	5.41	1.1

Table 22 Correction factors for transferring dynamic stiffness from center of mass to ground surface - pile 1.

TEST	COMPUTER MODEL		DYNAMIC STIFFNESS @ C.G.M. (KIPS/INCH)	CORRECTION FACTOR
	LATERAL FREQUENCY (HERTZ)	DYNAMIC STIFFNESS (KIPS/INCH)		
D	11.60	138	62.8	2.20
E	12.66	164	56.6	2.90
L	11.04	125	32.6	3.83
M	11.02	124	27.8	4.46
N	10.82	120	25.6	4.69
R	10.12	105	19.5	5.38

Table 23 Correction factors for transferring dynamic stiffness from center of mass to ground surface - pile 2.

TEST	COMPUTER MODEL LATERAL FREQUENCY (HERTZ)	COMPUTER MODEL DYNAMIC STIFFNESS (KIPS/INCH)	DYNAMIC STIFFNESS @ C.G.M. (KIPS/INCH)	CORRECTION FACTOR
D	10.02	103.0	38.0	2.71
E	9.27	88.0	38.9	2.26
F	9.41	90.6	38.9	2.33
M	8.30	70.5	33.4	2.11
N	8.12	67.4	32.4	2.08
O	8.03	65.9	32.4	2.03
P	8.19	68.7	31.7	2.17
Q	8.13	67.6	31.0	2.18
R	8.13	67.6	30.6	2.21

Table 24 Dynamic stiffness (kips/inch) of piles 1 and 2 at the ground surface.

TEST	PILE 1	PILE 2		
		12/17/94 TESTS	3/20/95 TESTS	
			Y PULL	X PULL
A	-----	-----	-----	-----
B	-----	87.2	92.8	99.7
C	-----	-----	98.3	-----
D	160	84.7	91.0	97.2
E	144	86.7	82.5	94.6
F	134	86.7	79.4	95.7
G	112	84.5	78.1	89.0
H	100	84.7	-----	87.2
I	-----	84.1	-----	85.6
J	145	78.5	-----	81.6
K	147	74.7	-----	80.9
L	141	-----	-----	79.6
M	121	74.5	-----	78.7
N	109	72.3	-----	76.7
O	110	72.3	-----	-----
P	109	70.7	-----	76.0
Q	104	69.1	-----	74.7
R	105	68.2	-----	76.3
S	88.9	-----	-----	78.3
T	77.4	-----	-----	84.5
U	80.5	-----	-----	-----
V	68.6	-----	-----	75.6

APPENDIX B

FIGURES

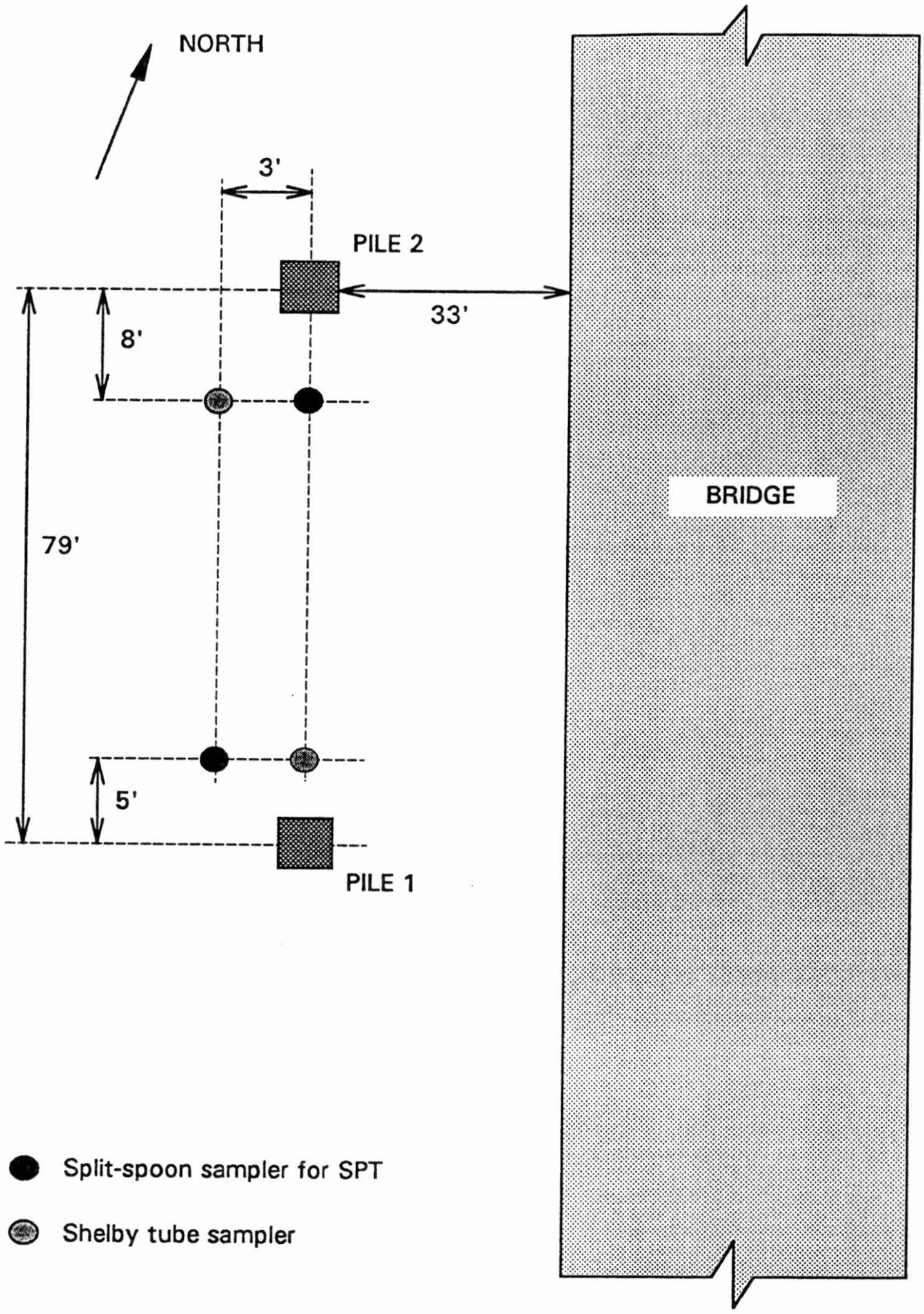

Figure 1 Location of boreholes from subsurface investigation with respect to test piles.

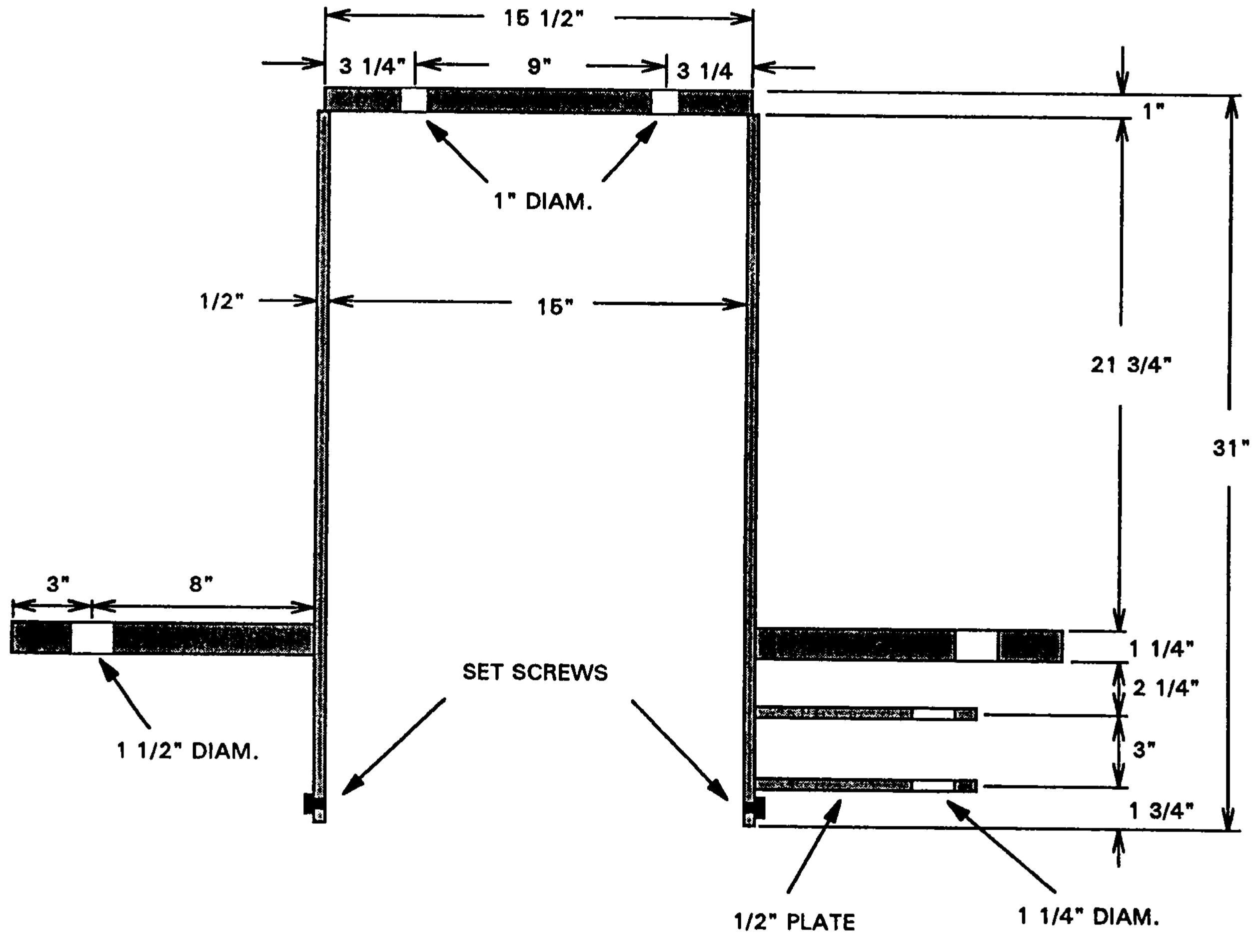

Figure 2   Cross-section view of pile mass holder.

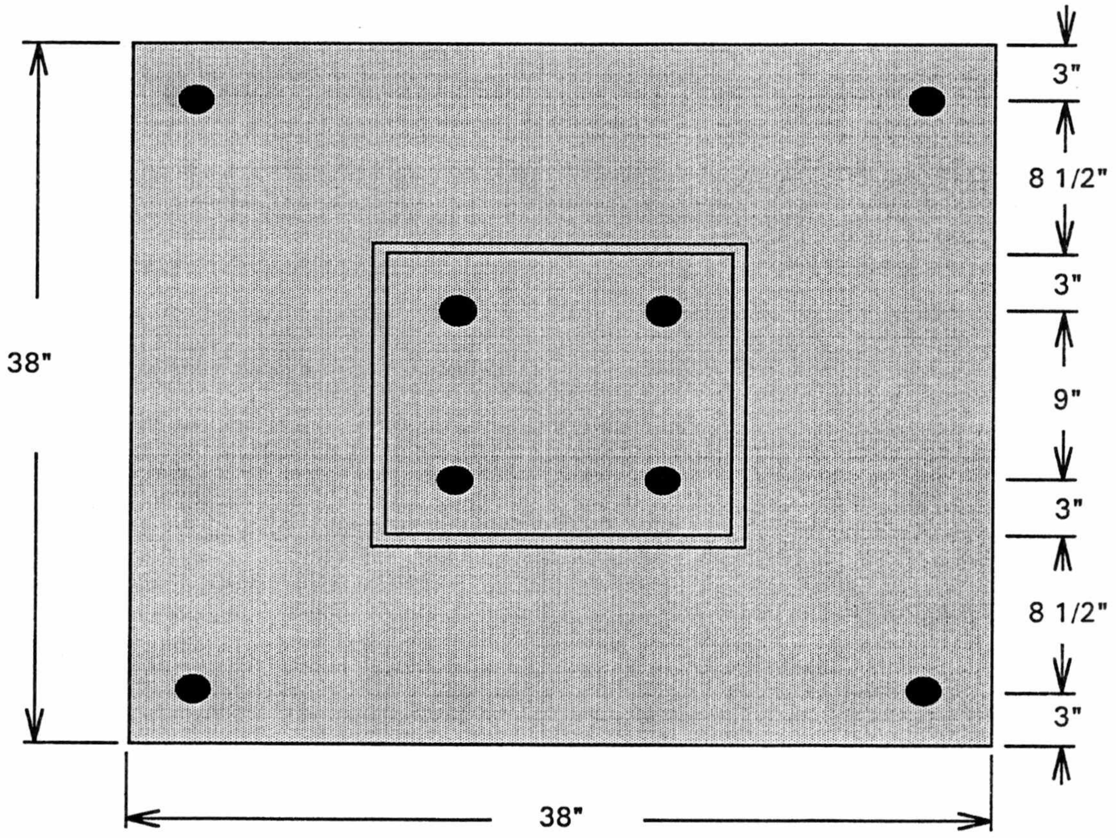

Figure 3 Top view of mass holder.

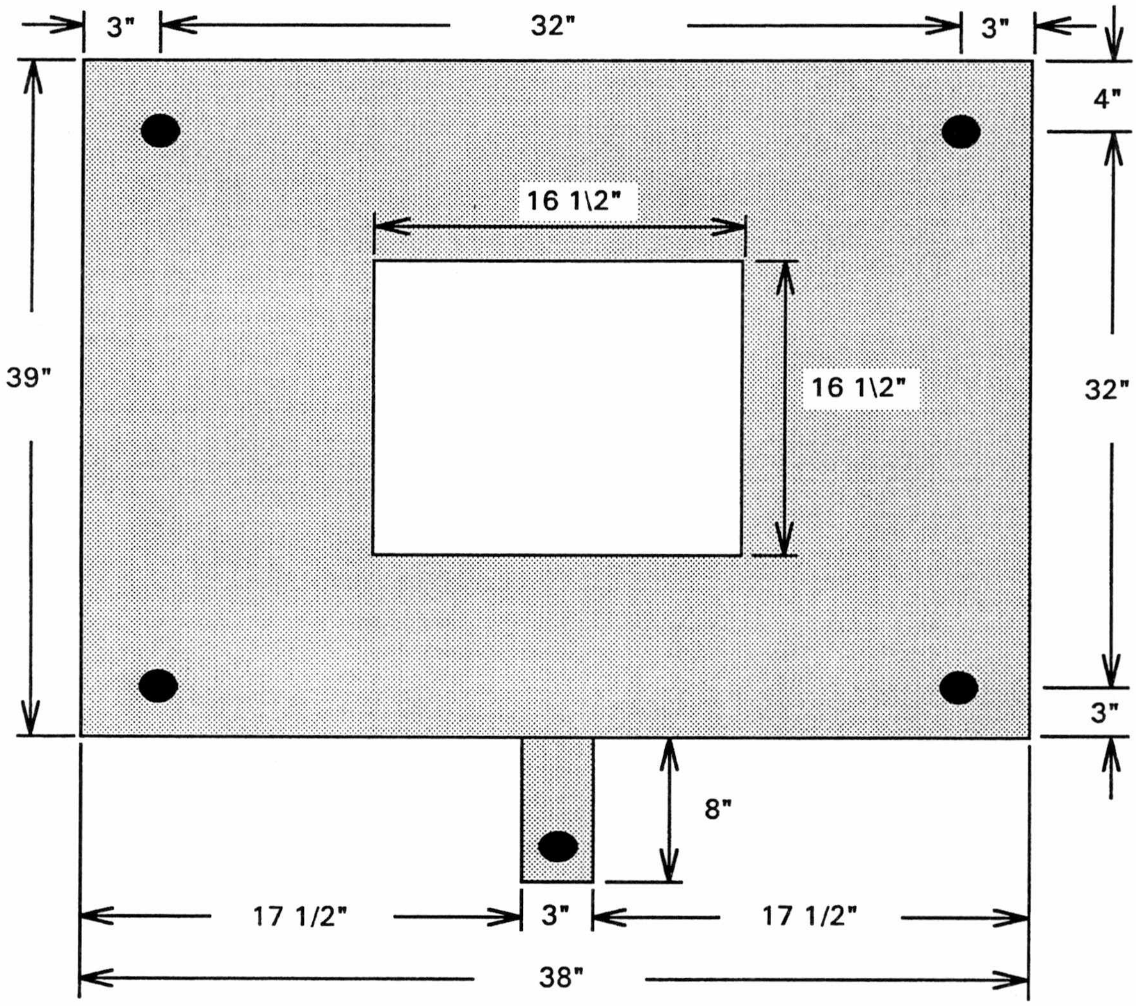

Figure 4 Pile mass pull plate.

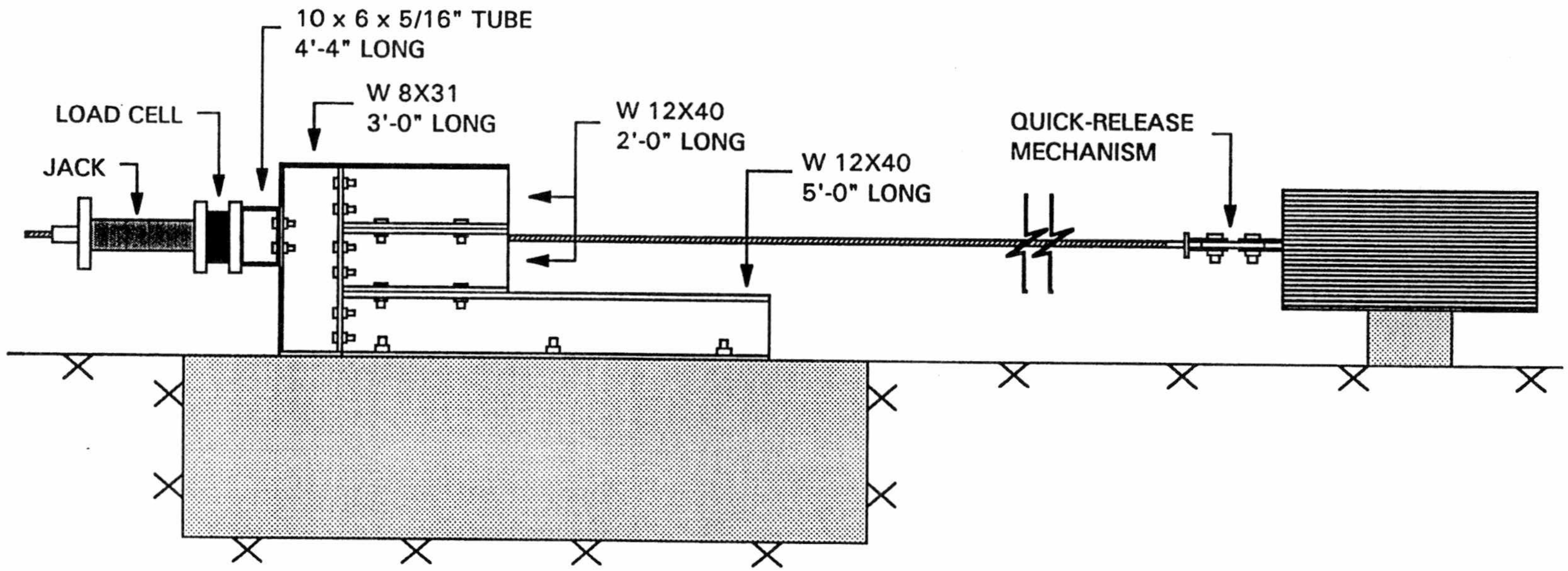

Figure 5 Load reaction frame and pile test set-up.

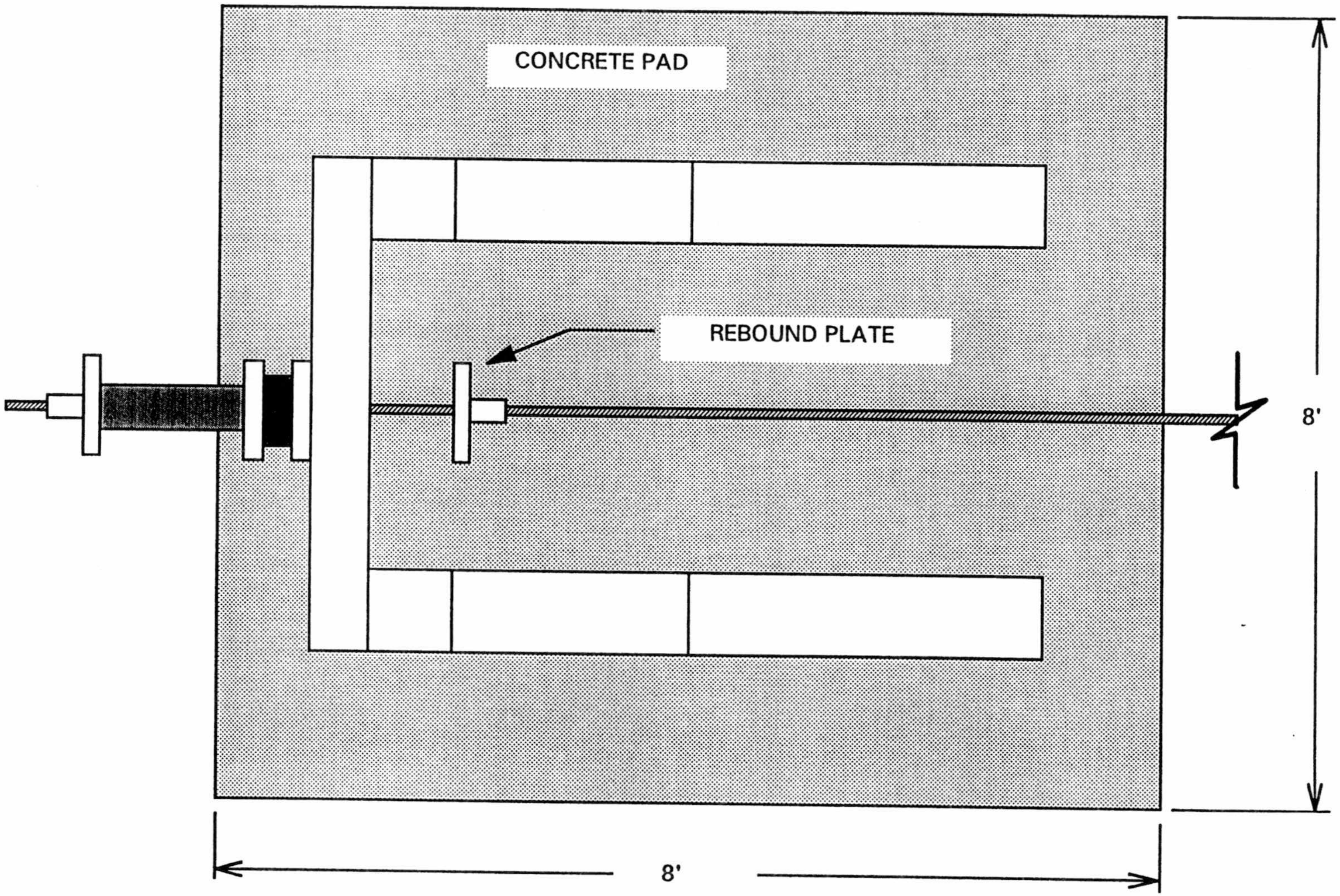

Figure 6 Top view of load reaction frame.

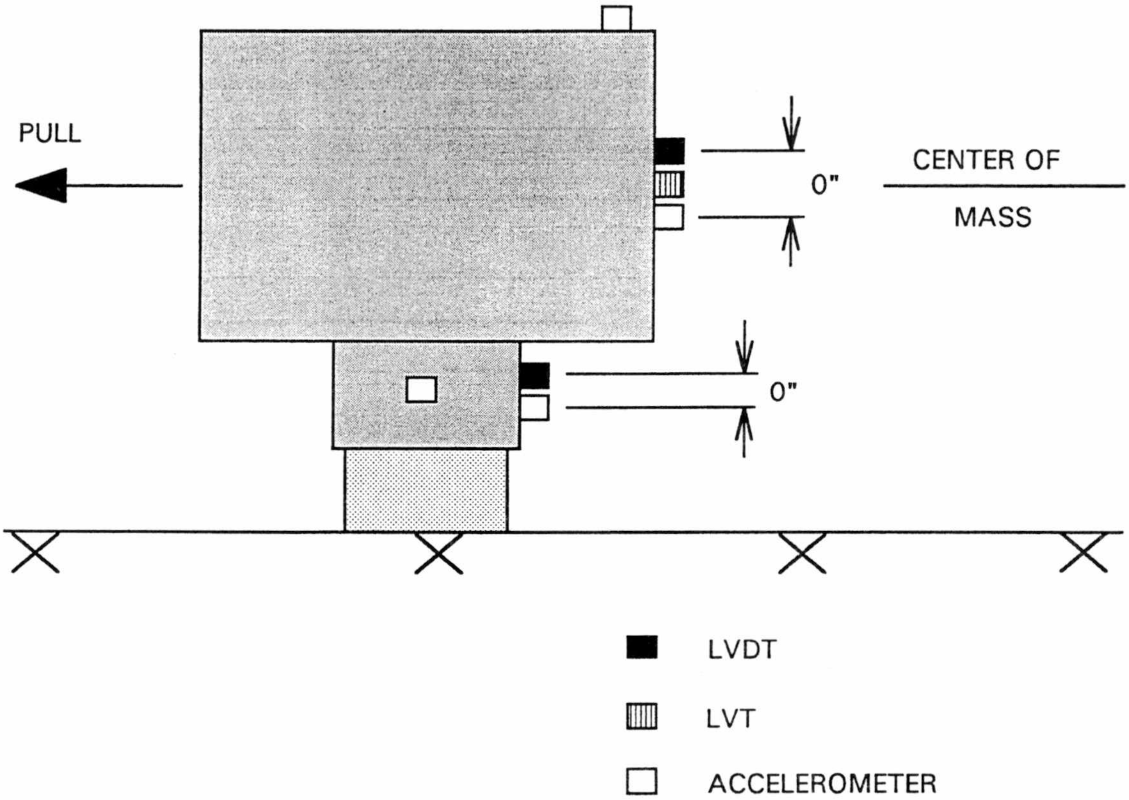

Figure 7 Location of motion sensing devices.

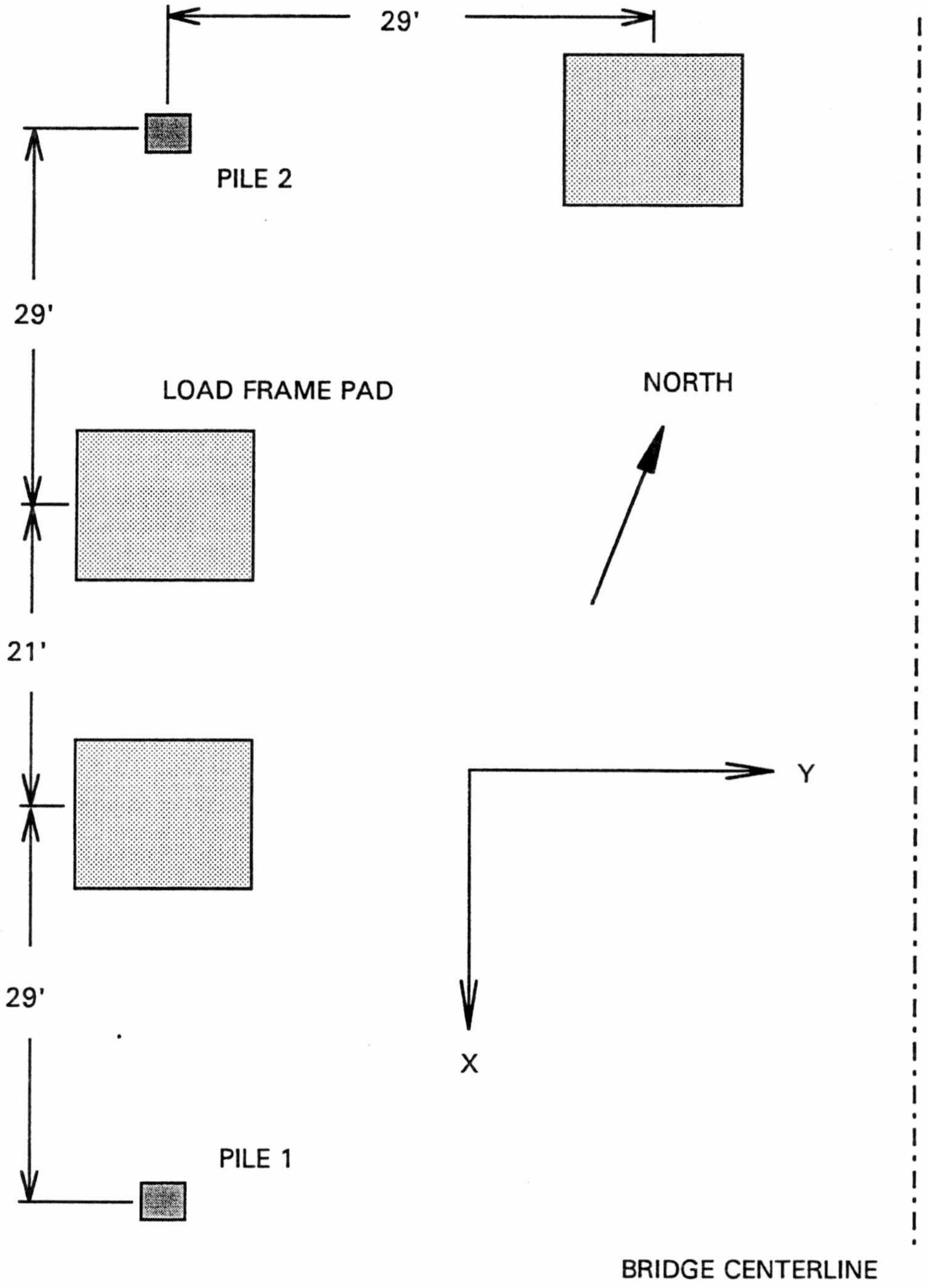

Figure 8 Test site layout.

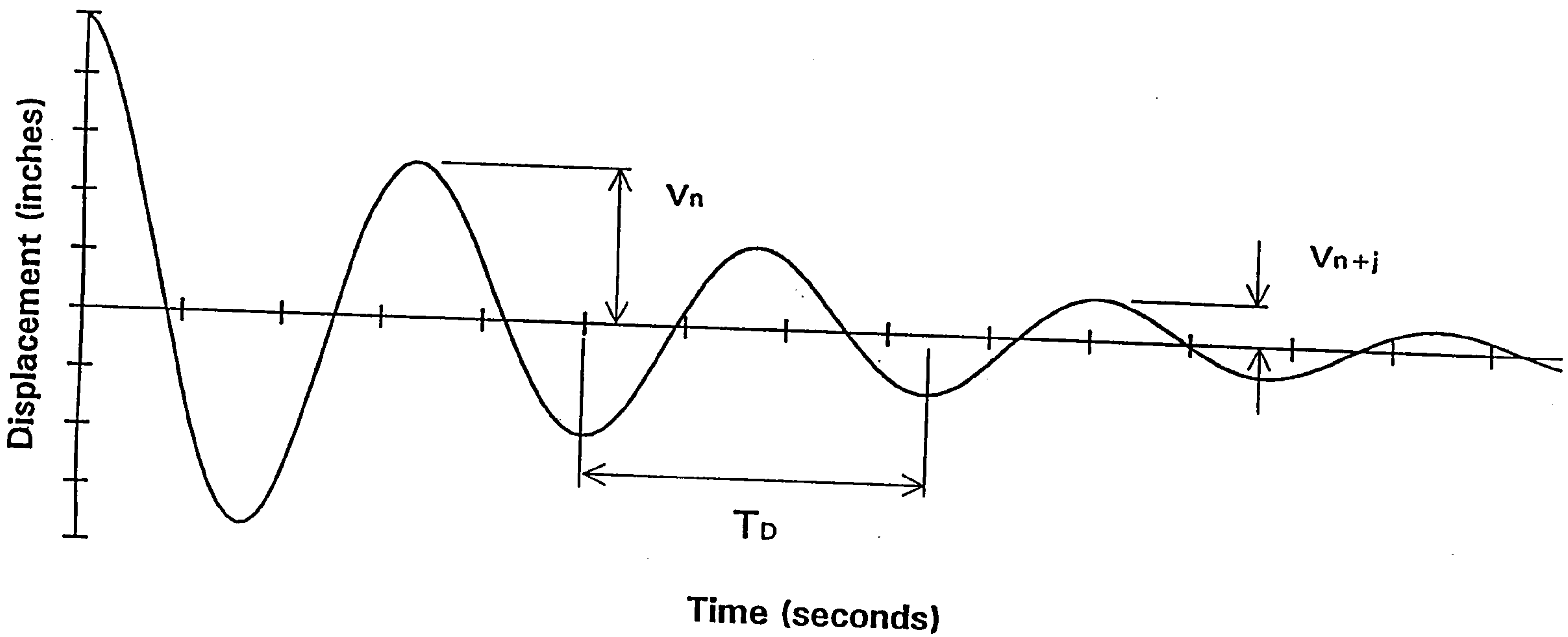

Figure 9 Idealized free-vibration response.

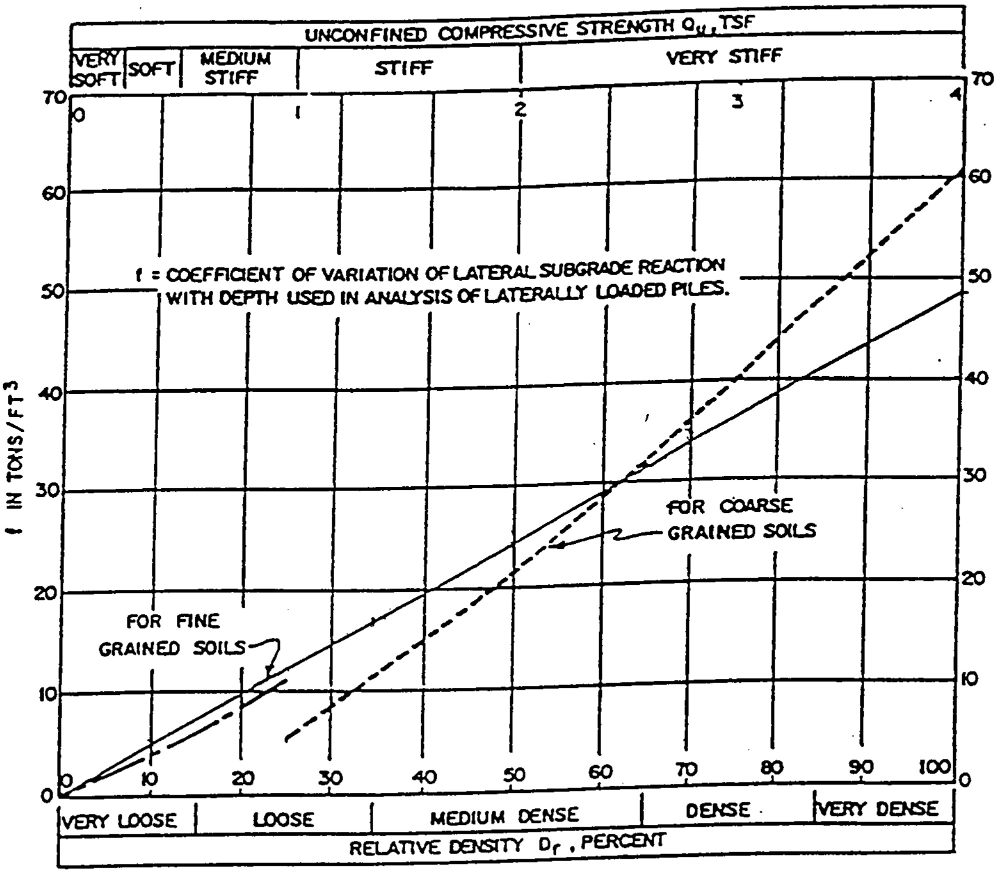

Figure 10 Subgrade modulus gradients for fine and coarse grained soils.

Source: Norris, G.M., and Sack, Robert L. 1986. "Evaluation of the Lateral Stiffness of Pile Groups for Seismic Analysis of Highway Bridges," Proceedings of the 22nd Symposium on Engineering Geology and Soils Engineering. Boise, Idaho.

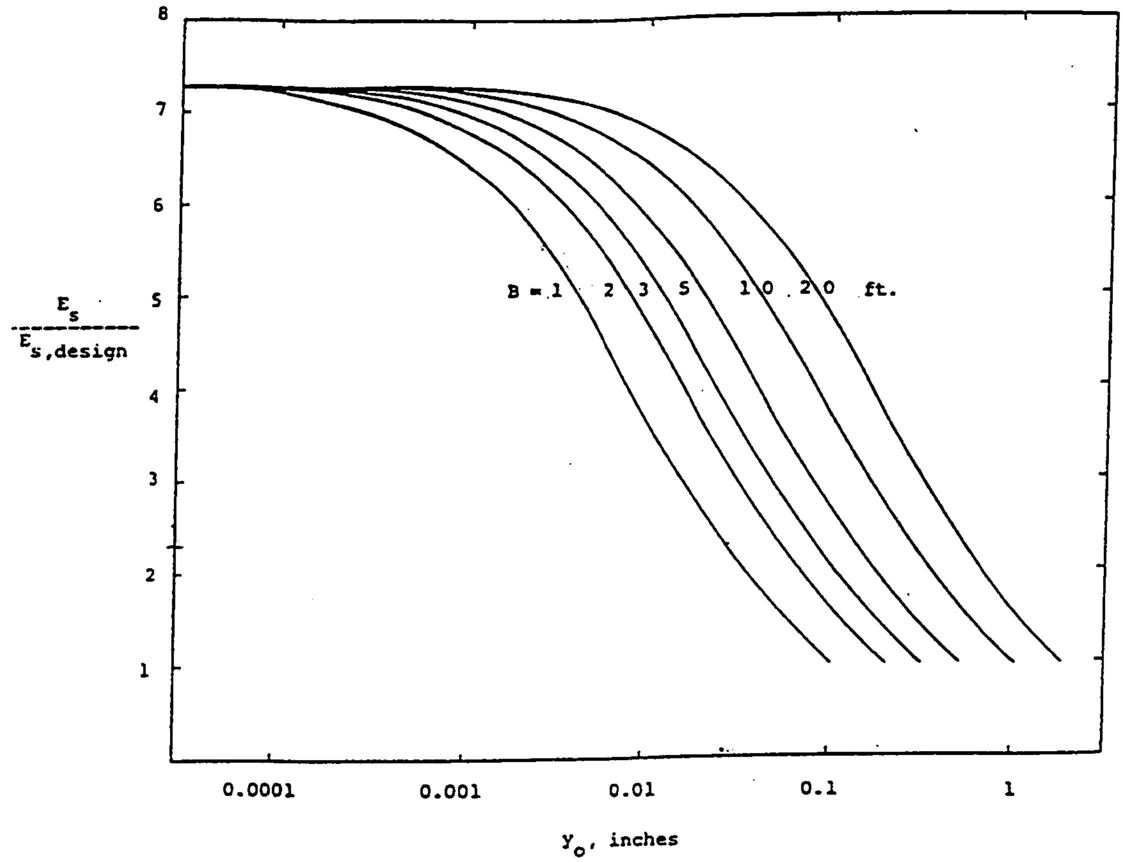

Figure 11 Subgrade modulus amplification curves.

Source: Norris, G.M., and Sack, Robert L. 1986. "Evaluation of the Lateral Stiffness of Pile Groups for Seismic Analysis of Highway Bridges," Proceedings of the 22nd Symposium on Engineering Geology and Soils Engineering. Boise, Idaho.

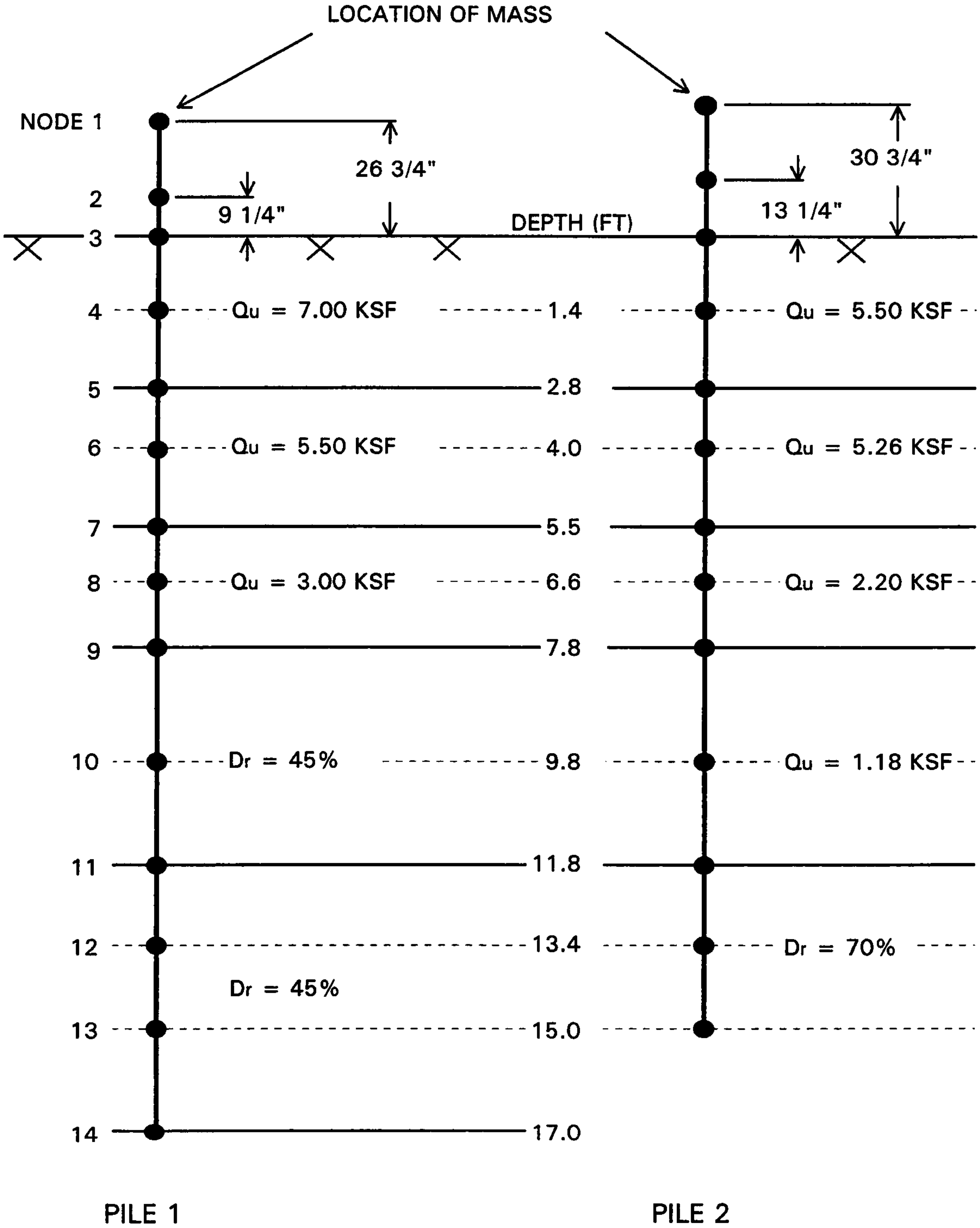

Figure 12 Computer models of test piles.

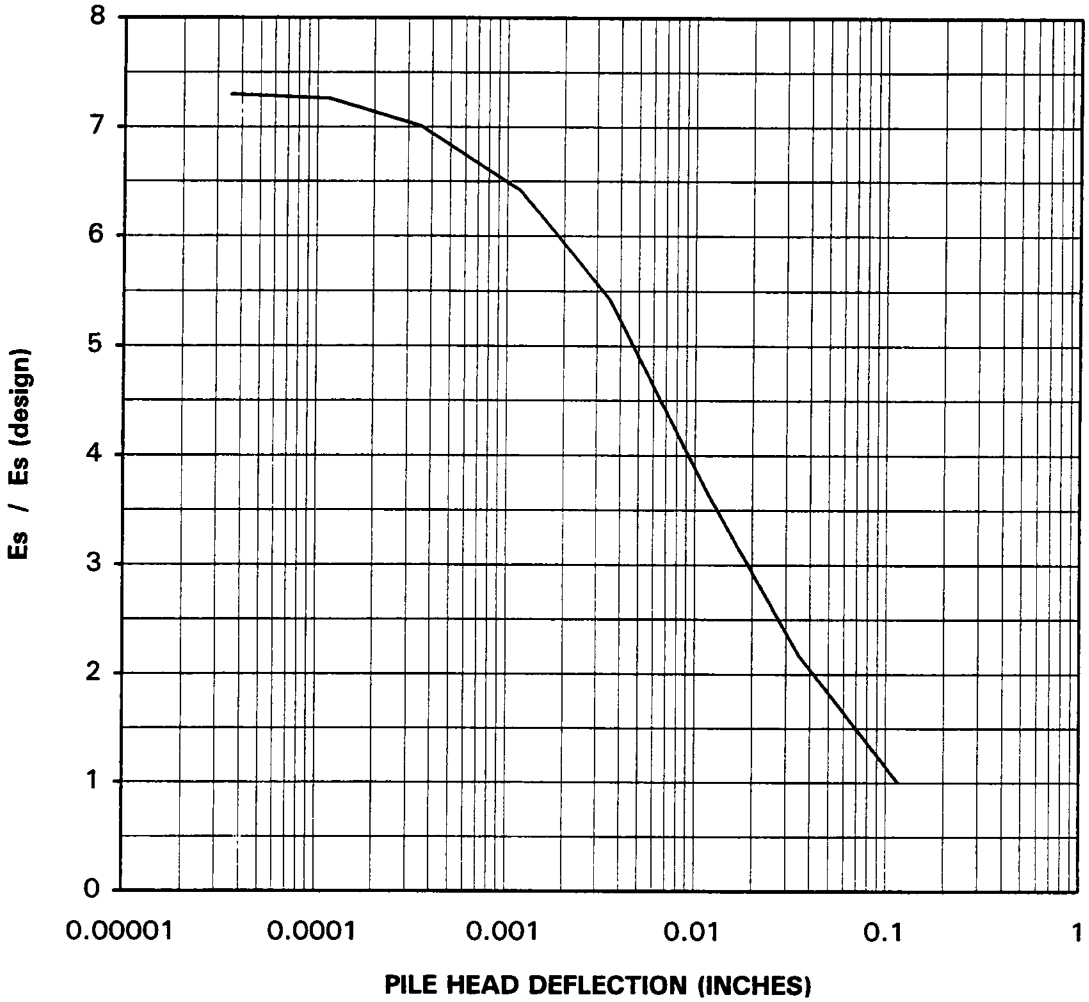

Figure 13 Subgrade modulus amplification curve for B=14".

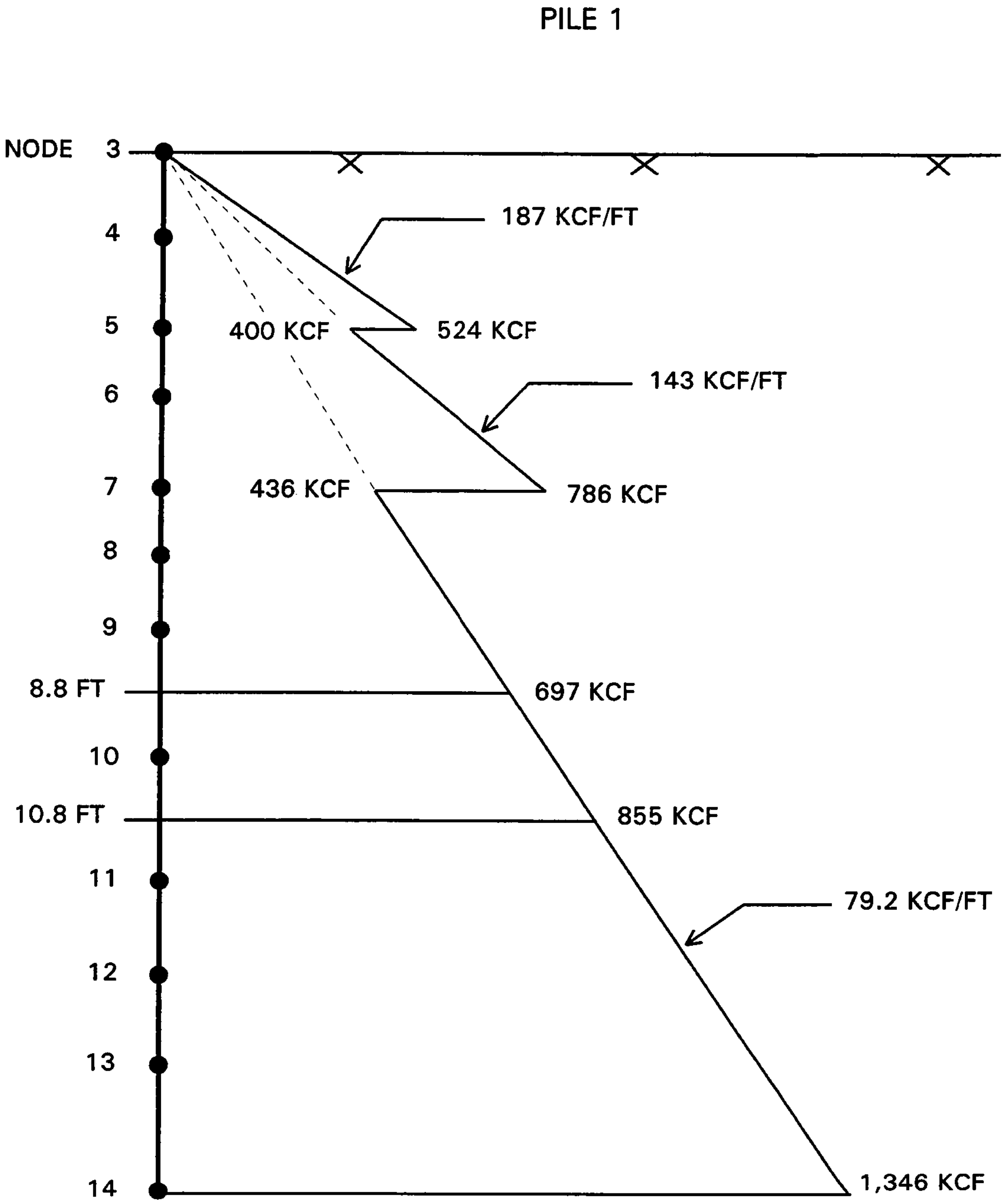

Figure 14 Example subgrade modulus profile.

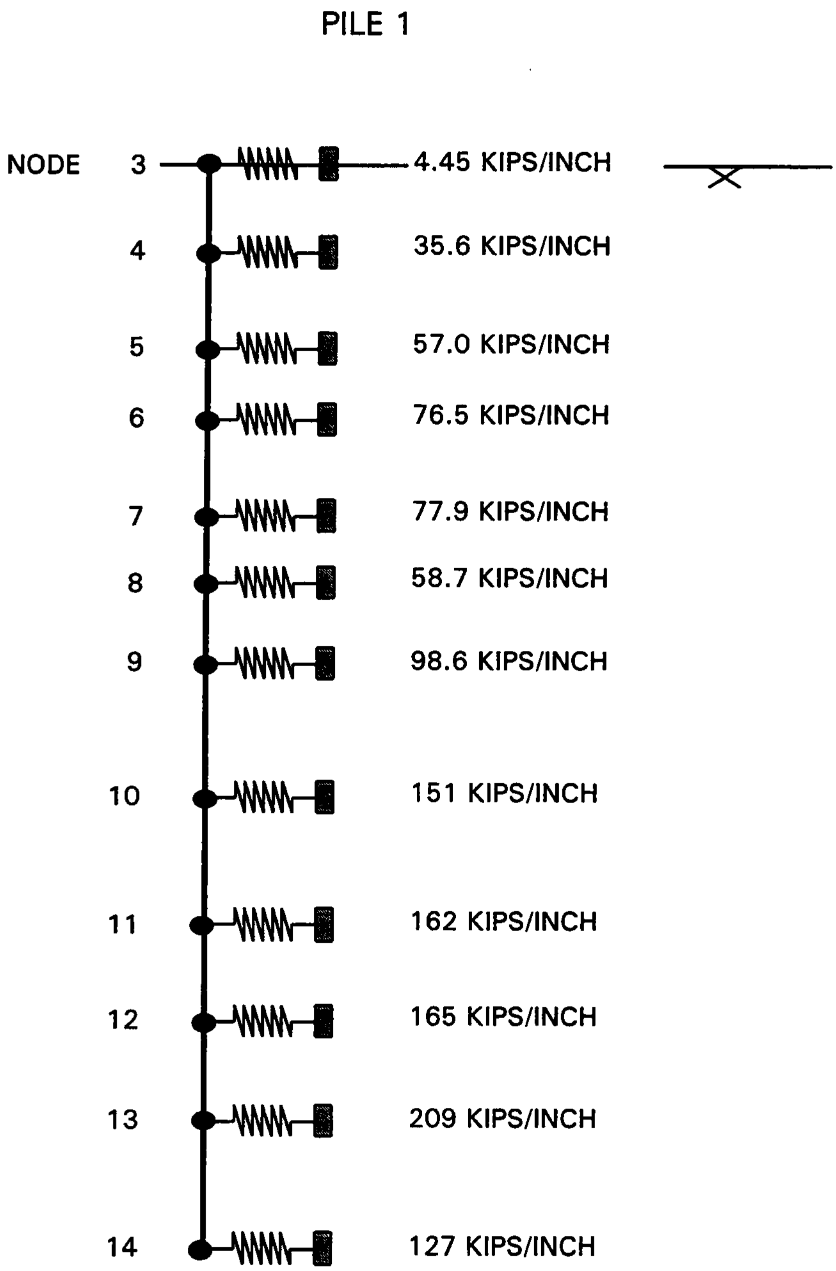

Figure 15 Example soil stiffness springs.

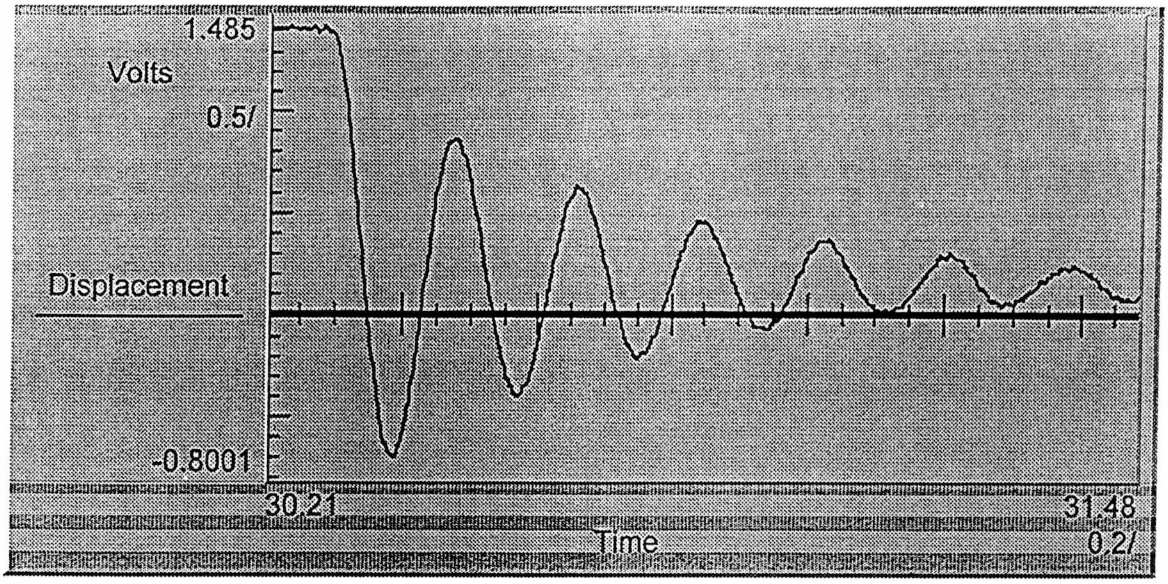

(b) Free-Vibration Response

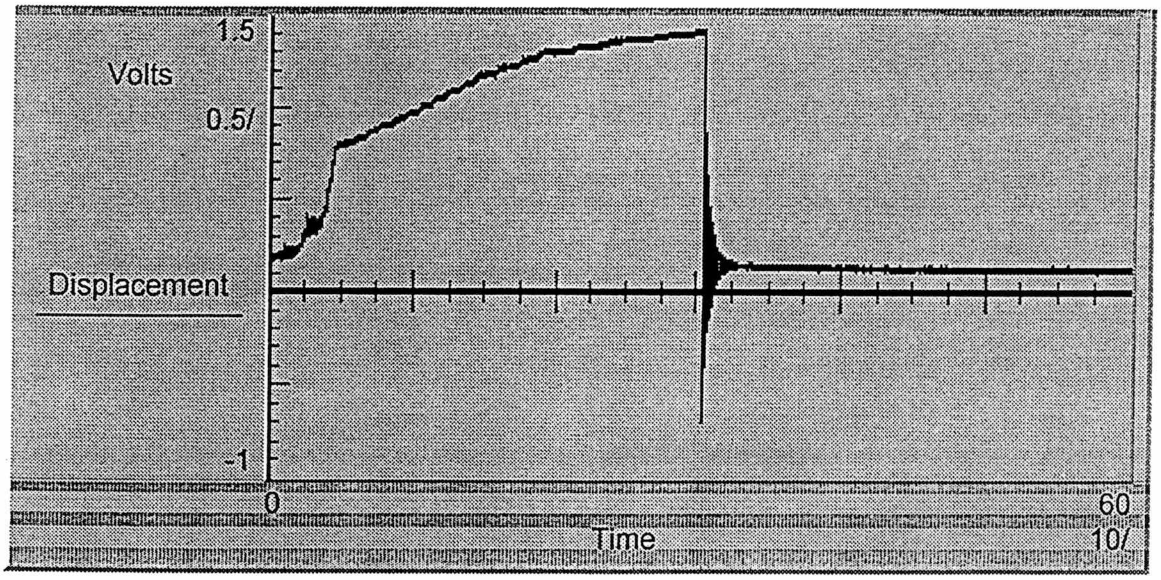

(a) Entire Test

Figure 16 Displacement at center of mass; pile 2; test R; 12-17-94 pile tests.

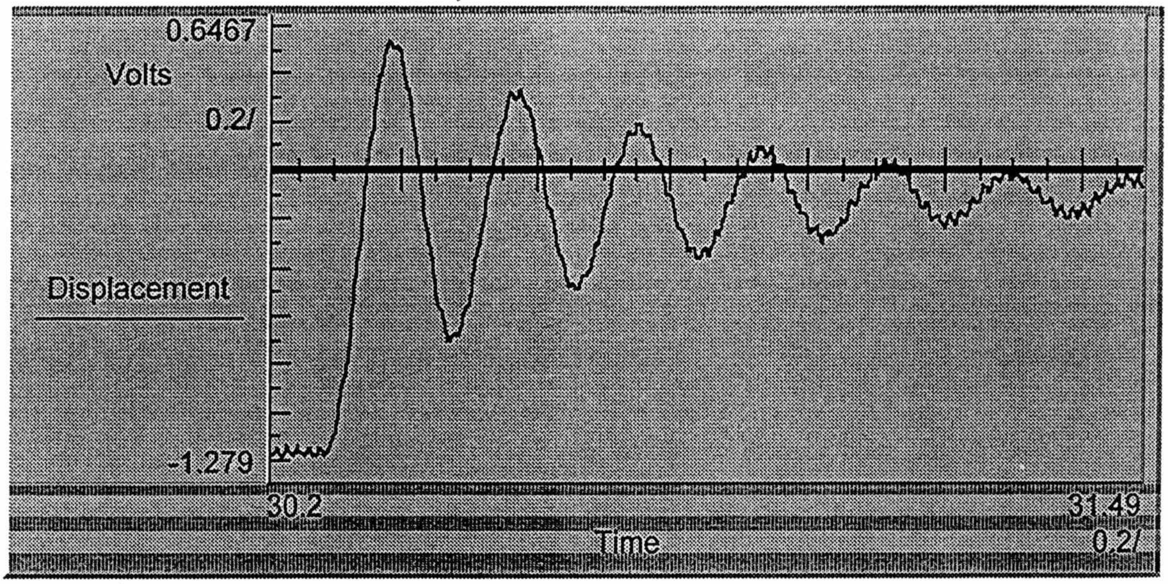

(b) Free-Vibration Response

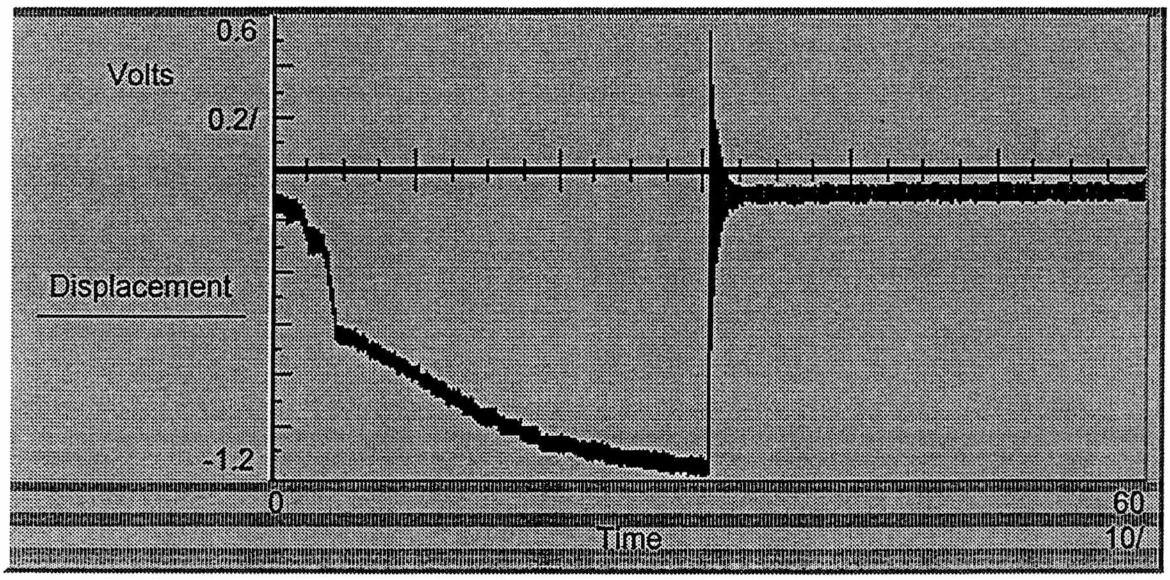

(a) Entire Test

Figure 17 Displacement at bottom of mass; pile 2; test R; 12-17-94 pile tests.

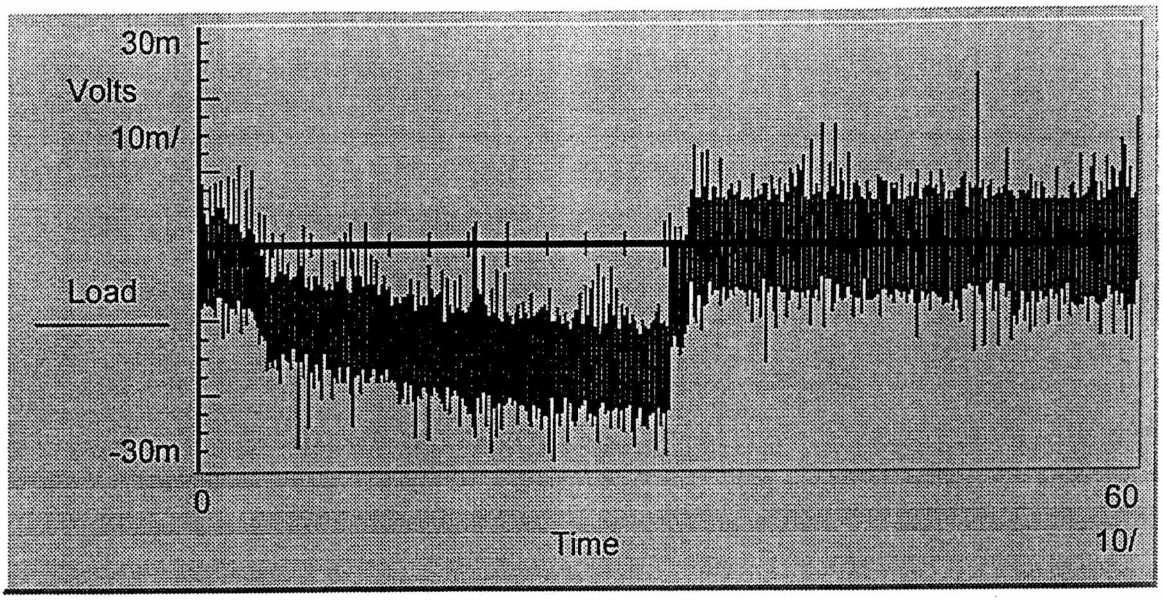

Figure 18 Load vs time; pile 2; test R; 12-17-94 pile tests.

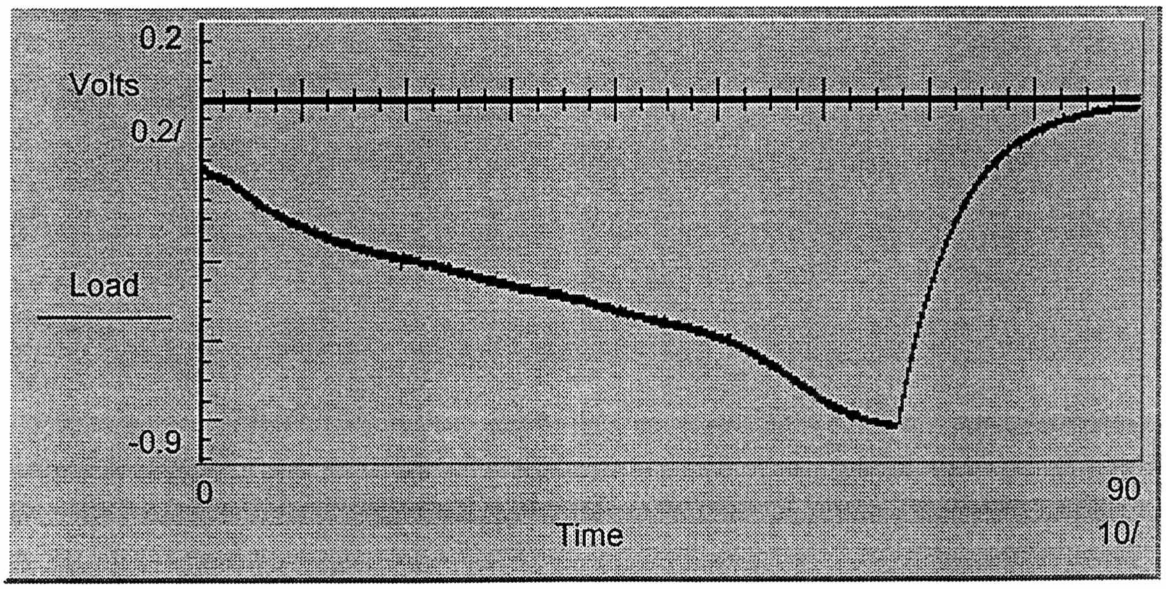

Figure 19 Load vs time; pile 2; test G; 3-20-95 pile tests; load in y-direction.

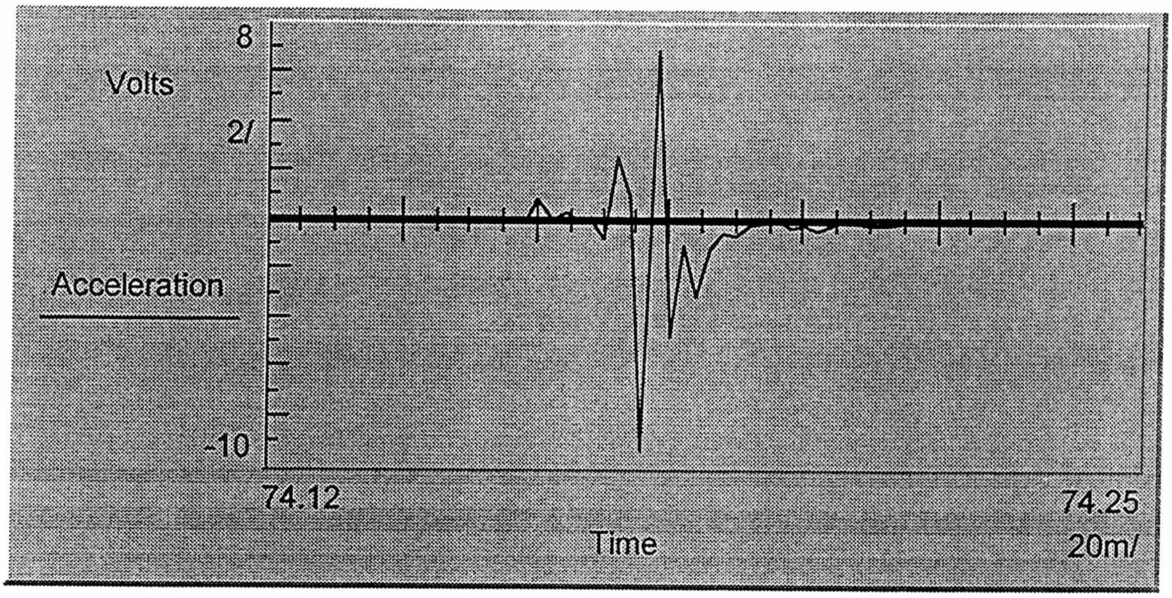

(b) Close-Up of Acceleration "Spike"

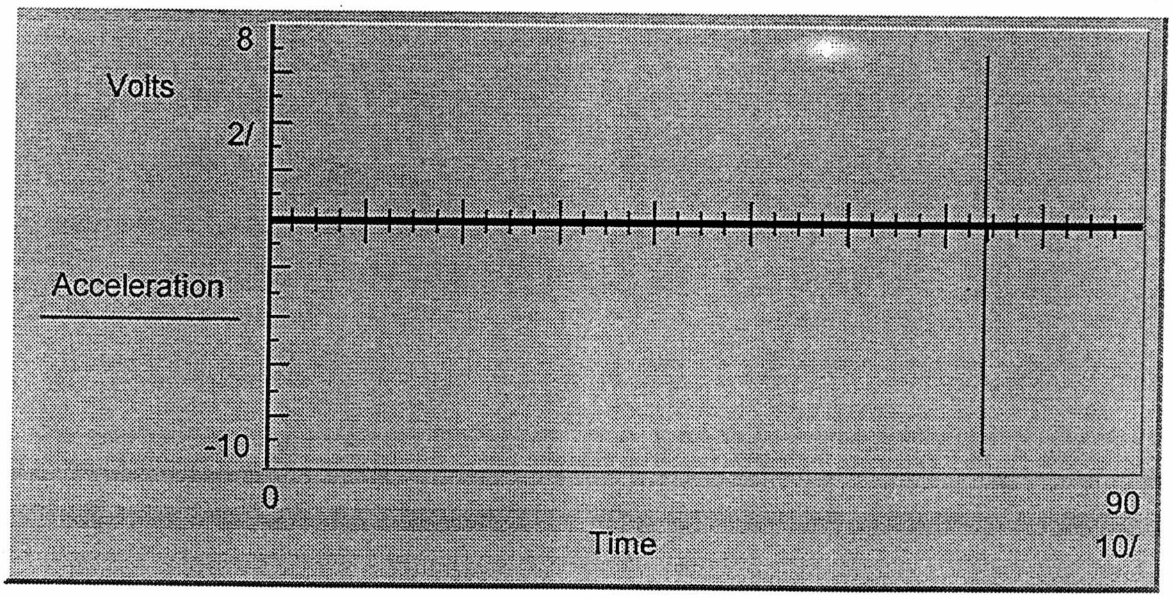

(a) Entire Test

Figure 20 Out-Of-Plane acceleration of pile mass; pile 1; test N; 12-16-94 pile tests.

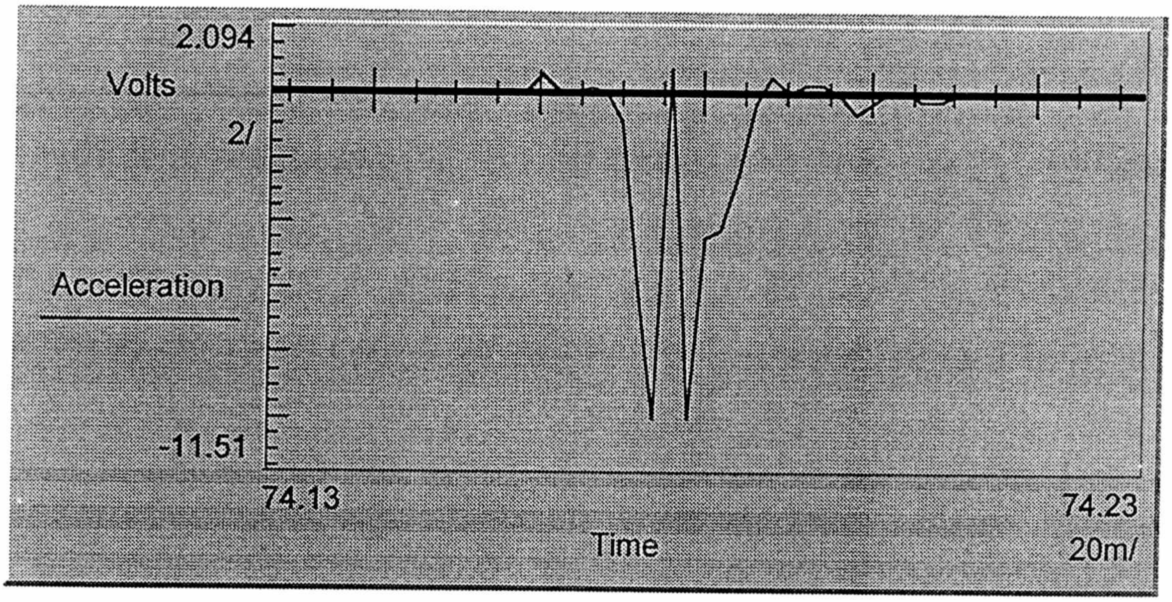

(b) Close-Up of Acceleration "Spike"

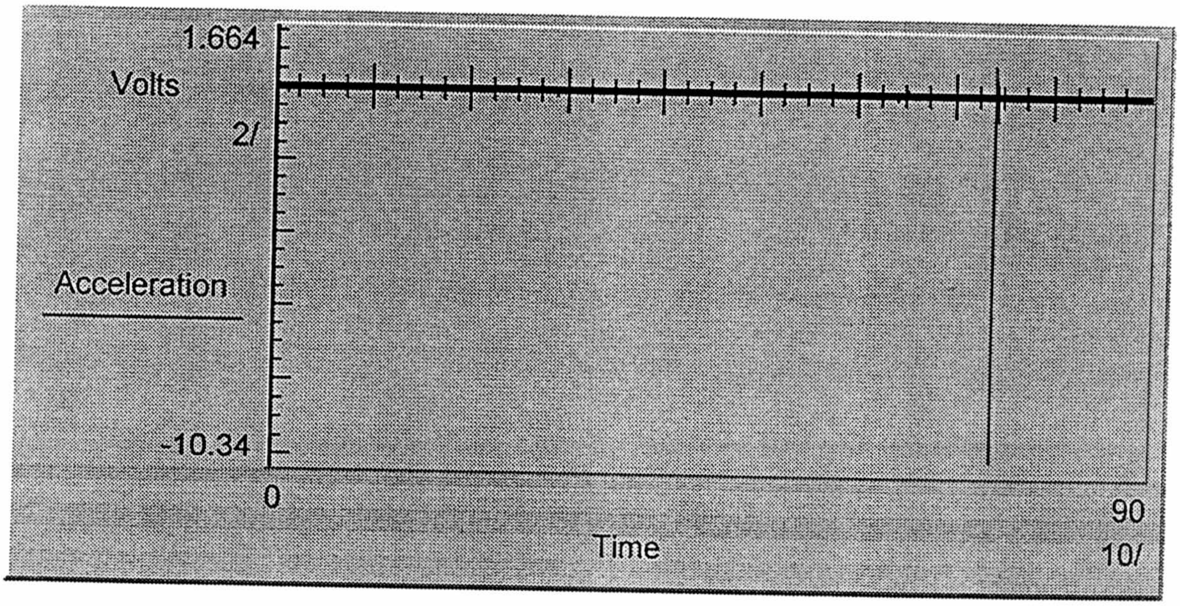

(a) Entire Test

Figure 21 Vertical acceleration of pile mass; pile 1; test N; 12-16-94 pile tests.

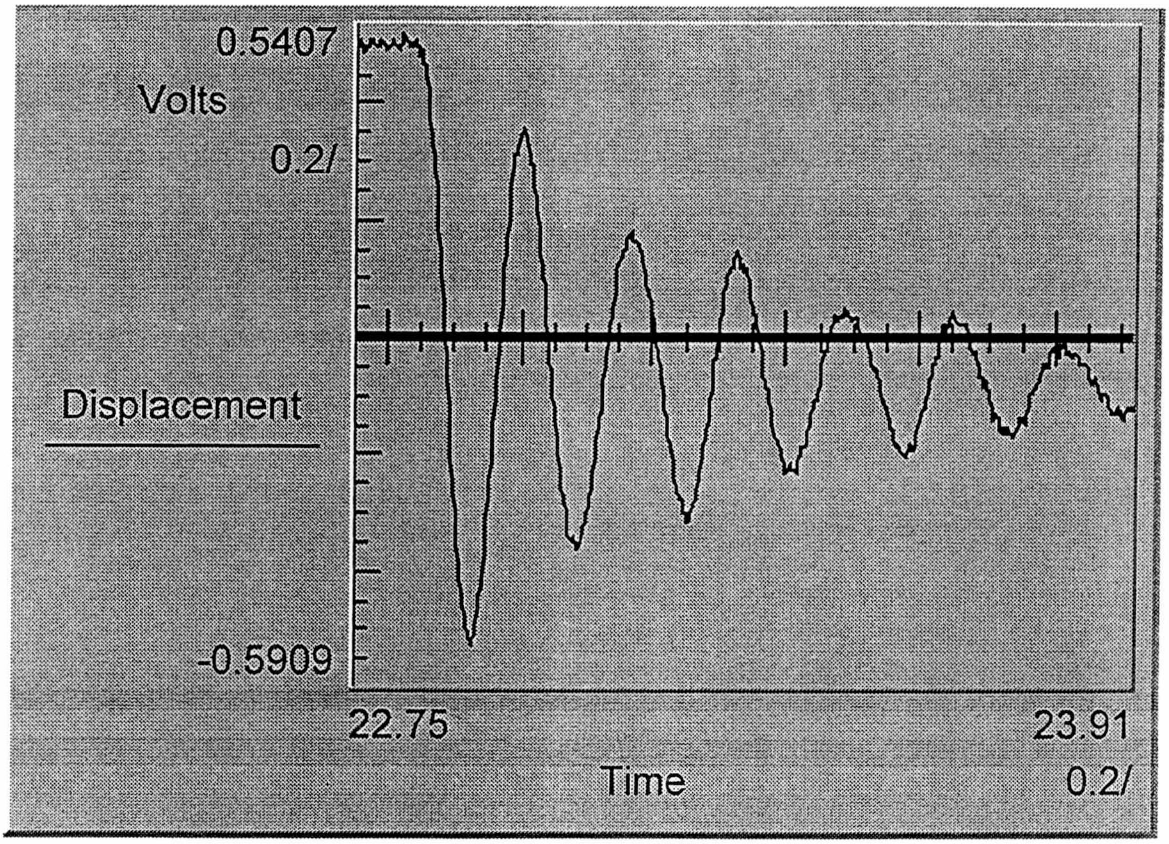

Figure 22 Free-vibration response of pile 2; test D; 12-17-94 pile tests.

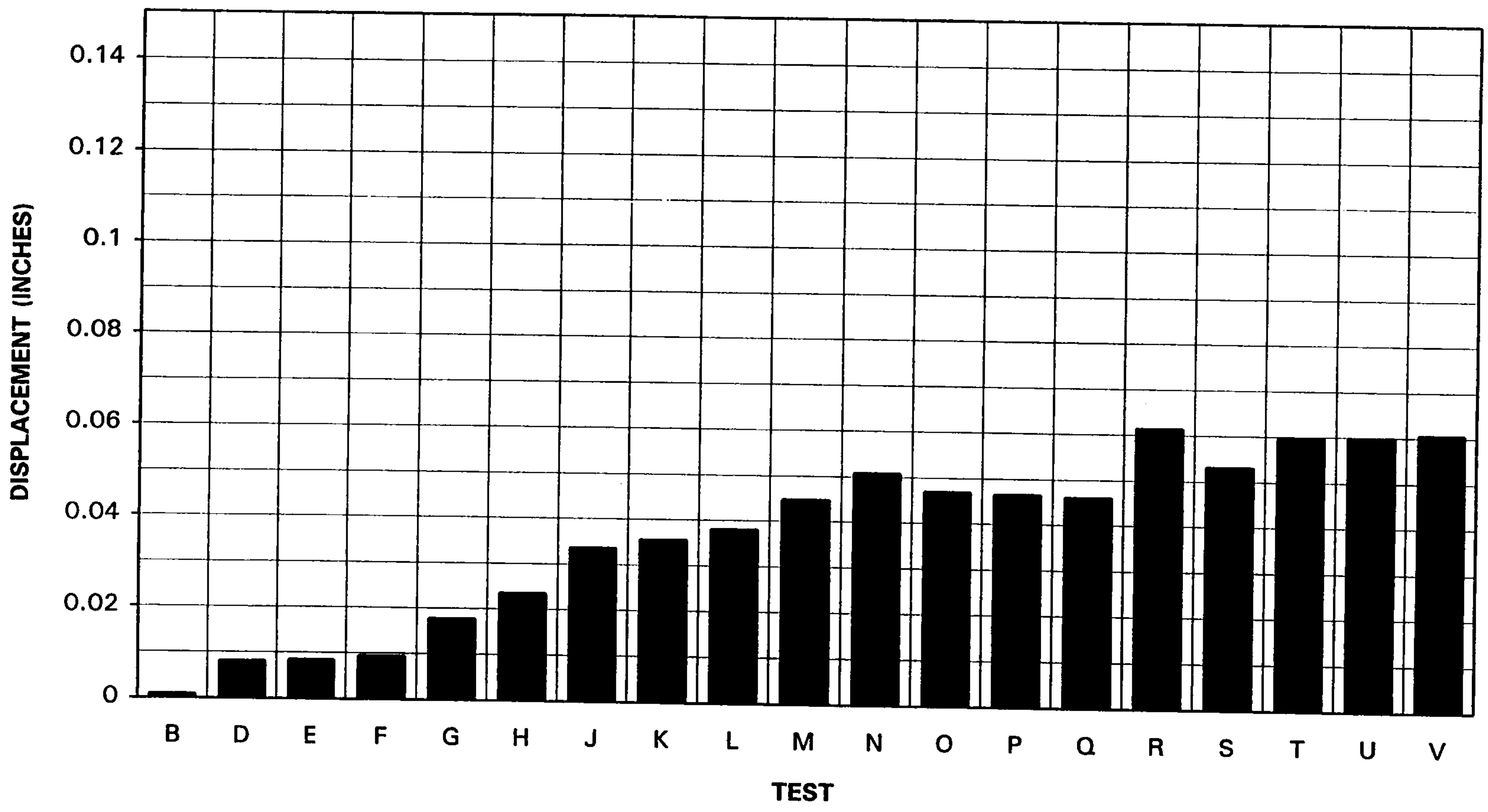

Figure 23   Pile mass resting positions; bottom of mass; pile 1.

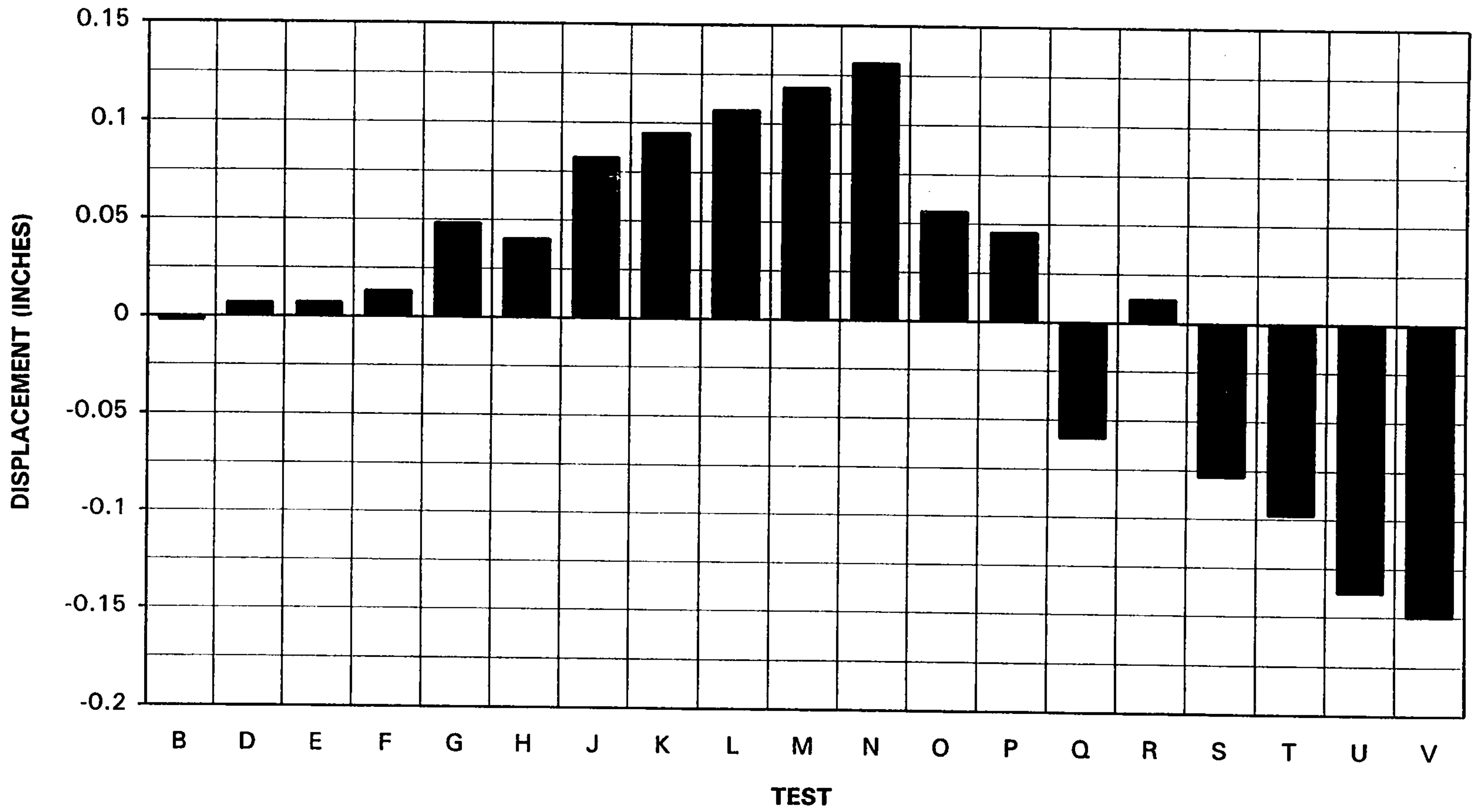

Figure 24   Pile mass resting positions; center of mass; pile 1.

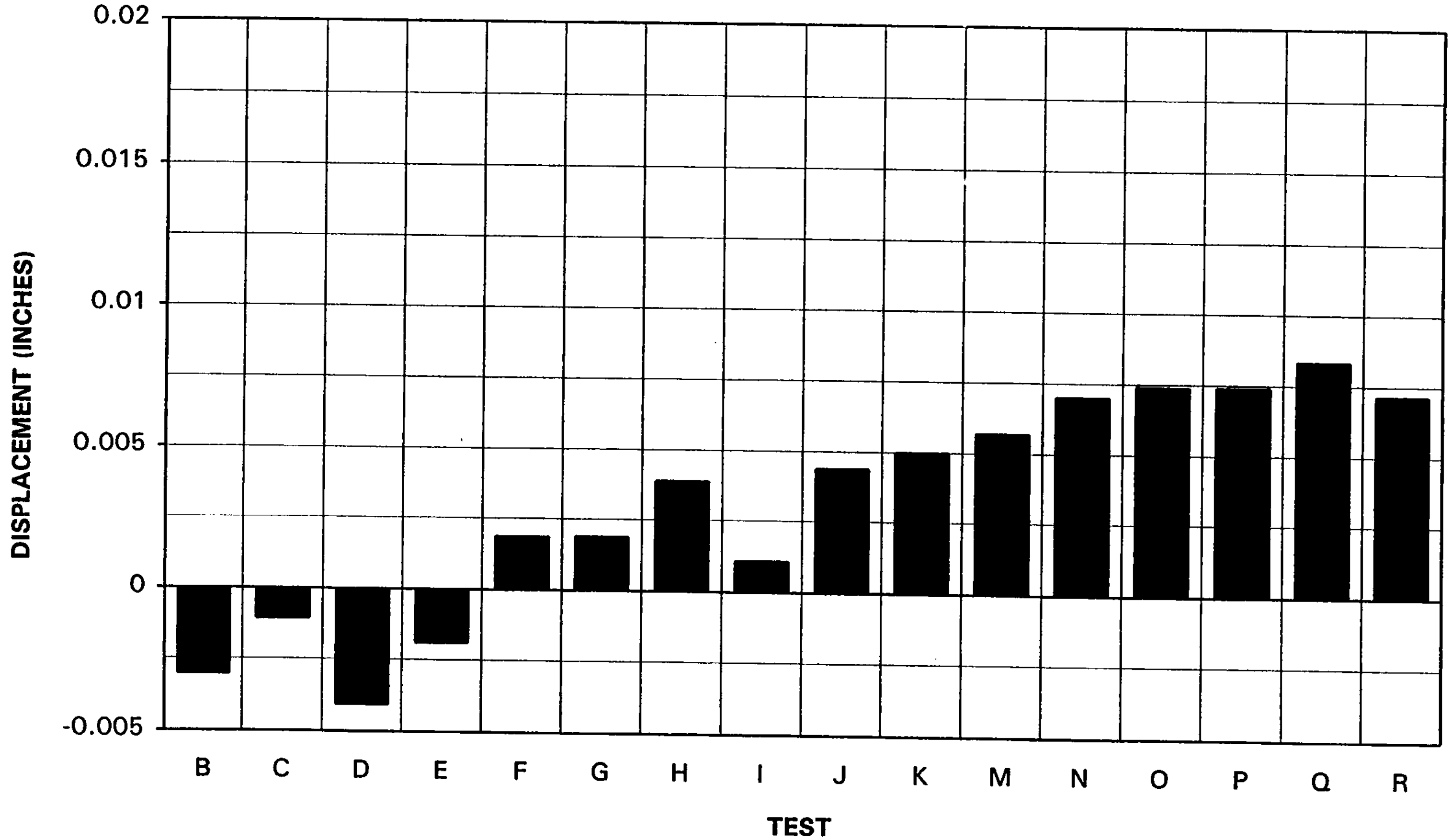

Figure 25 Pile mass resting positions; bottom of mass; pile 2; 12-17-94 pile tests.

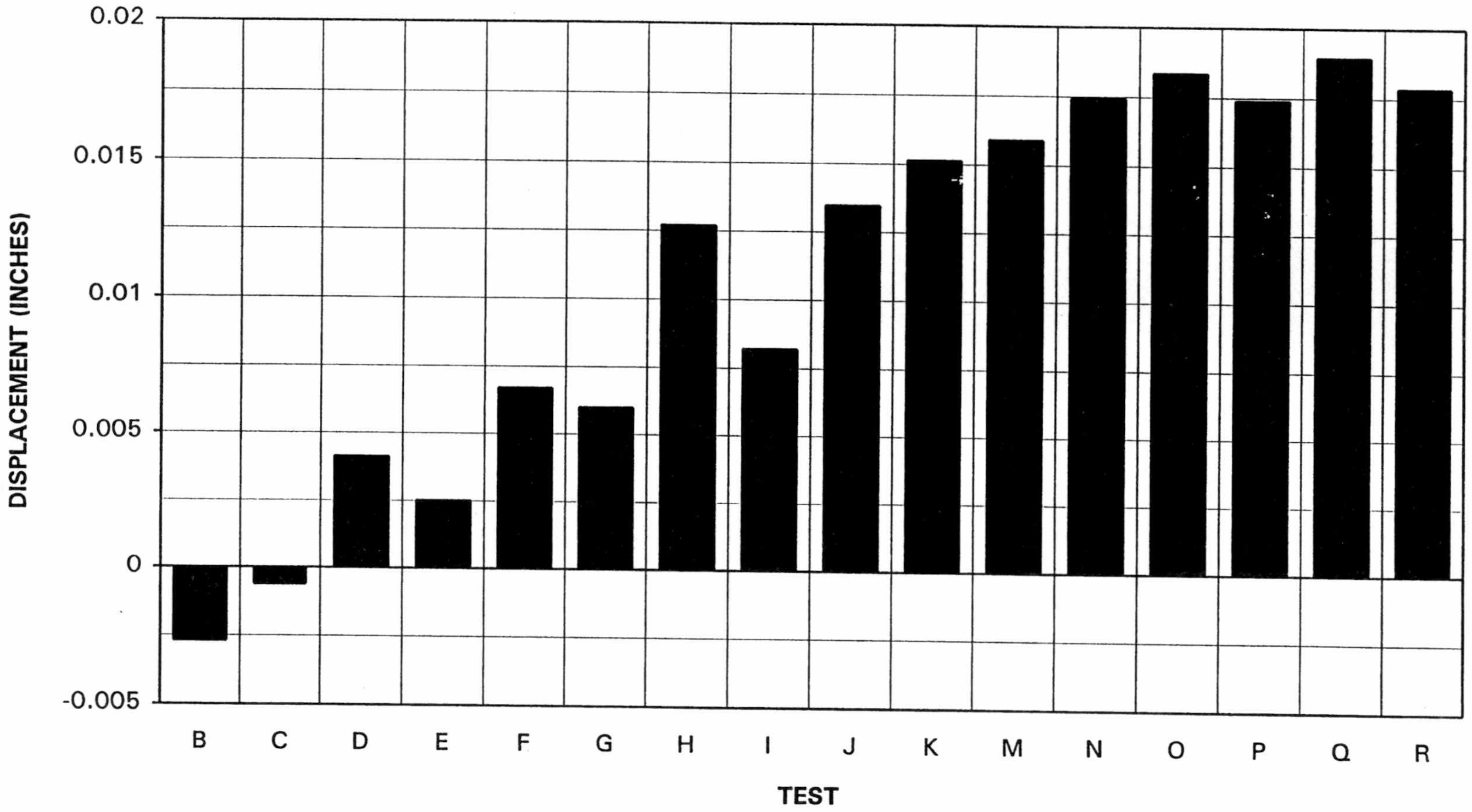

Figure 26 Pile mass resting positions; center of mass; pile 2; 12-17-94 pile tests.

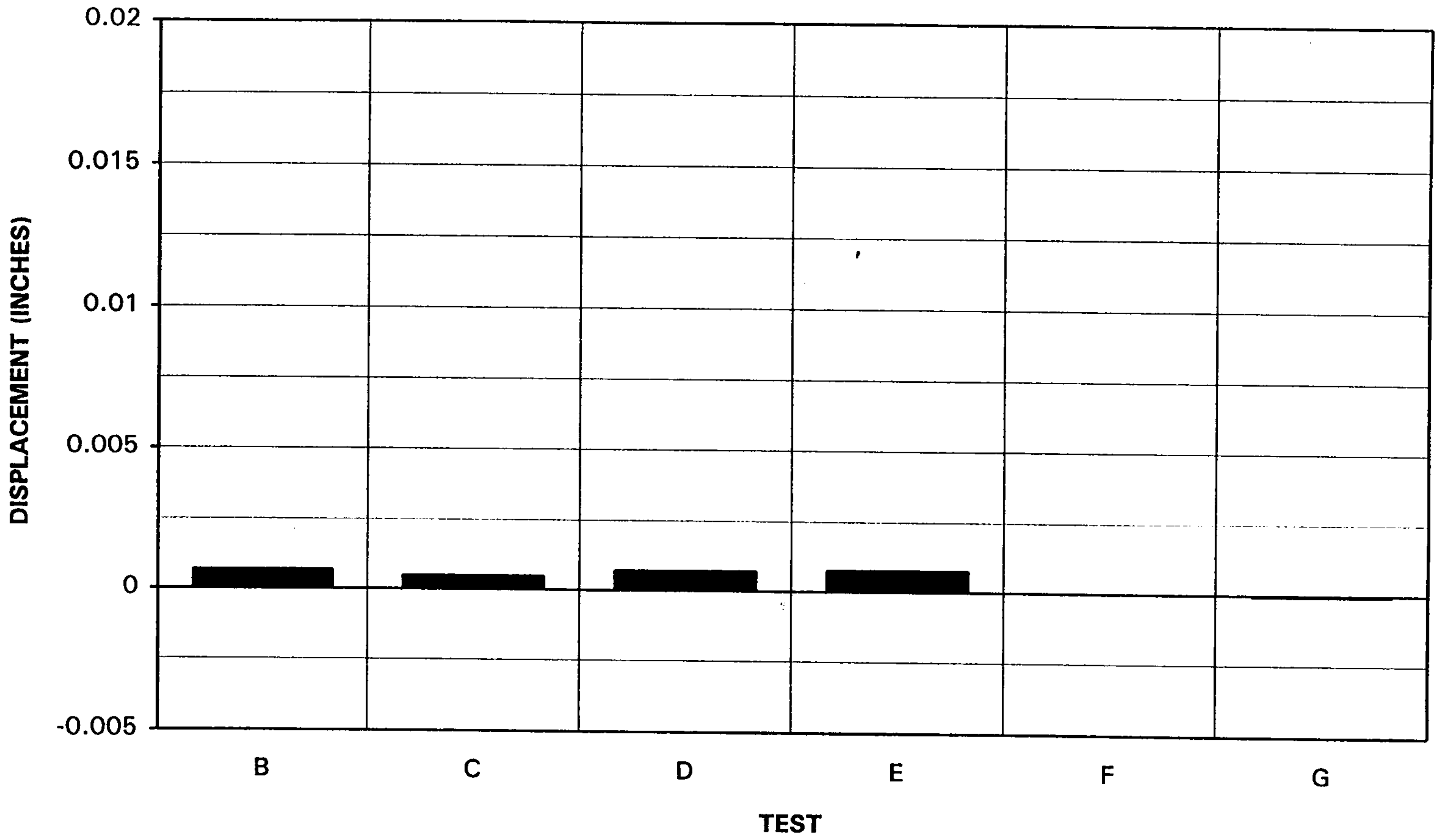

Figure 27 Pile mass resting positions; bottom of mass; pile 2; 3-20-95 pile tests; load in y-direction.

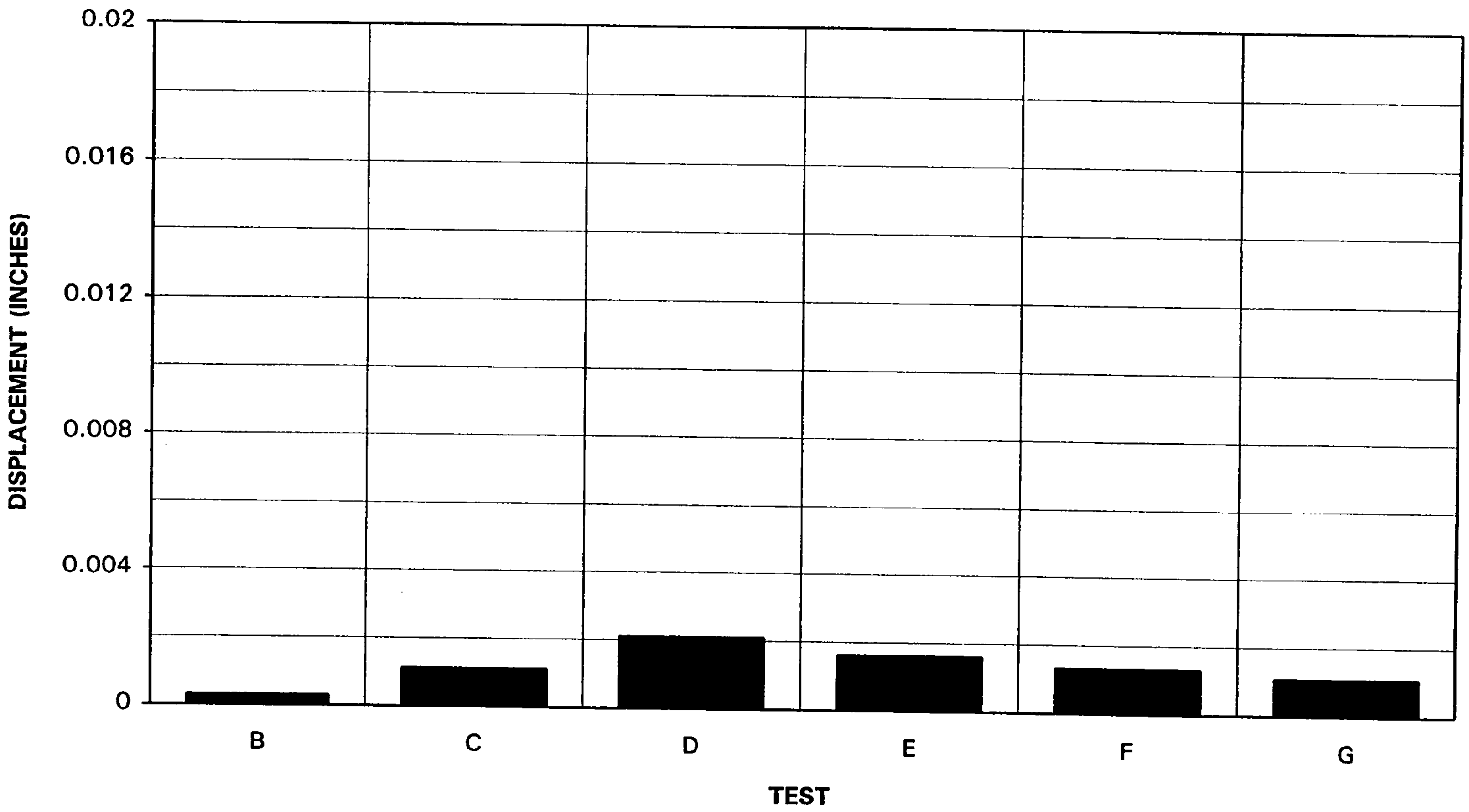

Figure 28 Pile mass resting positions; center of mass; pile 2; 3-20-95 pile tests; load in y-direction.

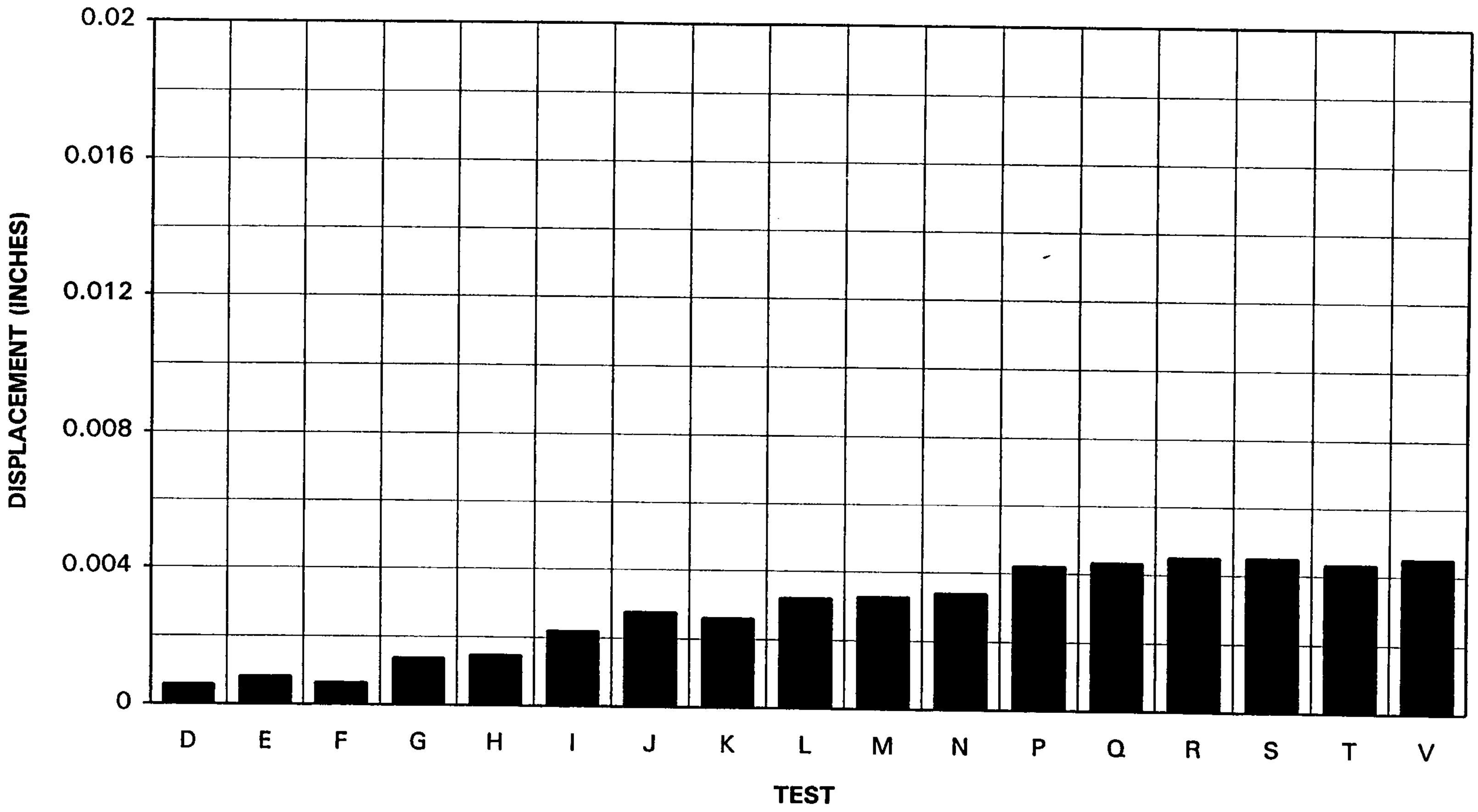

Figure 29 Pile mass resting positions; bottom of mass; pile 2; 3-20-95 pile tests; load in x-direction.

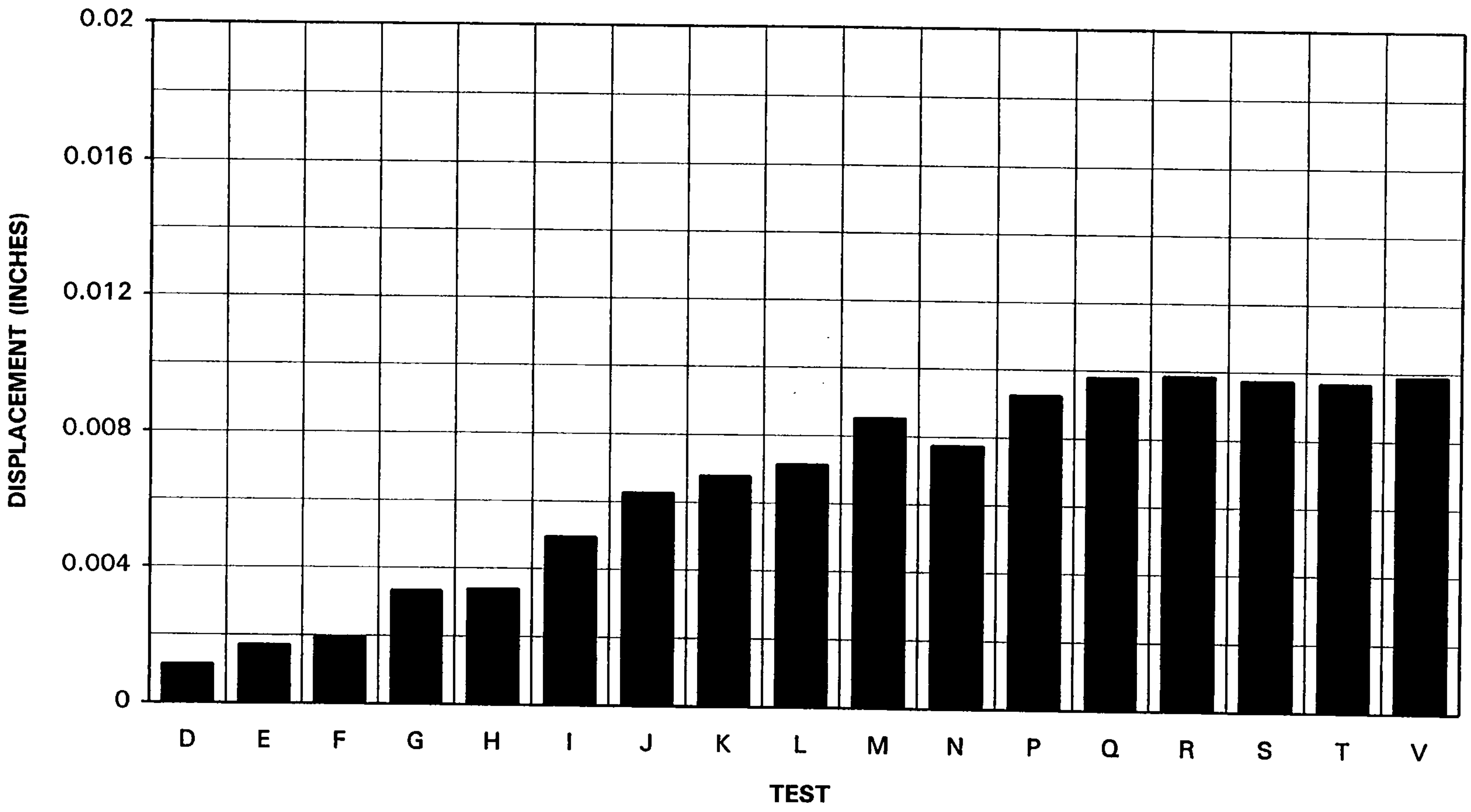

Figure 30 Pile mass resting positions; center of mass; pile 2; 3-20-95 pile tests; load in x-direction.

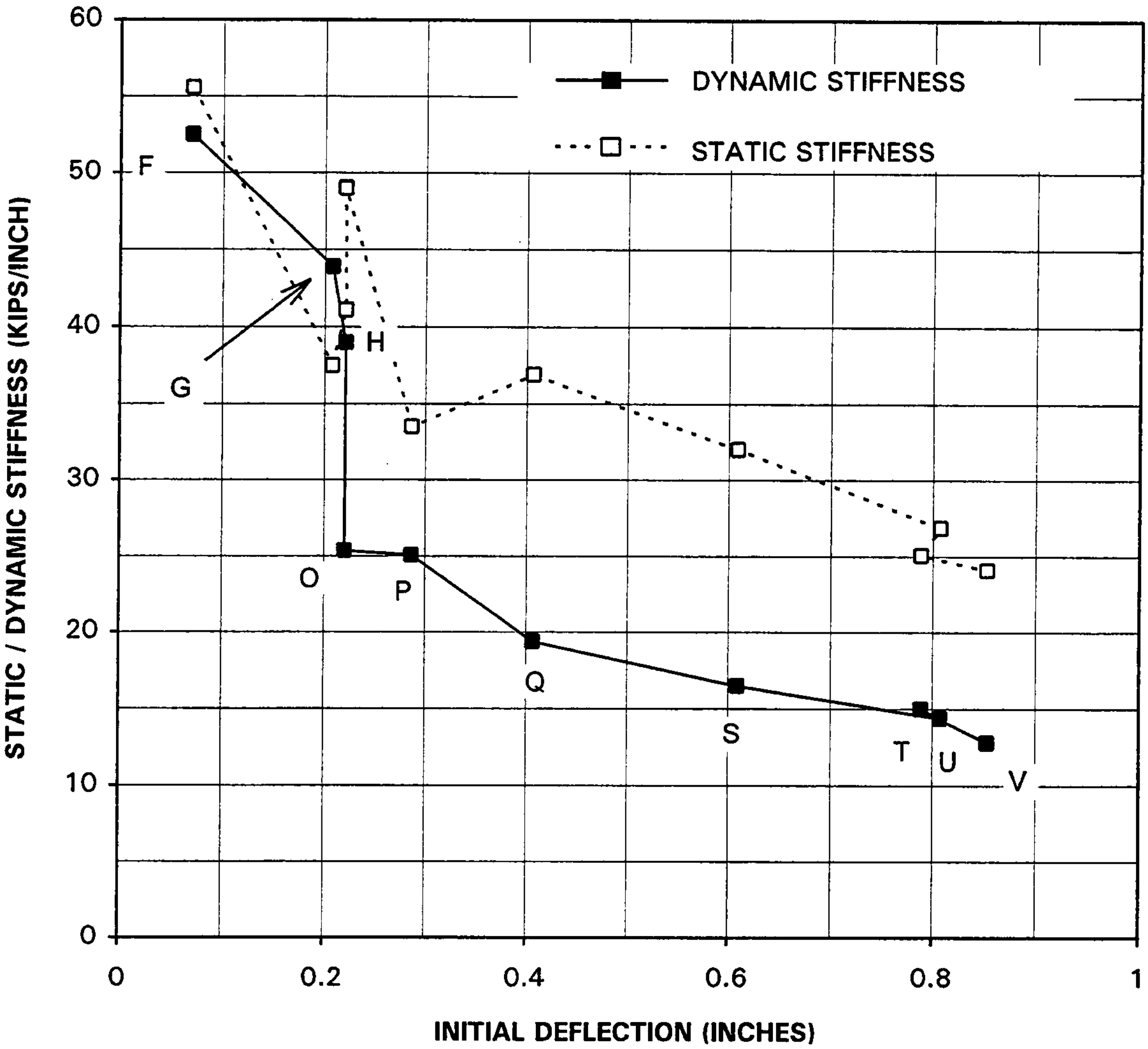

NOTE:

Only values of static and dynamic stiffness resulting from pile tests in which the load was applied at the center of mass are plotted.

Figure 31 Static and dynamic stiffness of pile 1 vs. initial deflection at the center of mass.

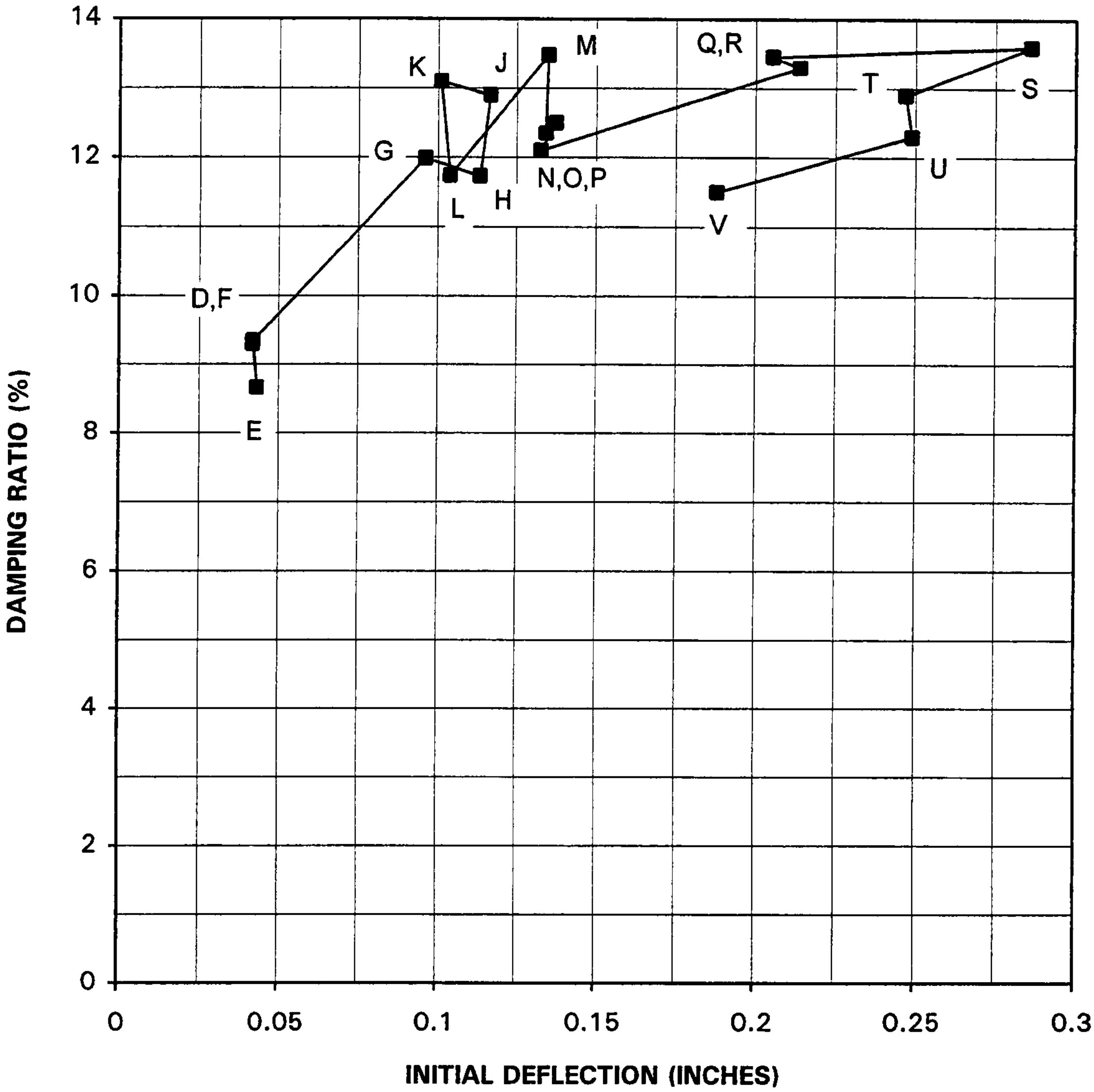

Figure 32 Damping ratio vs initial deflection at bottom of mass; pile 1.

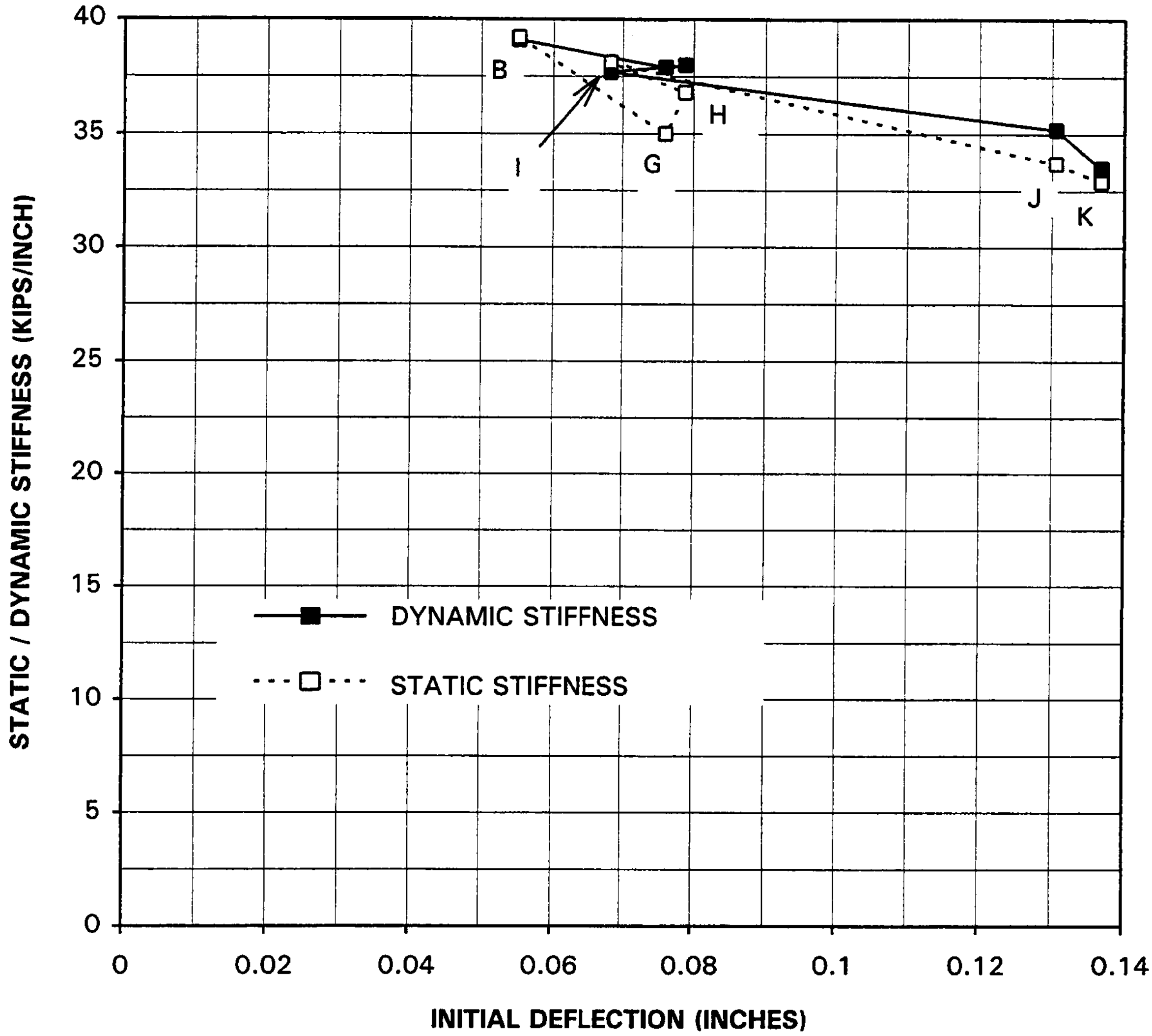

NOTE:

Only values of static and dynamic stiffness resulting from pile tests in which the load was applied at the center of mass are plotted.

Figure 33 Static and dynamic stiffness of pile 2 vs. initial deflection at the center of mass.

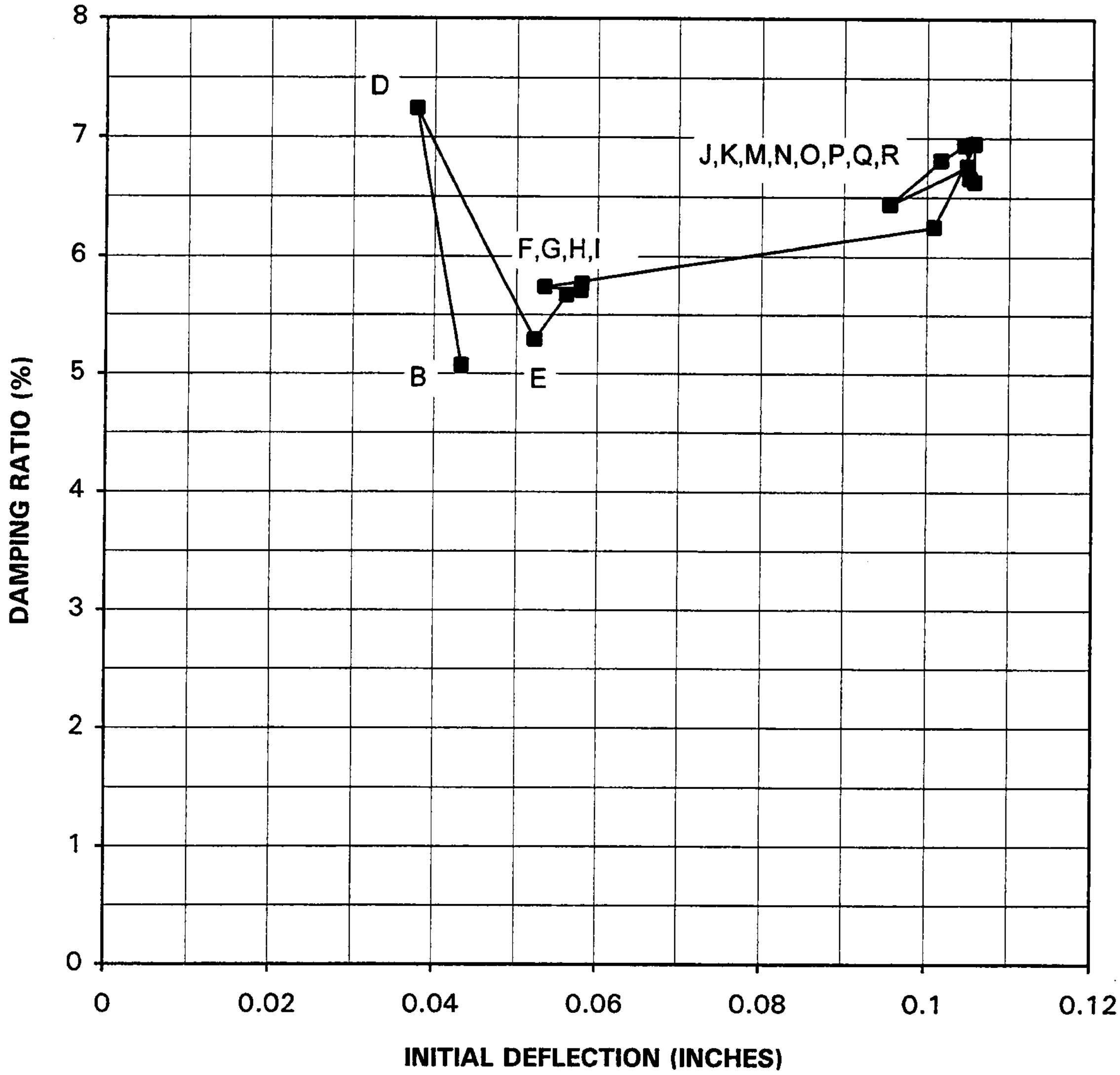

Figure 34 Damping ratio vs initial deflection at bottom of mass; pile 2.

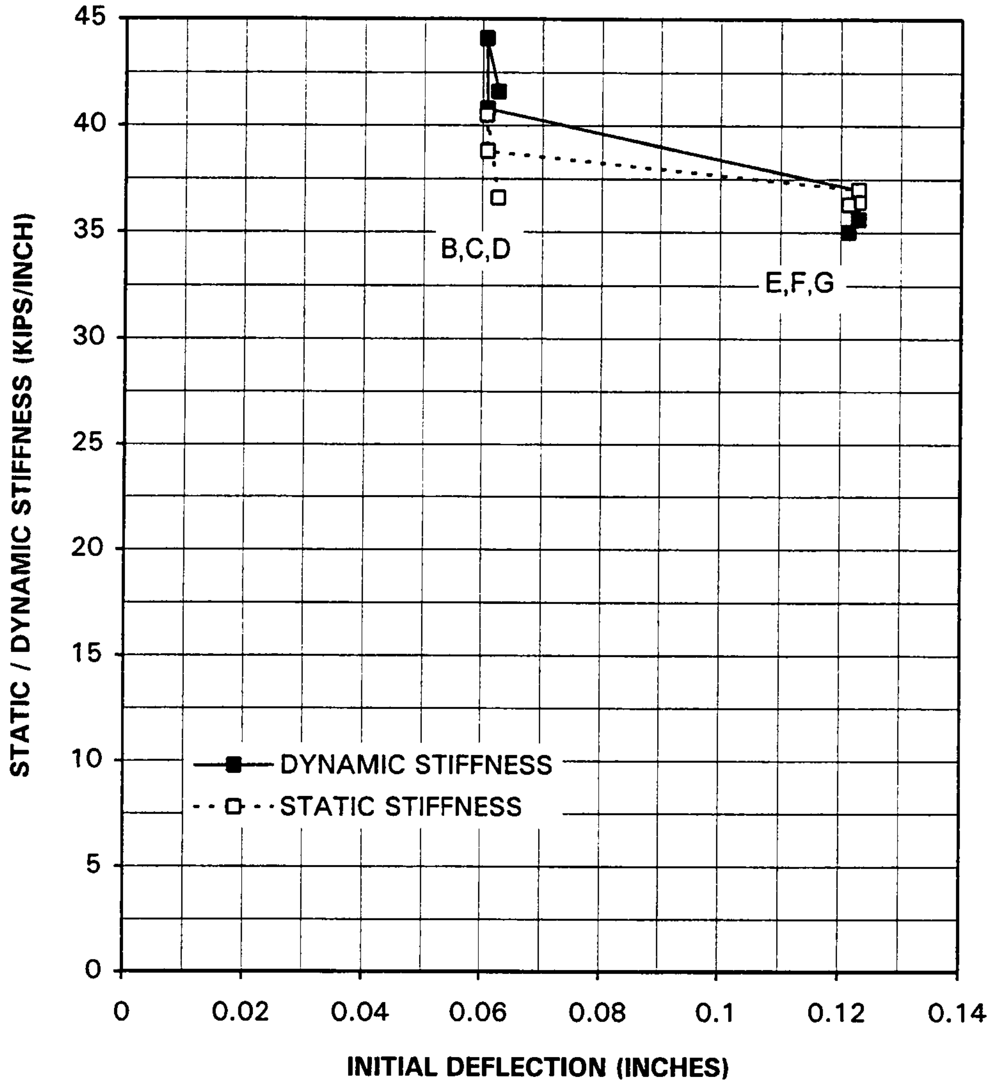

Figure 35 Static and dynamic stiffness vs initial deflection at center of mass; pile 2; 3-20-95 pile tests; load in y-direction.

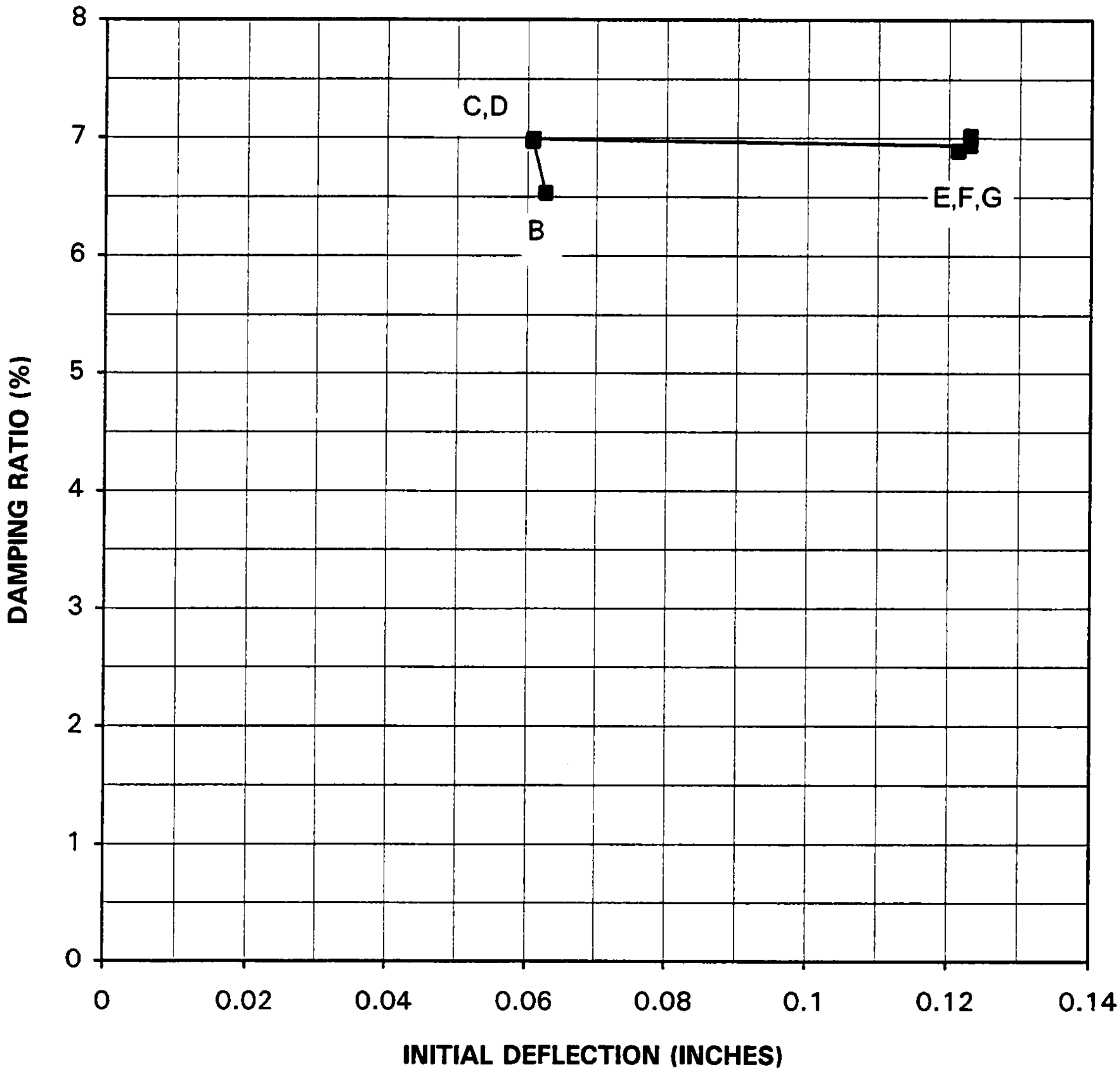

Figure 36 Damping ratio vs initial deflection at center of mass; pile 2; 3-20-95 pile tests; load in y-direction.

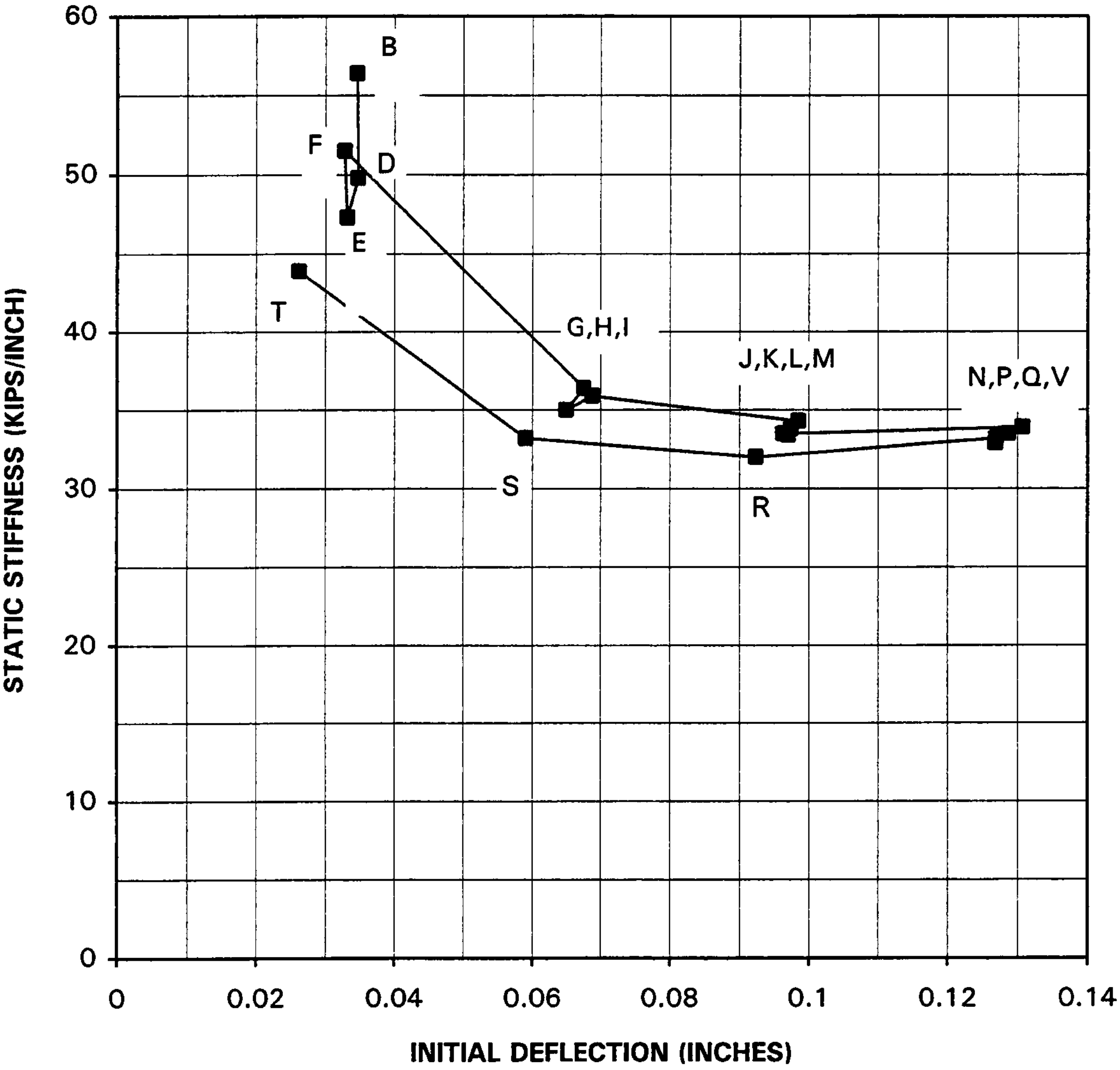

Figure 37 Static stiffness vs initial deflection at center of mass; pile 2; 3-20-95 pile tests; load in x-direction.

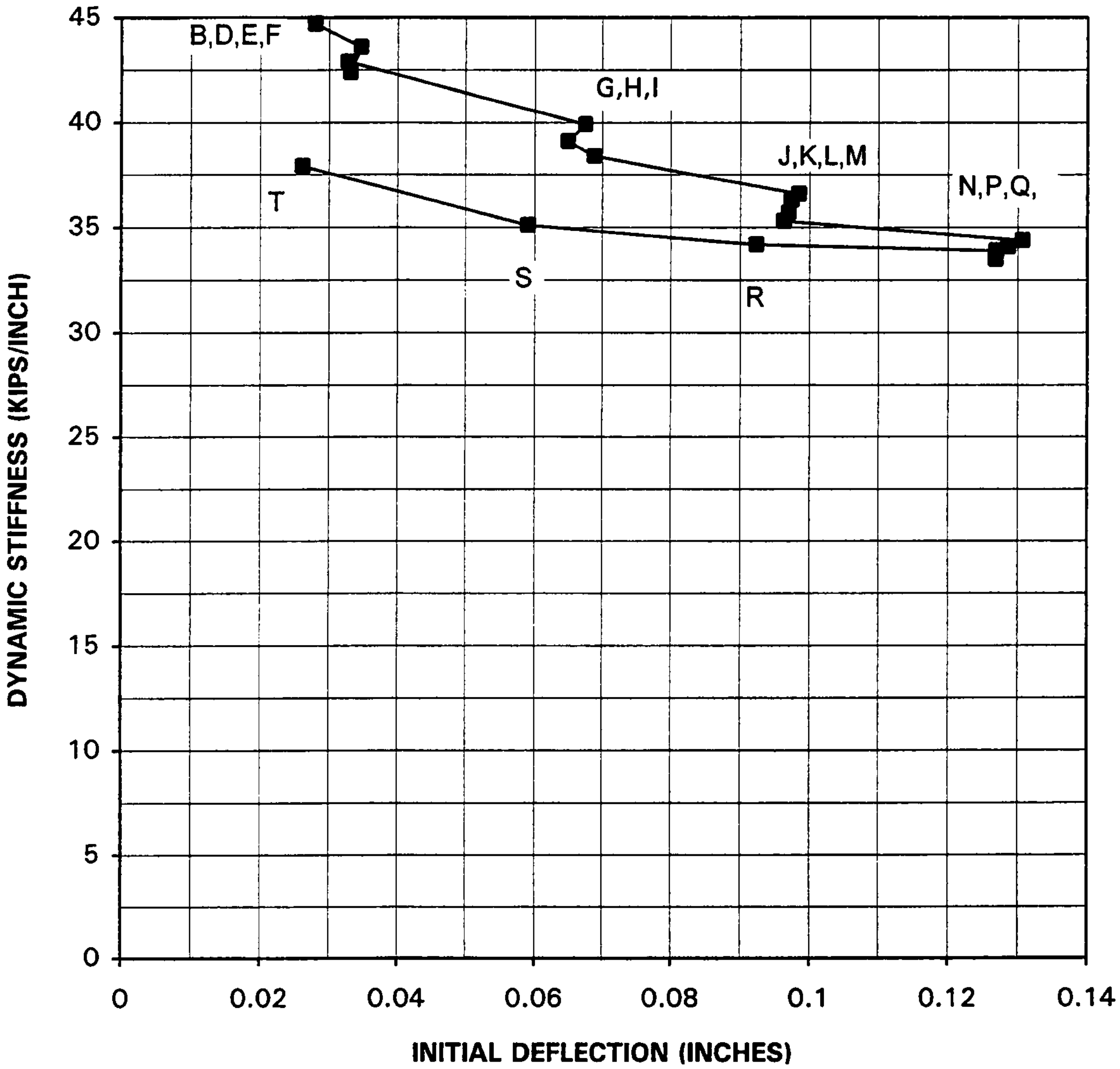

Figure 38 Dynamic stiffness vs initial deflection at center of mass; pile 2; 3-20-95 pile tests; load in x-direction.

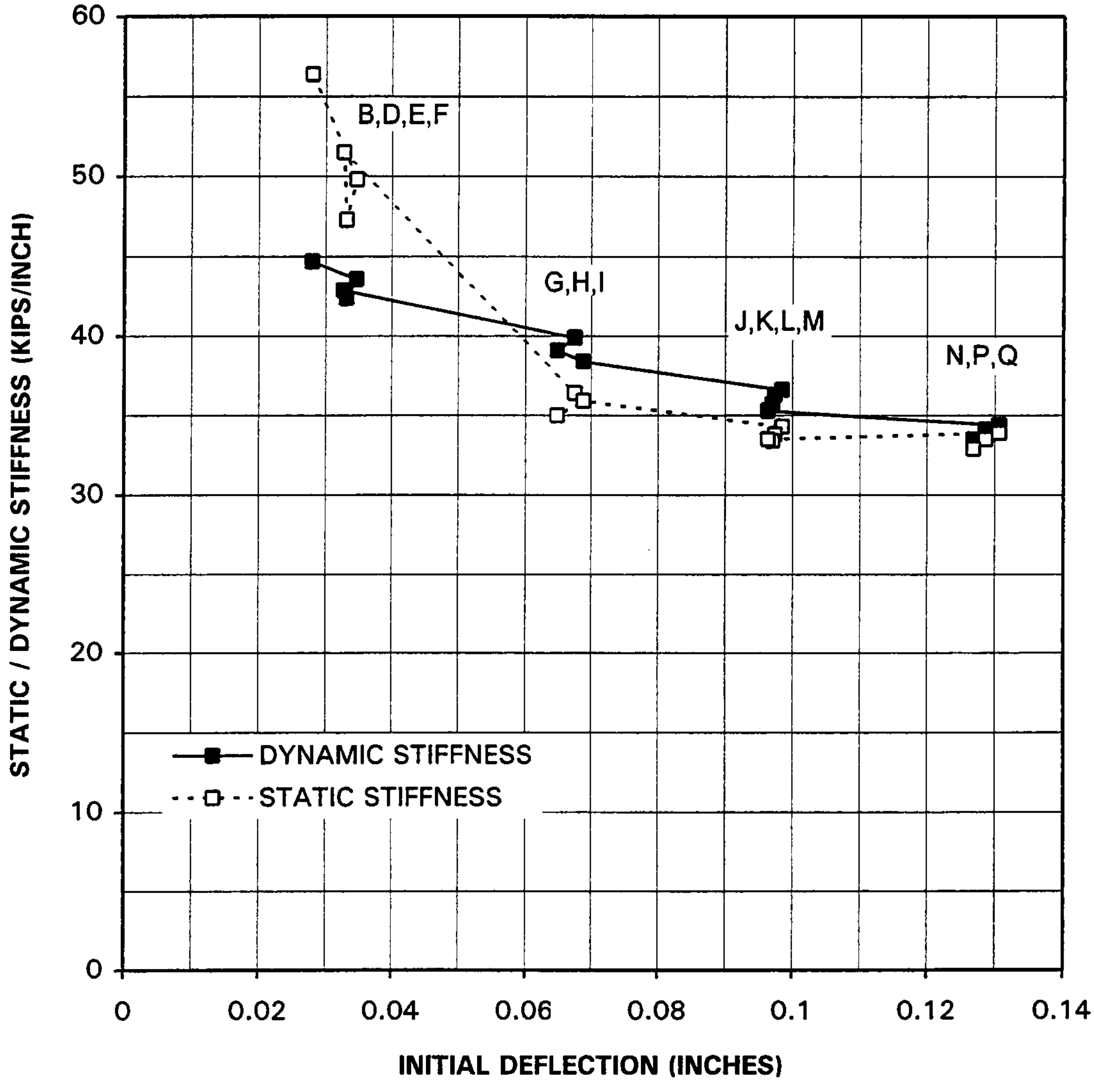

Figure 39 Static and dynamic stiffness vs initial defl. at center of mass; pile 2; 3-20-95 pile tests; load in x-direction.

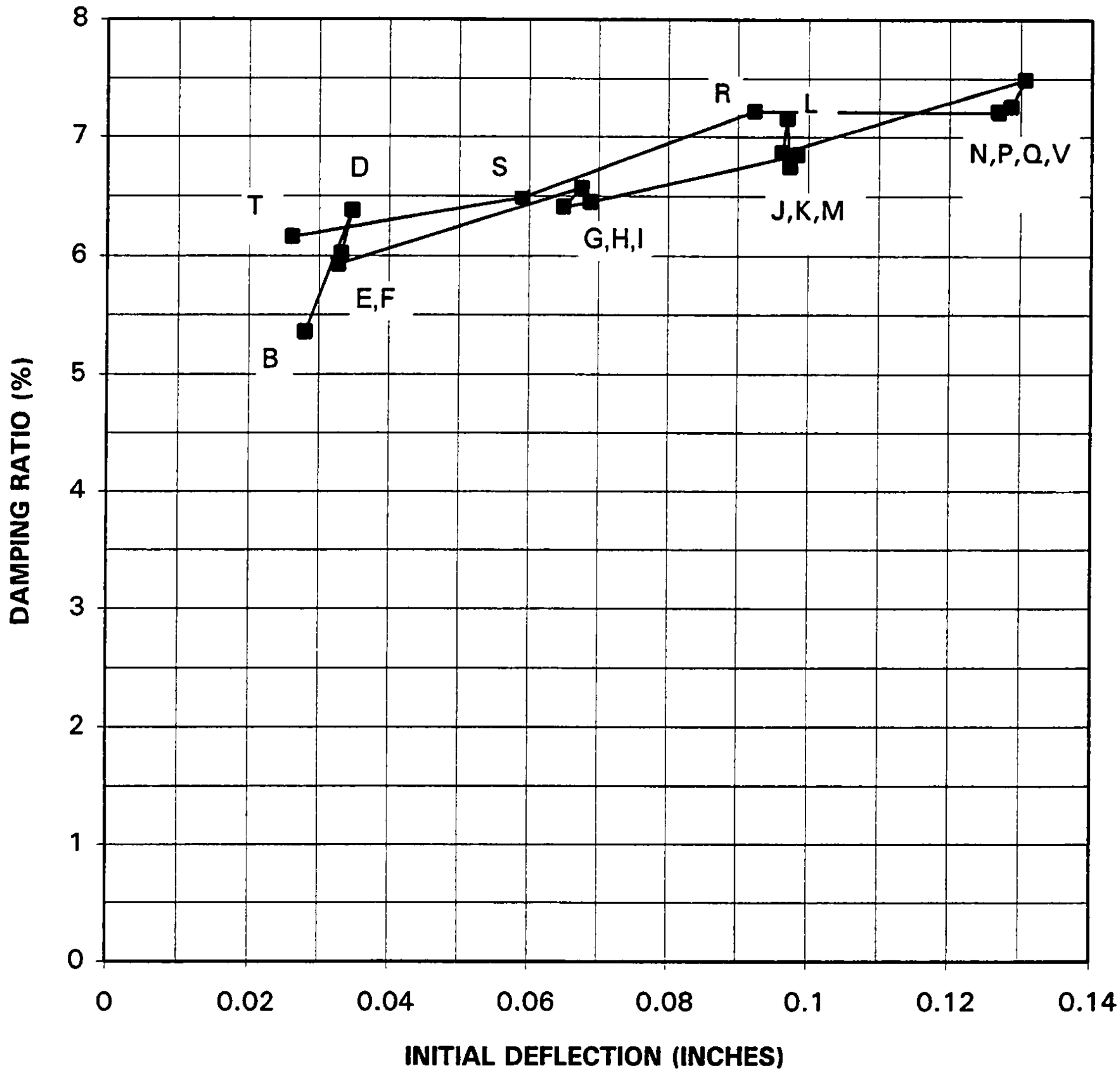

Figure 40 Damping ratio vs initial deflection at center of mass; pile 2; 3-20-95 pile tests; load in x-direction.

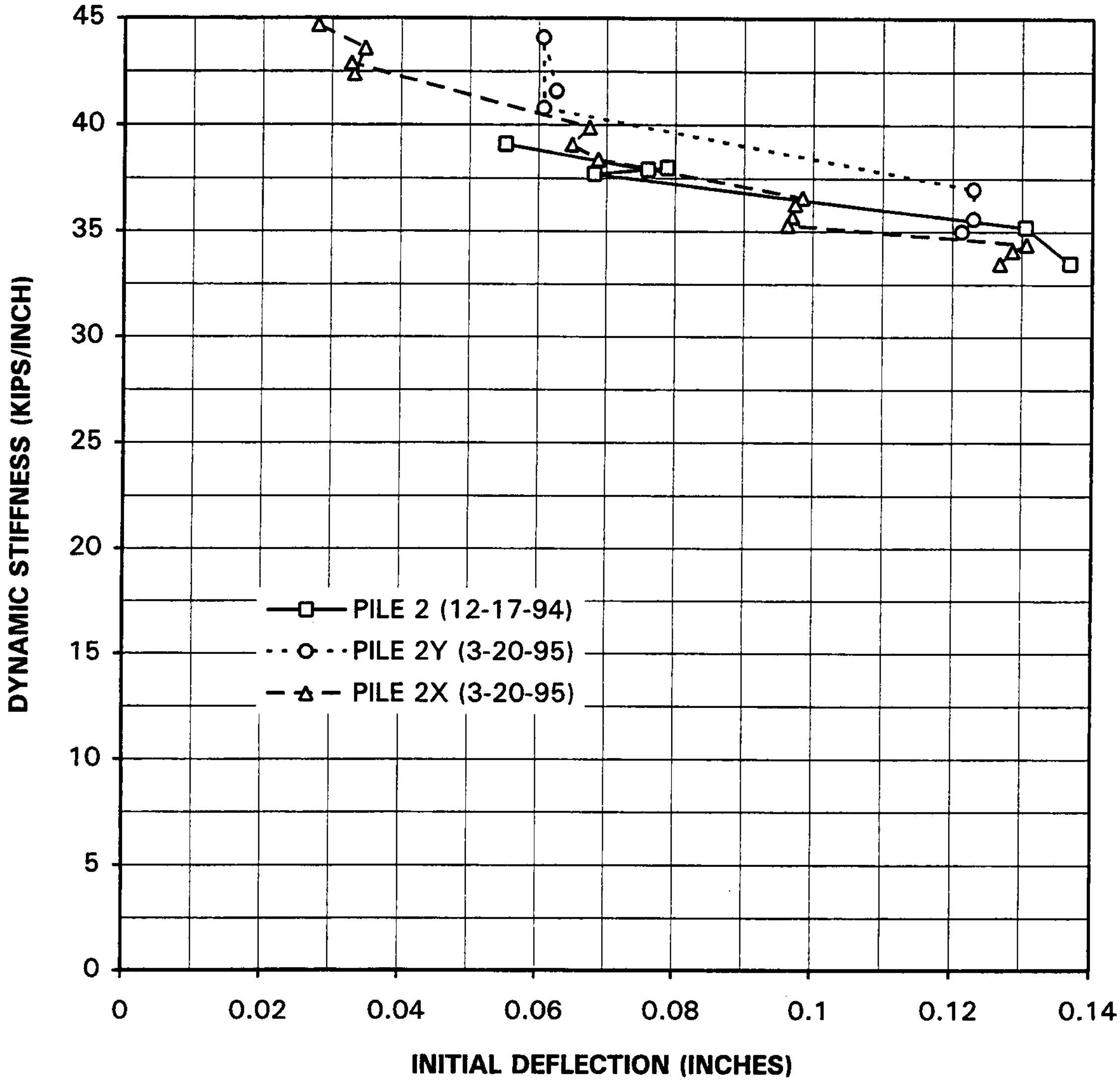

Figure 41 Dynamic stiffness vs initial deflection at center of mass; pile 2; all series of tests.

APPENDIX C

SAMPLE INPUT FILE FOR COMPUTER MODEL

```
STRUDL 'DECEMBER 17, 1994 PILE TESTS' 'PILE 1'
UNITS KIPS INCHES
TYPE PLANE FRAME
JOINT COORDINATES
1 0 26.75
2 0 9.25
3 0 0
4 0 -16.8
5 0 -33.6
6 0 -48.
7 0 -66.
8 0 -79.2
9 0 -93.6
10 0 -117.6
11 0 -141.6
12 0 -160.8
13 0 -180.
14 0 -204.
STATUS SUPPORT 3 TO 14
JOINT RELEASE
3 FORCE Y MOM Z KFX 4.45
4 FORCE Y MOM Z KFX 35.6
5 FORCE Y MOM Z KFX 57.0
6 FORCE Y MOM Z KFX 76.5
7 FORCE Y MOM Z KFX 77.9
8 FORCE Y MOM Z KFX 58.7
9 FORCE Y MOM Z KFX 98.6
10 FORCE Y MOM Z KFX 151.
11 FORCE Y MOM Z KFX 162.
12 FORCE Y MOM Z KFX 165.
13 FORCE Y MOM Z KFX 209.
14 MOM Z KFX 127.
GENERATE 13 MEMBERS ID 1,1 FROM 1,1 TO 2,1
CONSTANTS
E 4030 ALL
MATERIAL CONCRETE ALL
MEMBER PROPERTIES PRISMATIC
1 TO 13 AX 196. IZ 3201.
ADDITIONS
INERTIA OF JOINT WEIGHT
1 TRANSLATION ALL 10.018
INERTIA OF JOINTS CONSISTENT
EIGENPROBLEM
SOLVE USING GTLANZCOS
NUMBER OF MODES 5
END OF EIGENPROBLEM
DYNAMIC ANALYSIS EIGENVALUE
FINISH
LOAD 1
JOINT LOAD
2 FORCE X 5.0
STIFFNESS ANALYSIS
LOAD LIST 1
LIST DISPLACEMENTS 1 2 3
FINISH
```

APPENDIX D

TEST DATA

CYCLE	DISPLACEMENT AMPLITUDE (INCHES)		PERIOD (SECONDS)	
	POS.	NEG.	POS.	NEG.
1	0.01874	-0.02487	0.132	0.136
2	0.01247	-0.01465	0.124	0.128
3	0.00628	-0.00838	0.124	0.126
4	0.00288	-0.00463	0.128	0.128
5	0.00214	-0.00222	0.122	0.120

DISPL. PEAKS	DAMPING RATIO	
	POS.	NEG.
1-2	0.0648	0.0839
1-3	0.0867	0.0863
1-4	0.0988	0.0889
1-5	0.0861	0.0957
2-3	0.1086	0.0886
2-4	0.1157	0.0914
2-5	0.0932	0.0996
3-4	0.1228	0.0942
3-5	0.0855	0.1051
4-5	0.0477	0.1159

MEAN	0.0910	0.0949

TEST D; 12-16-94 PILE TESTS

CYCLE	DISPLACEMENT AMPLITUDE (INCHES)		PERIOD (SECONDS)	
	POS.	NEG.	POS.	NEG.
1	0.02568	-0.03578	0.140	0.146
2	0.01761	-0.02262	0.128	0.132
3	0.00883	-0.01289	0.132	0.132
4	0.00556	-0.00652	-----	-----
5	-----	-----	-----	-----

DISPL. PEAKS	DAMPING RATIO	
	POS.	NEG.
1-2	0.0600	0.0728
1-3	0.0846	0.0810
1-4	0.0809	0.0900
1-5	-----	-----
2-3	0.1092	0.0892
2-4	0.0914	0.0986
2-5	-----	-----
3-4	0.0735	0.1079
3-5	-----	-----
4-5	-----	-----

MEAN 0.0833 0.0899

TEST E; 12-16-94 PILE TESTS

CYCLE	DISPLACEMENT AMPLITUDE (INCHES)		PERIOD (SECONDS)	
	POS.	NEG.	POS.	NEG.
1	0.03578	-0.04911	0.148	0.154
2	0.02367	-0.03004	0.138	0.142
3	0.01268	-0.01604	0.142	0.140
4	0.00841	-0.00580	0.124	0.134
5	0.00535	-0.00330	-----	-----

DISPL. PEAKS	DAMPING RATIO	
	POS.	NEG.
1-2	0.0656	0.0780
1-3	0.0823	0.0887
1-4	0.0766	0.1126
1-5	0.0754	0.1068
2-3	0.0989	0.0994
2-4	0.0821	0.1298
2-5	0.0787	0.1163
3-4	0.0651	0.1598
3-5	0.0685	0.1248
4-5	0.0719	0.0893

MEAN 0.0765 0.1105

TEST F; 12-16-94 PILE TESTS

CYCLE	DISPLACEMENT AMPLITUDE (INCHES)		PERIOD (SECONDS)	
	POS.	NEG.	POS.	NEG.
1	0.04296	-0.07136	0.166	0.170
2	0.02442	-0.03220	0.158	0.166
3	0.01478	-0.01309	0.146	0.148
4	0.00920	-0.00540	0.134	0.142
5	0.00589	-0.00105	-----	-----

DISPL. PEAKS	DAMPING RATIO	
	POS.	NEG.
1-2	0.0895	0.1257
1-3	0.0846	0.1337
1-4	0.0815	0.1357
1-5	0.0788	0.1657
2-3	0.0796	0.1418
2-4	0.0775	0.1406
2-5	0.0752	0.1788
3-4	0.0753	0.1395
3-5	0.0730	0.1971
4-5	0.0707	0.2527

MEAN 0.0786 0.1611

TEST G; 12-16-94 PILE TESTS

CYCLE	DISPLACEMENT AMPLITUDE (INCHES)		PERIOD (SECONDS)	
	POS.	NEG.	POS.	NEG.
1	0.04004	-0.07545	0.191	0.188
2	0.02169	-0.03097	0.164	0.170
3	0.01202	-0.01367	0.150	0.160
4	0.00723	-0.00466	0.142	0.140
5	0.00559	-0.00142	-----	-----

DISPL. PEAKS	DAMPING RATIO	
	POS.	NEG.
1-2	0.0971	0.1403
1-3	0.0953	0.1347
1-4	0.0901	0.1462
1-5	0.0781	0.1563
2-3	0.0936	0.1291
2-4	0.0867	0.1491
2-5	0.0718	0.1616
3-4	0.0797	0.1689
3-5	0.0608	0.1776
4-5	0.0418	0.1862
MEAN	0.0795	0.1550

TEST H; 12-16-94 PILE TESTS

CYCLE	DISPLACEMENT AMPLITUDE (INCHES)		PERIOD (SECONDS)	
	POS.	NEG.	POS.	NEG.
1	0.04646	-0.08221	0,190	0.190
2	0.02595	-0.03833	0.183	0.178
3	0.01456	-0.01562	0.161	0.180
4	0.00814	-0.00634	0.162	0.169
5	0.00549	-0.00084	-----	-----

DISPL. PEAKS	DAMPING RATIO	
	POS.	NEG.
1-2	0.0923	0.1206
1-3	0.0919	0.1310
1-4	0.0920	0.1347
1-5	0.0846	0.1794
2-3	0.0916	0.1415
2-4	0.0919	0.1418
2-5	0.0821	0.1986
3-4	0.0922	0.1421
3-5	0.0773	0.2264
4-5	0.0624	0.3060

MEAN 0.0858 0.1722

TEST J; 12-16-94 PILE TESTS

CYCLE	DISPLACEMENT AMPLITUDE (INCHES)		PERIOD (SECONDS)	
	POS.	NEG.	POS.	NEG.
1	0.05323	-0.09449	0.190	0.192
2	0.02989	-0.04487	0.182	0.178
3	0.01631	-0.01850	0.160	0.178
4	0.00874	-0.00814	0.156	0.166
5	0.00655	-0.00081	-----	-----

DISPL. PEAKS	DAMPING RATIO	
	POS.	NEG.
1-2	0.0915	0.1177
1-3	0.0937	0.1287
1-4	0.0954	0.1290
1-5	0.0831	0.1861
2-3	0.0959	0.1396
2-4	0.0974	0.1346
2-5	0.0803	0.2084
3-4	0.0988	0.1296
3-5	0.0724	0.2417
4-5	0.0459	0.3449

MEAN 0.0854 0.1760

TEST K; 12-16-94 PILE TESTS

CYCLE	DISPLACEMENT AMPLITUDE (INCHES)		PERIOD (SECONDS)	
	POS.	NEG.	POS.	NEG.
1	0.05527	-0.10072	0.196	0.194
2	0.02974	-0.05095	0.180	0.184
3	0.01583	-0.02199	0.174	0.178
4	0.00751	-0.00919	0.156	0.166
5	0.00514	-0.00294	-----	-----

DISPL. PEAKS	DAMPING RATIO	
	POS.	NEG.
1-2	0.0982	0.1078
1-3	0.0990	0.1202
1-4	0.1053	0.1260
1-5	0.0941	0.1392
2-3	0.0998	0.1326
2-4	0.1089	0.1350
2-5	0.0928	0.1496
3-4	0.1179	0.1375
3-5	0.0892	0.1580
4-5	0.0603	0.1783

MEAN 0.0965 0.1384

TEST L; 12-16-94 PILE TESTS

CYCLE	DISPLACEMENT AMPLITUDE (INCHES)		PERIOD (SECONDS)	
	POS.	NEG.	POS.	NEG.
1	0.06329	-0.11558	0.206	0.206
2	0.03406	-0.05710	0.196	0.204
3	0.01977	-0.02184	0.192	0.188
4	0.01208	-0.00676	0.182	0.174
5	0.00700	-0.00096	-----	-----

DISPL. PEAKS	DAMPING RATIO	
	POS.	NEG.
1-2	0.0981	0.1115
1-3	0.0922	0.1315
1-4	0.0875	0.1490
1-5	0.0873	0.1873
2-3	0.0863	0.1512
2-4	0.0822	0.1674
2-5	0.0836	0.2118
3-4	0.0782	0.1835
3-5	0.0823	0.2413
4-5	0.0865	0.2966

MEAN 0.0864 0.1831

TEST M; 12-16-94 PILE TESTS

CYCLE	DISPLACEMENT AMPLITUDE (INCHES)		PERIOD (SECONDS)	
	POS.	NEG.	POS.	NEG.
1	0.06148	-0.12117	0.212	0.208
2	0.02907	-0.06362	0.204	0.210
3	0.01411	-0.02779	0.198	0.202
4	0.00817	-0.01004	0.194	0.198
5	0.00471	-0.00298	-----	-----

DISPL. PEAKS	DAMPING RATIO	
	POS.	NEG.
1-2	0.1184	0.1020
1-3	0.1163	0.1164
1-4	0.1065	0.1310
1-5	0.1017	0.1459
2-3	0.1143	0.1307
2-4	0.1005	0.1454
2-5	0.0961	0.1603
3-4	0.0866	0.1600
3-5	0.0869	0.1749
4-5	0.0873	0.1897
MEAN	0.1015	0.1456

TEST N; 12-16-94 PILE TESTS

CYCLE	DISPLACEMENT AMPLITUDE (INCHES)		PERIOD (SECONDS)	
	POS.	NEG.	POS.	NEG.
1	0.04334	-0.09747	0.212	0.208
2	0.02076	-0.04172	0.204	0.208
3	0.01018	-0.01673	0.198	0.202
4	0.00394	-0.00711	0.182	0.198
5	0.00249	-0.00327	-----	-----

DISPL. PEAKS	DAMPING RATIO	
	POS.	NEG.
1-2	0.1164	0.1338
1-3	0.1145	0.1389
1-4	0.1263	0.1375
1-5	0.1129	0.1338
2-3	0.1126	0.1439
2-4	0.1312	0.1394
2-5	0.1117	0.1338
3-4	0.1496	0.1349
3-5	0.1113	0.1287
4-5	0.0725	0.1226

MEAN 0.1159 0.1347

TEST O; 12-16-94 PILE TESTS

CYCLE	DISPLACEMENT AMPLITUDE (INCHES)		PERIOD (SECONDS)	
	POS.	NEG.	POS.	NEG.
1	0.03390	-0.07662	0.214	0.216
2	0.01469	-0.02928	0.196	0.204
3	0.00700	-0.01030	0.186	0.204
4	0.00508	-0.00550	-----	-----
5	-----	-----	-----	-----

DISPL. PEAKS	DAMPING RATIO	
	POS.	NEG.
1-2	0.1319	0.1513
1-3	0.1246	0.1577
1-4	0.1002	0.1385
1-5	-----	-----
2-3	0.1172	0.1640
2-4	0.0842	0.1320
2-5	-----	-----
3-4	0.0510	0.0995
3-5	-----	-----
4-5	-----	-----

MEAN 0.1015 0.1405

TEST P; 12-16-94 PILE TESTS

CYCLE	DISPLACEMENT AMPLITUDE (INCHES)		PERIOD (SECONDS)	
	POS.	NEG.	POS.	NEG.
1	0.06966	-0.15526	0.238	0.234
2	0.03025	-0.05626	0.240	0.240
3	0.01199	-0.02550	0.220	0.220
4	0.00622	-0.01084	-----	-----
5	-----	-----	-----	-----

DISPL. PEAKS	DAMPING RATIO	
	POS.	NEG.
1-2	0.1316	0.1595
1-3	0.1387	0.1423
1-4	0.1271	0.1398
1-5	-----	-----
2-3	0.1458	0.1250
2-4	0.1249	0.1299
2-5	-----	-----
3-4	0.1039	0.1349
3-5	-----	-----

TEST Q; 12-16-94 PILE TESTS

CYCLE	DISPLACEMENT AMPLITUDE (INCHES)		PERIOD (SECONDS)	
	POS.	NEG.	POS.	NEG.
1	0.06960	-0.13535	0.244	0.234
2	0.03764	-0.06263	0.234	0.256
3	0.01619	-0.01976	0.228	0.232
4	0.00652	-0.00730	0.210	0.214
5	0.00436	-0.00282	-----	-----

DISPL. PEAKS	DAMPING RATIO	
	POS.	NEG.
1-2	0.0974	0.1217
1-3	0.1153	0.1513
1-4	0.1247	0.1531
1-5	0.1096	0.1522
2-3	0.1331	0.1806
2-4	0.1382	0.1686
2-5	0.1136	0.1623
3-4	0.1433	0.1566
3-5	0.1038	0.1531
4-5	0.0639	0.1497
MEAN	0.1143	0.1549

TEST R; 12-16-94 PILE TESTS

CYCLE	DISPLACEMENT AMPLITUDE (INCHES)		PERIOD (SECONDS)	
	POS.	NEG.	POS.	NEG.
1	0.12186	-0.23017	0.278	0.256
2	0.05722	-0.10330	0.246	0.260
3	0.02646	-0.03938	0.252	0.260
4	0.00820	-0.01775	0.232	0.226
5	0.00435	-0.00718	-----	-----

DISPL. PEAKS	DAMPING RATIO	
	POS.	NEG.
1-2	0.1195	0.1265
1-3	0.1206	0.1391
1-4	0.1217	0.1347
1-5	0.1315	0.1367
2-3	0.1218	0.1517
2-4	0.1528	0.1388
2-5	0.1354	0.1401
3-4	0.1833	0.1258
3-5	0.1422	0.1342
4-5	0.1004	0.1426

MEAN 0.1329 0.1370

TEST S; 12-16-94 PILE TESTS

CYCLE	DISPLACEMENT AMPLITUDE (INCHES)		PERIOD (SECONDS)	
	POS.	NEG.	POS.	NEG.
1	0.17656	-0.36507	0.276	0.262
2	0.09750	-0.15601	0.286	0.282
3	0.04632	-0.07575	0.310	0.278
4	0.01749	-0.02865	0.206	0.252
5	0.00884	-0.01135	-----	-----

DISPL. PEAKS	DAMPING RATIO	
	POS.	NEG.
1-2	0.0941	0.1341
1-3	0.1059	0.1242
1-4	0.1218	0.1338
1-5	0.1183	0.1368
2-3	0.1176	0.1142
2-4	0.1355	0.1337
2-5	0.1263	0.1377
3-4	0.1532	0.1529
3-5	0.1307	0.1494
4-5	0.1079	0.1458

MEAN 0.1211 0.1363

TEST T; 12-16-94 PILE TESTS

CYCLE	DISPLACEMENT AMPLITUDE (INCHES)		PERIOD (SECONDS)	
	POS.	NEG.	POS.	NEG.
1	0.16934	-0.28578	0.286	0.272
2	0.09437	-0.15169	0.296	0.292
3	0.04439	-0.07287	0.260	0.282
4	0.01940	-0.02674	0.162	0.258
5	0.00979	-0.01040	-----	-----

DISPL. PEAKS	DAMPING RATIO	
	POS.	NEG.
1-2	0.0927	0.1003
1-3	0.1059	0.1081
1-4	0.1142	0.1247
1-5	0.1127	0.1307
2-3	0.1192	0.1159
2-4	0.1249	0.1368
2-5	0.1194	0.1408
3-4	0.1306	0.1576
3-5	0.1194	0.1531
4-5	0.1082	0.1486

MEAN 0.1147 0.1317

TEST U; 12-16-94 PILE TESTS

CYCLE	DISPLACEMENT AMPLITUDE (INCHES)		PERIOD (SECONDS)	
	POS.	NEG.	POS.	NEG.
1	0.19403	-0.34039	0.292	0.276
2	0.11137	-0.18275	0.296	0.294
3	0.05370	-0.09144	0.286	0.294
4	0.02246	-0.03762	0.262	0.282
5	-----	-----	-----	-----

DISPL. PEAKS	DAMPING RATIO	
	POS.	NEG.
1-2	0.0880	0.0985
1-3	0.1017	0.1040
1-4	0.1137	0.1161
1-5	-----	-----
2-3	0.1153	0.1095
2-4	0.1264	0.1248
2-5	-----	-----
3-4	0.1374	0.1400
3-5	-----	-----
4-5	-----	-----

MEAN 0.1137 0.1155

TEST V; 12-16-94 PILE TESTS

CYCLE	DISPLACEMENT AMPLITUDE (INCHES)		PERIOD (SECONDS)	
	POS.	NEG.	POS.	NEG.
1	0.04316	-0.04349	0.166	0.160
2	0.02586	-0.02727	0.160	0.166
3	0.02241	-0.02324	0.164	0.158
4	0.01283	-0.01490	0.160	0.170
5	0.01247	-0.01184	0.158	0.158

DISPL. PEAKS	DAMPING RATIO	
	POS.	NEG.
1-2	0.0813	0.0741
1-3	0.0521	0.0498
1-4	0.0643	0.0567
1-5	0.0494	0.0517
2-3	0.0228	0.0254
2-4	0.0557	0.0481
2-5	0.0387	0.0442
3-4	0.0884	0.0706
3-5	0.0466	0.0536
4-5	0.0045	0.0366

MEAN 0.0504 0.0511

TEST B; 12-17-94 PILE TESTS

CYCLE	DISPLACEMENT AMPLITUDE (INCHES)		PERIOD (SECONDS)	
	POS.	NEG.	POS.	NEG.
1	0.03235	-0.03340	0.166	0.164
2	0.01926	-0.02238	0.164	0.164
3	0.01384	-0.01508	0.166	0.164
4	0.00712	-0.00982	0.166	0.164
5	0.00436	-0.00643	-----	-----

DISPL. PEAKS	DAMPING RATIO	
	POS.	NEG.
1-2	0.0823	0.0636
1-3	0.0674	0.0631
1-4	0.0801	0.0648
1-5	0.0795	0.0654
2-3	0.0525	0.0627
2-4	0.0790	0.0654
2-5	0.0786	0.0660
3-4	0.1053	0.0682
3-5	0.0916	0.0677
4-5	0.0779	0.0673

MEAN 0.0794 0.0654

TEST D; 12-17-94 PILE TESTS

CYCLE	DISPLACEMENT AMPLITUDE (INCHES)		PERIOD (SECONDS)	
	POS.	NEG.	POS.	NEG.
1	0.03689	-0.03118	0.164	0.162
2	0.02424	-0.02106	0.162	0.164
3	0.01772	-0.01508	0.160	0.160
4	0.01214	-0.01006	0.164	0.164
5	0.01105	-0.00757	-----	-----

DISPL. PEAKS	DAMPING RATIO	
	POS.	NEG.
1-2	0.0667	0.0624
1-3	0.0582	0.0577
1-4	0.0589	0.0599
1-5	0.0479	0.0562
2-3	0.0498	0.0530
2-4	0.0550	0.0587
2-5	0.0416	0.0542
3-4	0.0602	0.0643
3-5	0.0376	0.0548
4-5	0.0148	0.0452

MEAN 0.0491 0.0566

TEST E; 12-17-94 PILE TESTS

CYCLE	DISPLACEMENT AMPLITUDE (INCHES)		PERIOD (SECONDS)	
	POS.	NEG.	POS.	NEG.
1	0.03959	-0.03703	0.162	0.166
2	0.02845	-0.02589	0.164	0.162
3	0.02031	-0.01727	0.160	0.164
4	0.01375	-0.01327	0.162	0.164
5	0.01046	-0.00799	0.160	0.160

DISPL. PEAKS	DAMPING RATIO	
	POS.	NEG.
1-2	0.0525	0.0569
1-3	0.0531	0.0606
1-4	0.0560	0.0544
1-5	0.0529	0.0609
2-3	0.0536	0.0643
2-4	0.0577	0.0531
2-5	0.0530	0.0623
3-4	0.0619	0.0419
3-5	0.0528	0.0612
4-5	0.0436	0.0805

MEAN 0.0537 0.0596

TEST F; 12-17-94 PILE TESTS

CYCLE	DISPLACEMENT AMPLITUDE (INCHES)		PERIOD (SECONDS)	
	POS.	NEG.	POS.	NEG.
1	0.04299	-0.03577	0.166	0.166
2	0.03018	-0.02421	0.166	0.166
3	0.02147	-0.01691	0.164	0.166
4	0.01646	-0.01115	0.160	0.166
5	0.01150	-0.00712	0.164	0.162

DISPL. PEAKS	DAMPING RATIO	
	POS.	NEG.
1-2	0.0562	0.0620
1-3	0.0552	0.0595
1-4	0.0509	0.0617
1-5	0.0524	0.0641
2-3	0.0541	0.0570
2-4	0.0482	0.0616
2-5	0.0511	0.0648
3-4	0.0423	0.0662
3-5	0.0496	0.0687
4-5	0.0570	0.0712

MEAN 0.0517 0.0637

TEST G; 12-17-94 PILE TESTS

CYCLE	DISPLACEMENT AMPLITUDE (INCHES)		PERIOD (SECONDS)	
	POS.	NEG.	POS.	NEG.
1	0.03868	-0.03671	0.166	0.166
2	0.02636	-0.02557	0.168	0.164
3	0.01756	-0.01815	0.164	0.164
4	0.01291	-0.01290	0.162	0.162
5	0.00876	-0.00902	0.164	0.164

DISPL. PEAKS	DAMPING RATIO	
	POS.	NEG.
1-2	0.0609	0.0575
1-3	0.0627	0.0560
1-4	0.0581	0.0554
1-5	0.0590	0.0558
2-3	0.0645	0.0545
2-4	0.0568	0.0544
2-5	0.0583	0.0552
3-4	0.0490	0.0543
3-5	0.0553	0.0555
4-5	0.0615	0.0568

MEAN 0.0586 0.0555

TEST H; 12-17-94 PILE TESTS

CYCLE	DISPLACEMENT AMPLITUDE (INCHES)		PERIOD (SECONDS)	
	POS.	NEG.	POS.	NEG.
1	0.04653	-0.04316	0.166	0.168
2	0.03409	-0.02943	0.166	0.166
3	0.02364	-0.02054	0.164	0.164
4	0.01688	-0.01412	0.164	0.164
5	0.01202	-0.00928	0.164	0.164

DISPL. PEAKS	DAMPING RATIO	
	POS.	NEG.
1-2	0.0495	0.0608
1-3	0.0538	0.0590
1-4	0.0537	0.0592
1-5	0.0538	0.0610
2-3	0.0582	0.0571
2-4	0.0559	0.0584
2-5	0.0552	0.0611
3-4	0.0536	0.0596
3-5	0.0538	0.0631
4-5	0.0540	0.0666

MEAN	0.0541	0.0606

TEST I; 12-17-94 PILE TESTS

CYCLE	DISPLACEMENT AMPLITUDE (INCHES)		PERIOD (SECONDS)	
	POS.	NEG.	POS.	NEG.
1	0.07329	-0.07761	0.174	0.174
2	0.04830	-0.05262	0.174	0.172
3	0.03196	-0.03532	0.170	0.172
4	0.02235	-0.02379	0.172	0.172
5	0.01514	-0.01610	0.164	0.164

DISPL. PEAKS	DAMPING RATIO	
	POS.	NEG.
1-2	0.0662	0.0617
1-3	0.0659	0.0625
1-4	0.0629	0.0626
1-5	0.0626	0.0625
2-3	0.0656	0.0633
2-4	0.0612	0.0630
2-5	0.0614	0.0627
3-4	0.0569	0.0627
3-5	0.0594	0.0624
4-5	0.0618	0.0621

MEAN 0.0624 0.0626

TEST J; 12-17-94 PILE TESTS

CYCLE	DISPLACEMENT AMPLITUDE (INCHES)		PERIOD (SECONDS)	
	POS.	NEG.	POS.	NEG.
1	0.07869	-0.08182	0.176	0.176
2	0.05178	-0.05831	0.176	0.178
3	0.03353	-0.03472	0.176	0.174
4	0.02295	-0.02295	0.174	0.174
5	0.01429	-0.01358	0.176	0.172

DISPL. PEAKS	DAMPING RATIO	
	POS.	NEG.
1-2	0.0665	0.0539
1-3	0.0677	0.0681
1-4	0.0653	0.0673
1-5	0.0677	0.0713
2-3	0.0690	0.0822
2-4	0.0646	0.0740
2-5	0.0681	0.0771
3-4	0.0602	0.0658
3-5	0.0677	0.0745
4-5	0.0751	0.0833

MEAN 0.0672 0.0717

TEST K; 12-17-94 PILE TESTS

CYCLE	DISPLACEMENT AMPLITUDE (INCHES)		PERIOD (SECONDS)	
	POS.	NEG.	POS.	NEG.
1	0.07286	-0.07179	0.178	0.178
2	0.04836	-0.04488	0.176	0.178
3	0.03322	-0.02713	0.176	0.176
4	0.02420	-0.01607	0.174	0.174
5	0.01649	-0.01148	0.170	0.174

DISPL. PEAKS	DAMPING RATIO	
	POS.	NEG.
1-2	0.0651	0.0746
1-3	0.0624	0.0772
1-4	0.0584	0.0792
1-5	0.0590	0.0728
2-3	0.0597	0.0799
2-4	0.0550	0.0815
2-5	0.0570	0.0722
3-4	0.0503	0.0830
3-5	0.0557	0.0683
4-5	0.0610	0.0535
MEAN	0.0584	0.0742

TEST M; 12-17-94 PILE TESTS

CYCLE	DISPLACEMENT AMPLITUDE (INCHES)		PERIOD (SECONDS)	
	POS.	NEG.	POS.	NEG.
1	0.07219	-0.07777	0.182	0.180
2	0.04911	-0.04893	0.178	0.178
3	0.03196	-0.02973	0.178	0.180
4	0.02332	-0.01790	0.176	0.174
5	0.01568	-0.01087	-----	-----

DISPL. PEAKS	DAMPING RATIO	
	POS.	NEG.
1-2	0.0612	0.0736
1-3	0.0647	0.0763
1-4	0.0598	0.0777
1-5	0.0606	0.0781
2-3	0.0682	0.0790
2-4	0.0592	0.0798
2-5	0.0605	0.0796
3-4	0.0501	0.0805
3-5	0.0566	0.0798
4-5	0.0630	0.0791

MEAN 0.0604 0.0783

TEST N; 12-17-94 PILE TESTS

CYCLE	DISPLACEMENT AMPLITUDE (INCHES)		PERIOD (SECONDS)	
	POS.	NEG.	POS.	NEG.
1	0.07215	-0.07209	0.182	0.182
2	0.04730	-0.04409	0.180	0.182
3	0.03139	-0.02767	0.180	0.178
4	0.02343	-0.01733	0.178	0.170
5	0.01474	-0.01103	0.170	0.180

DISPL. PEAKS	DAMPING RATIO	
	POS.	NEG.
1-2	0.0670	0.0780
1-3	0.0661	0.0760
1-4	0.0596	0.0754
1-5	0.0631	0.0745
2-3	0.0651	0.0740
2-4	0.0558	0.0741
2-5	0.0617	0.0733
3-4	0.0465	0.0742
3-5	0.0600	0.0730
4-5	0.0735	0.0718

MEAN 0.0618 0.0744

TEST O; 12-17-94 PILE TESTS

CYCLE	DISPLACEMENT AMPLITUDE (INCHES)		PERIOD (SECONDS)	
	POS.	NEG.	POS.	NEG.
1	0.06509	-0.07140	0.184	0.182
2	0.04347	-0.04593	0.180	0.182
3	0.02929	-0.03054	0.180	0.182
4	0.02136	-0.01901	0.180	0.176
5	0.01463	-0.01228	0.180	0.176

DISPL. PEAKS	DAMPING RATIO	
	POS.	NEG.
1-2	0.0641	0.0701
1-3	0.0634	0.0674
1-4	0.0590	0.0700
1-5	0.0593	0.0699
2-3	0.0627	0.0648
2-4	0.0565	0.0700
2-5	0.0577	0.0698
3-4	0.0502	0.0752
3-5	0.0552	0.0723
4-5	0.0602	0.0694

MEAN 0.0588 0.0699

TEST P; 12-17-94 PILE TESTS

CYCLE	DISPLACEMENT AMPLITUDE (INCHES)		PERIOD (SECONDS)	
	POS.	NEG.	POS.	NEG.
1	0.07389	-0.07539	0.184	0.184
2	0.04982	-0.04680	0.182	0.182
3	0.03421	-0.02920	0.182	0.182
4	0.02363	-0.01797	0.180	0.180
5	0.01712	-0.01082	-----	-----

DISPL. PEAKS	DAMPING RATIO	
	POS.	NEG.
1-2	0.0626	0.0757
1-3	0.0612	0.0753
1-4	0.0604	0.0759
1-5	0.0581	0.0770
2-3	0.0597	0.0749
2-4	0.0593	0.0760
2-5	0.0566	0.0775
3-4	0.0588	0.0771
3-5	0.0550	0.0788
4-5	0.0513	0.0805

MEAN 0.0583 0.0768

TEST Q; 12-17-94 PILE TESTS

CYCLE	DISPLACEMENT AMPLITUDE (INCHES)		PERIOD (SECONDS)	
	POS.	NEG.	POS.	NEG.
1	0.07338	-0.08090	0.184	0.186
2	0.04935	-0.05109	0.184	0.182
3	0.03253	-0.03283	0.180	0.184
4	0.02481	-0.01932	0.184	0.182
5	0.01808	-0.01139	0.180	0.180

DISPL. PEAKS	DAMPING RATIO	
	POS.	NEG.
1-2	0.0630	0.0729
1-3	0.0646	0.0716
1-4	0.0574	0.0758
1-5	0.0557	0.0778
2-3	0.0662	0.0702
2-4	0.0546	0.0772
2-5	0.0532	0.0794
3-4	0.0431	0.0841
3-5	0.0467	0.0840
4-5	0.0503	0.0838
MEAN	0.0555	0.0777

TEST R; 12-17-94 PILE TESTS

CYCLE	DISPLACEMENT AMPLITUDE (INCHES)		PERIOD (SECONDS)	
	POS.	NEG.	POS.	NEG.
1	0.03388	-0.02325	0.158	0.160
2	0.02313	-0.01496	0.156	0.156
3	0.01574	-0.00988	0.158	0.158
4	0.01229	-0.00496	0.148	0.154
5	0.00994	-0.00306	0.158	-----

DISPL. PEAKS	DAMPING RATIO	
	POS.	NEG.
1-2	0.0607	0.0700
1-3	0.0609	0.0679
1-4	0.0537	0.0817
1-5	0.0487	0.0804
2-3	0.0611	0.0658
2-4	0.0503	0.0876
2-5	0.0447	0.0838
3-4	0.0394	0.1092
3-5	0.0365	0.0928
4-5	0.0337	0.0763

MEAN 0.0490 0.0816

TEST B; 3-20-95 PILE TESTS; LOAD IN Y-DIRECTION

CYCLE	DISPLACEMENT AMPLITUDE (INCHES)		PERIOD (SECONDS)	
	POS.	NEG.	POS.	NEG.
1	0.03154	-0.02634	0.156	0.160
2	0.02211	-0.01454	0.156	0.158
3	0.01493	-0.00850	0.160	0.158
4	0.01238	-0.00384	-----	0.154
5	0.00874	-0.00300	0.160	0.156

DISPL. PEAKS	DAMPING RATIO	
	POS.	NEG.
1-2	0.0565	0.0942
1-3	0.0594	0.0896
1-4	0.0496	0.1016
1-5	0.0510	0.0861
2-3	0.0624	0.0851
2-4	0.0461	0.1053
2-5	0.0492	0.0834
3-4	0.0298	0.1253
3-5	0.0426	0.0825
4-5	0.0553	0.0393

MEAN 0.0502 0.0892

TEST C; 3-20-95 PILE TESTS; LOAD IN Y-DIRECTION

CYCLE	DISPLACEMENT AMPLITUDE (INCHES)		PERIOD (SECONDS)	
	POS.	NEG.	POS.	NEG.
1	0.03586	-0.03283	0.160	0.160
2	0.02328	-0.02307	0.162	0.158
3	0.01556	-0.01556	0.158	0.162
4	0.01259	-0.00652	0.158	0.158
5	0.00808	-0.00451	0.156	0.156

DISPL. PEAKS	DAMPING RATIO	
	POS.	NEG.
1-2	0.0686	0.0561
1-3	0.0663	0.0593
1-4	0.0555	0.0855
1-5	0.0592	0.0788
2-3	0.0640	0.0626
2-4	0.0489	0.1001
2-5	0.0560	0.0863
3-4	0.0337	0.1372
3-5	0.0521	0.0981
4-5	0.0704	0.0587

MEAN 0.0575 0.0823

TEST D; 3-20-95 PILE TESTS; LOAD IN Y-DIRECTION

CYCLE	DISPLACEMENT AMPLITUDE (INCHES)		PERIOD (SECONDS)	
	POS.	NEG.	POS.	NEG.
1	0.07317	-0.06524	0.168	0.170
2	0.05031	-0.04166	0.172	0.168
3	0.03139	-0.02685	0.166	0.160
4	0.02235	-0.01688	0.170	0.160
5	0.01670	-0.00856	-----	-----

DISPL. PEAKS	DAMPING RATIO	
	POS.	NEG.
1-2	0.0595	0.0712
1-3	0.0672	0.0705
1-4	0.0628	0.0715
1-5	0.0587	0.0805
2-3	0.0749	0.0697
2-4	0.0644	0.0717
2-5	0.0584	0.0837
3-4	0.0540	0.0737
3-5	0.0502	0.0906
4-5	0.0463	0.1074

MEAN 0.0596 0.0791

TEST E; 3-20-95 PILE TESTS; LOAD IN Y-DIRECTION

CYCLE	DISPLACEMENT AMPLITUDE (INCHES)		PERIOD (SECONDS)	
	POS.	NEG.	POS.	NEG.
1	0.07419	-0.06446	0.172	0.172
2	0.05070	-0.04250	0.174	0.174
3	0.03403	-0.02358	0.166	0.168
4	0.02391	-0.01568	0.170	0.172
5	0.01679	-0.00823	0.164	0.168

DISPL. PEAKS	DAMPING RATIO	
	POS.	NEG.
1-2	0.0605	0.0661
1-3	0.0619	0.0798
1-4	0.0600	0.0748
1-5	0.0590	0.0816
2-3	0.0633	0.0934
2-4	0.0597	0.0791
2-5	0.0585	0.0868
3-4	0.0561	0.0648
3-5	0.0561	0.0835
4-5	0.0562	0.1020
MEAN	0.0591	0.0812

TEST F; 3-20-95 PILE TESTS; LOAD IN Y-DIRECTION

CYCLE	DISPLACEMENT AMPLITUDE (INCHES)		PERIOD (SECONDS)	
	POS.	NEG.	POS.	NEG.
1	0.07263	-0.06623	0.172	0.176
2	0.04893	-0.04421	0.174	0.172
3	0.03385	-0.02580	0.170	0.172
4	0.02298	-0.01694	0.168	0.172
5	0.01697	-0.00874	0.172	0.166

DISPL. PEAKS	DAMPING RATIO	
	POS.	NEG.
1-2	0.0627	0.0642
1-3	0.0606	0.0748
1-4	0.0609	0.0721
1-5	0.0578	0.0803
2-3	0.0585	0.0854
2-4	0.0600	0.0761
2-5	0.0561	0.0857
3-4	0.0615	0.0668
3-5	0.0549	0.0858
4-5	0.0482	0.1047

MEAN 0.0581 0.0796

TEST G; 3-20-95 PILE TESTS; LOAD IN Y-DIRECTION

CYCLE	DISPLACEMENT AMPLITUDE (INCHES)		PERIOD (SECONDS)	
	POS.	NEG.	POS.	NEG.
1	0.01727	-0.01379	0.154	0.154
2	0.01397	-0.00874	0.148	0.156
3	0.00871	-0.00826	0.152	0.150
4	0.00646	-0.00487	0.148	0.150
5	0.00571	-0.00282	-----	-----

DISPL. PEAKS	DAMPING RATIO	
	POS.	NEG.
1-2	0.0338	0.0723
1-3	0.0544	0.0407
1-4	0.0521	0.0552
1-5	0.0440	0.0630
2-3	0.0749	0.0090
2-4	0.0613	0.0466
2-5	0.0474	0.0598
3-4	0.0476	0.0839
3-5	0.0336	0.0851
4-5	0.0197	0.0863

MEAN 0.0469 0.0602

TEST B; 3-20-95 PILE TESTS; LOAD IN X-DIRECTION

CYCLE	DISPLACEMENT AMPLITUDE (INCHES)		PERIOD (SECONDS)	
	POS.	NEG.	POS.	NEG.
1	0.02148	-0.02006	0.154	0.156
2	0.01451	-0.01283	0.154	0.152
3	0.00961	-0.00883	0.152	0.154
4	0.00670	-0.00553	0.154	0.152
5	0.00469	-0.00372	-----	-----

DISPL. PEAKS	DAMPING RATIO	
	POS.	NEG.
1-2	0.0623	0.0710
1-3	0.0638	0.0652
1-4	0.0617	0.0682
1-5	0.0605	0.0669
2-3	0.0654	0.0593
2-4	0.0614	0.0668
2-5	0.0598	0.0655
3-4	0.0574	0.0744
3-5	0.0571	0.0685
4-5	0.0568	0.0627

MEAN 0.0606 0.0669

TEST D; 3-20-95 PILE TESTS; LOAD IN X-DIRECTION

CYCLE	DISPLACEMENT AMPLITUDE (INCHES)		PERIOD (SECONDS)	
	POS.	NEG.	POS.	NEG.
1	0.02064	-0.01907	0.156	0.158
2	0.01370	-0.01367	0.158	0.154
3	0.00913	-0.00889	0.150	0.156
4	0.00580	-0.00685	-----	0.158
5	0.00484	-0.00399	-----	-----

DISPL. PEAKS	DAMPING RATIO	
	POS.	NEG.
1-2	0.0651	0.0530
1-3	0.0647	0.0606
1-4	0.0672	0.0543
1-5	0.0576	0.0621
2-3	0.0644	0.0683
2-4	0.0683	0.0549
2-5	0.0551	0.0651
3-4	0.0721	0.0415
3-5	0.0505	0.0635
4-5	0.0288	0.0855
MEAN	0.0594	0.0609

TEST E; 3-20-95 PILE TESTS; LOAD IN X-DIRECTION

CYCLE	DISPLACEMENT AMPLITUDE (INCHES)		PERIOD (SECONDS)	
	POS.	NEG.	POS.	NEG.
1	0.02088	-0.01922	0.156	0.158
2	0.01409	-0.01295	0.154	0.156
3	0.00919	-0.00934	0.154	0.154
4	0.00631	-0.00580	0.152	0.154
5	0.00469	-0.00454	-----	-----

DISPL. PEAKS	DAMPING RATIO	
	POS.	NEG.
1-2	0.0625	0.0628
1-3	0.0651	0.0573
1-4	0.0634	0.0635
1-5	0.0593	0.0574
2-3	0.0678	0.0519
2-4	0.0638	0.0638
2-5	0.0583	0.0556
3-4	0.0598	0.0757
3-5	0.0535	0.0574
4-5	0.0473	0.0390

MEAN 0.0601 0.0584

TEST F; 3-20-95 PILE TESTS; LOAD IN X-DIRECTION

CYCLE	DISPLACEMENT AMPLITUDE (INCHES)		PERIOD (SECONDS)	
	POS.	NEG.	POS.	NEG.
1	0.04025	-0.03725	0.164	0.162
2	0.02661	-0.02388	0.162	0.164
3	0.01805	-0.01547	0.164	0.160
4	0.01250	-0.01039	0.158	0.160
5	0.00808	-0.00661	0.154	0.158

DISPL. PEAKS	DAMPING RATIO	
	POS.	NEG.
1-2	0.0657	0.0706
1-3	0.0637	0.0698
1-4	0.0619	0.0676
1-5	0.0638	0.0686
2-3	0.0617	0.0689
2-4	0.0601	0.0661
2-5	0.0631	0.0680
3-4	0.0585	0.0632
3-5	0.0638	0.0675
4-5	0.0692	0.0719

MEAN 0.0631 0.0682

TEST G; 3-20-95 PILE TESTS; LOAD IN X-DIRECTION

CYCLE	DISPLACEMENT AMPLITUDE (INCHES)		PERIOD (SECONDS)	
	POS.	NEG.	POS.	NEG.
1	0.04022	-0.03725	0.164	0.166
2	0.02718	-0.02376	0.166	0.162
3	0.01817	-0.01502	0.162	0.164
4	0.01223	-0.01015	0.158	0.162
5	0.00889	-0.00676	0.156	0.162

DISPL. PEAKS	DAMPING RATIO	
	POS.	NEG.
1-2	0.0622	0.0714
1-3	0.0631	0.0721
1-4	0.0631	0.0688
1-5	0.0599	0.0678
2-3	0.0640	0.0728
2-4	0.0635	0.0675
2-5	0.0592	0.0665
3-4	0.0630	0.0622
3-5	0.0568	0.0634
4-5	0.0506	0.0646

MEAN	0.0605	0.0677

TEST H; 3-20-95 PILE TESTS; LOAD IN X-DIRECTION

CYCLE	DISPLACEMENT AMPLITUDE (INCHES)		PERIOD (SECONDS)	
	POS.	NEG.	POS.	NEG.
1	0.04028	-0.03842	0.166	0.166
2	0.02634	-0.02490	0.166	0.168
3	0.01901	-0.01619	0.164	0.164
4	0.01298	-0.01000	0.164	0.160
5	0.00886	-0.00679	0.156	0.162

DISPL. PEAKS	DAMPING RATIO	
	POS.	NEG.
1-2	0.0674	0.0688
1-3	0.0596	0.0686
1-4	0.0600	0.0712
1-5	0.0601	0.0688
2-3	0.0518	0.0684
2-4	0.0563	0.0724
2-5	0.0577	0.0688
3-4	0.0607	0.0764
3-5	0.0606	0.0690
4-5	0.0606	0.0616

MEAN 0.0595 0.0694

TEST I; 3-20-95 PILE TESTS; LOAD IN X-DIRECTION

CYCLE	DISPLACEMENT AMPLITUDE (INCHES)		PERIOD (SECONDS)	
	POS.	NEG.	POS.	NEG.
1	0.05719	-0.05560	0.170	0.170
2	0.03788	-0.03469	0.170	0.170
3	0.02463	-0.02148	0.168	0.166
4	0.01742	-0.01289	0.170	0.166
5	0.01235	-0.00832	0.164	0.162

DISPL. PEAKS	DAMPING RATIO	
	POS.	NEG.
1-2	0.0654	0.0749
1-3	0.0669	0.0755
1-4	0.0629	0.0773
1-5	0.0609	0.0754
2-3	0.0683	0.0761
2-4	0.0617	0.0786
2-5	0.0594	0.0755
3-4	0.0550	0.0810
3-5	0.0549	0.0752
4-5	0.0547	0.0695

MEAN	0.0610	0.0759

TEST J; 3-20-95 PILE TESTS; LOAD IN X-DIRECTION

CYCLE	DISPLACEMENT AMPLITUDE (INCHES)		PERIOD (SECONDS)	
	POS.	NEG.	POS.	NEG.
1	0.05860	-0.05506	0.172	0.172
2	0.03575	-0.03487	0.168	0.170
3	0.02577	-0.02130	0.170	0.170
4	0.01814	-0.01328	0.166	0.166
5	0.01304	-0.00805	0.166	0.164

DISPL. PEAKS	DAMPING RATIO	
	POS.	NEG.
1-2	0.0784	0.0725
1-3	0.0652	0.0754
1-4	0.0621	0.0752
1-5	0.0597	0.0763
2-3	0.0520	0.0783
2-4	0.0539	0.0766
2-5	0.0534	0.0775
3-4	0.0558	0.0750
3-5	0.0542	0.0772
4-5	0.0525	0.0794

MEAN 0.0587 0.0763

TEST K; 3-20-95 PILE TESTS; LOAD IN X-DIRECTION

CYCLE	DISPLACEMENT AMPLITUDE (INCHES)		PERIOD (SECONDS)	
	POS.	NEG.	POS.	NEG.
1	0.05854	-0.05461	0.172	0.174
2	0.03863	-0.03388	0.172	0.172
3	0.02688	-0.02085	0.170	0.170
4	0.01841	-0.01213	0.166	0.168
5	0.01289	-0.00661	0.170	0.164

DISPL. PEAKS	DAMPING RATIO	
	POS.	NEG.
1-2	0.0660	0.0757
1-3	0.0618	0.0764
1-4	0.0612	0.0795
1-5	0.0601	0.0837
2-3	0.0576	0.0771
2-4	0.0589	0.0814
2-5	0.0581	0.0864
3-4	0.0601	0.0858
3-5	0.0584	0.0910
4-5	0.0567	0.0963

MEAN 0.0599 0.0833

TEST L; 3-20-95 PILE TESTS; LOAD IN X-DIRECTION

CYCLE	DISPLACEMENT AMPLITUDE (INCHES)		PERIOD (SECONDS)	
	POS.	NEG.	POS.	NEG.
1	0.05746	-0.05581	0.170	0.174
2	0.03746	-0.03472	0.174	0.174
3	0.02529	-0.02109	0.170	0.174
4	0.01718	-0.01271	0.168	0.170
5	0.01244	-0.00829	0.166	0.166

DISPL. PEAKS	DAMPING RATIO	
	POS.	NEG.
1-2	0.0680	0.0753
1-3	0.0652	0.0772
1-4	0.0639	0.0783
1-5	0.0608	0.0757
2-3	0.0624	0.0791
2-4	0.0619	0.0797
2-5	0.0584	0.0758
3-4	0.0614	0.0804
3-5	0.0564	0.0741
4-5	0.0514	0.0678

MEAN 0.0610 0.0763

TEST M; 3-20-95 PILE TESTS; LOAD IN X-DIRECTION

CYCLE	DISPLACEMENT AMPLITUDE (INCHES)		PERIOD (SECONDS)	
	POS.	NEG.	POS.	NEG.
1	0.07780	-0.06999	0.174	0.176
2	0.05079	-0.04322	0.174	0.176
3	0.03355	-0.02520	0.174	0.174
4	0.02412	-0.01403	0.172	0.170
5	0.01706	-0.00727	0.170	0.170

DISPL. PEAKS	DAMPING RATIO	
	POS.	NEG.
1-2	0.0677	0.0765
1-3	0.0668	0.0810
1-4	0.0620	0.0850
1-5	0.0603	0.0897
2-3	0.0659	0.0855
2-4	0.0592	0.0892
2-5	0.0578	0.0942
3-4	0.0525	0.0928
3-5	0.0537	0.0985
4-5	0.0550	0.1041

MEAN 0.0601 0.0896

TEST N; 3-20-95 PILE TESTS; LOAD IN X-DIRECTION

CYCLE	DISPLACEMENT AMPLITUDE (INCHES)		PERIOD (SECONDS)	
	POS.	NEG.	POS.	NEG.
1	0.07422	-0.06743	0.174	0.176
2	0.04875	-0.04124	0.174	0.178
3	0.03109	-0.02550	0.174	0.176
4	0.02124	-0.01469	0.174	0.174
5	0.01655	-0.00790	0.170	0.168

DISPL. PEAKS	DAMPING RATIO	
	POS.	NEG.
1-2	0.0668	0.0780
1-3	0.0691	0.0772
1-4	0.0662	0.0806
1-5	0.0596	0.0850
2-3	0.0714	0.0763
2-4	0.0660	0.0819
2-5	0.0572	0.0873
3-4	0.0605	0.0875
3-5	0.0501	0.0929
4-5	0.0396	0.0982

MEAN 0.0607 0.0845

TEST P; 3-20-95 PILE TESTS; LOAD IN X-DIRECTION

CYCLE	DISPLACEMENT AMPLITUDE (INCHES)		PERIOD (SECONDS)	
	POS.	NEG.	POS.	NEG.
1	0.07428	-0.06866	0.178	0.180
2	0.04752	-0.04304	0.176	0.178
3	0.03076	-0.02562	0.174	0.178
4	0.02136	-0.01508	0.174	0.174
5	0.01505	-0.00901	0.170	0.170

DISPL. PEAKS	DAMPING RATIO	
	POS.	NEG.
1-2	0.0709	0.0741
1-3	0.0700	0.0782
1-4	0.0660	0.0802
1-5	0.0634	0.0805
2-3	0.0691	0.0823
2-4	0.0635	0.0832
2-5	0.0609	0.0827
3-4	0.0580	0.0841
3-5	0.0568	0.0829
4-5	0.0556	0.0817
MEAN	0.0634	0.0810

TEST Q; 3-20-95 PILE TESTS; LOAD IN X-DIRECTION

CYCLE	DISPLACEMENT AMPLITUDE (INCHES)		PERIOD (SECONDS)	
	POS.	NEG.	POS.	NEG.
1	0.05449	-0.05013	0.176	0.178
2	0.03692	-0.03121	0.176	0.176
3	0.02415	-0.01907	0.172	0.174
4	0.01733	-0.01030	0.170	0.172
5	0.01256	-0.00583	0.172	0.168

DISPL. PEAKS	DAMPING RATIO	
	POS.	NEG.
1-2	0.0618	0.0752
1-3	0.0646	0.0767
1-4	0.0607	0.0836
1-5	0.0583	0.0853
2-3	0.0674	0.0781
2-4	0.0601	0.0879
2-5	0.0571	0.0887
3-4	0.0527	0.0976
3-5	0.0520	0.0939
4-5	0.0512	0.0903

MEAN 0.0586 0.0857

TEST R; 3-20-95 PILE TESTS

CYCLE	DISPLACEMENT AMPLITUDE (INCHES)		PERIOD (SECONDS)	
	POS.	NEG.	POS.	NEG.
1	0.03653	-0.03466	0.172	0.176
2	0.02412	-0.02199	0.170	0.174
3	0.01682	-0.01412	0.170	0.172
4	0.01186	-0.00820	0.168	0.170
5	0.00868	-0.00571	0.168	-----

DISPL. PEAKS	DAMPING RATIO	
	POS.	NEG.
1-2	0.0659	0.0723
1-3	0.0616	0.0713
1-4	0.0595	0.0763
1-5	0.0571	0.0716
2-3	0.0573	0.0703
2-4	0.0564	0.0782
2-5	0.0541	0.0714
3-4	0.0555	0.0861
3-5	0.0526	0.0719
4-5	0.0497	0.0576

MEAN 0.0570 0.0727

TEST S; 3-20-95 PILE TESTS; LOAD IN X-DIRECTION

CYCLE	DISPLACEMENT AMPLITUDE (INCHES)		PERIOD (SECONDS)	
	POS.	NEG.	POS.	NEG.
1	0.01754	-0.01583	0.168	0.168
2	0.01186	-0.01039	0.164	0.164
3	0.00811	-0.00685	0.164	0.164
4	0.00580	-0.00421	0.164	0.162
5	0.00421	-0.00306	-----	-----

DISPL. PEAKS	DAMPING RATIO	
	POS.	NEG.
1-2	0.0621	0.0668
1-3	0.0613	0.0665
1-4	0.0586	0.0702
1-5	0.0567	0.0652
2-3	0.0604	0.0662
2-4	0.0569	0.0718
2-5	0.0549	0.0647
3-4	0.0534	0.0774
3-5	0.0522	0.0639
4-5	0.0510	0.0503

MEAN 0.0568 0.0663

TEST T; 3-20-95 PILE TESTS; LOAD IN X-DIRECTION

CYCLE	DISPLACEMENT AMPLITUDE (INCHES)		PERIOD (SECONDS)	
	POS.	NEG.	POS.	NEG.
1	0.07626	-0.06915	0.176	0.178
2	0.04980	-0.04277	0.176	0.178
3	0.03205	-0.02664	0.174	0.176
4	0.02157	-0.01511	0.172	0.174
5	0.01583	-0.00904	0.168	0.170

DISPL. PEAKS	DAMPING RATIO	
	POS.	NEG.
1-2	0.0677	0.0762
1-3	0.0688	0.0757
1-4	0.0669	0.0804
1-5	0.0624	0.0807
2-3	0.0700	0.0751
2-4	0.0665	0.0825
2-5	0.0607	0.0822
3-4	0.0629	0.0899
3-5	0.0560	0.0857
4-5	0.0492	0.0815

MEAN 0.0631 0.0810

TEST V; 3-20-95 PILE TESTS; LOAD IN X-DIRECTION

VITA

Richard Lee Graves was born April 17, 1961 in Laon, France. As the son of an Air Force enlisted man, Richard spent much of his childhood moving from one place to the next. The family finally settled in Moore, Oklahoma in 1972. Soon after graduating from Moore high School, he enlisted in the United States Coast Guard and spent the next eight years of his life much like the first several years. During his enlistment, Richard met and married Laura Marie Schmidt. In 1988, he left the Coast Guard to continue his education. After one year of classes at Virginia Western Community College in Roanoke, Virginia, the couple moved to Knoxville, Tennessee. Richard then entered the College of Engineering at The University of Tennessee. There, he received his Bachelor of Science degree in Civil Engineering in December of 1993 and his Master of Science degree in December of 1995.